LA-UR-20-23733
Approved for public release; distribution is unlimited.

Title: Beryllium (Be) Handbook

Author(s): Haertling, Carol Lynn

Intended for: Report

Issued: 2020-05-19

Beryllium (Be) Handbook

Los Alamos National Laboratory
Los Alamos, NM 87545

May, 2020

Contacts: Carol Haertling, Sigma-2, 505-665-9058, chaert@lanl.gov

TABLE OF CONTENTS

1. General

Beryllium (Be), atomic number 4, is a silver gray metal of low density (1.85g/cm^3), moderately high melting point (1289°C), and quite good stability in the atmosphere. Favorable mechanical properties, particularly specific stiffness (elastic modulus/density), have resulted in a number of weight-critical structural applications. Other notable properties of beryllium include good dimensional stability, high specific heat and extremely high transparency to X-radiation. The nuclear properties of beryllium include a high neutron scattering cross section (6 barns for thermal neutrons) and a low neutron absorption cross section (0.009 barns for thermal neutrons) making it a good choice for a neutron reflector. The (n, 2n) reaction in beryllium also makes it suitable for a neutron multiplier.

The use of Be for structural applications is limited by its low temperature brittleness which results in poor resistance to impact and low fracture toughness. This brittleness is a result of the hexagonal closed packed (HCP) crystal structure and cannot be substantially reduced by purification or heat treatment. However, the mechanical and physical properties of beryllium are affected by the grain size, microchemistry, thermal treatment and mechanical working.

Be is processed to different grades for various applications. Structural grades (e.g. Materion Corporation S65C, S200E, S200F) provide the best combination of ductility and strength. Furthermore, these grades are the most versatile. Instrument grade materials are optimized to provide the least distortion in aerospace guidance instruments. Also, instrument grades are optimized to provide the best precision elastic limit, which is the maximum stress which can be applied before one μin of plastic strain is produced. Optical grade materials are optimized for reflectivity, thermal expansion and polishing characteristics. The principal application is satellite mirrors.

Structural grades of Be are emphasized in this compilation of data, and specifically, block forms of structural grade material are emphasized. Several excellent compilations of information on Be already exist (see bibliography). In 2010, the American Society of Materials (ASM) published a handbook on Be, "Beryllium and Beryllium Alloys." The reader should refer to these compilations as well as the considerable more data available in the references, for additional insight into specific properties and behavior of Be. Furthermore, the reader should consult the listed references for experimental details before using data in this handbook.

1.01 Commercial Designations

There have been two commercial manufacturers of Be products, Materion Corporation and Kawicki Berylco Industries.

1.011 Materion Corporation:

Materion Corporation is currently the only U.S. commercial source of Be products. The organization originated in 1931 as Brush Wellman, Inc. In 2011, the name was changed to Materion Corporation. Materion Corporation manufactures beryllium and beryllium containing alloys beginning with ore reserves and mining operations to processing of raw material through

extraction refinement to fabrication of shapes. Material Corporation produces mill products including powders and pressed forms, wrought forms, machined forms, and coatings.

Materion Corporation has manufactured and continues to manufacture several structural grades of Be block. These include the S100 series and the S200 series (D, E, and F) and S65. The S200 series is versatile, and is most frequently used for parts machined from pressed block. The S65 material is a premium Be which is guaranteed to exhibit a minimum 3% tensile elongation at room temperature in any test direction. Control of both chemistry and powder characteristics allow this strain capacity.

S200D and S200E have the same specified impurity limits, however, the difference in powder origins can make the actual impurity levels and subsequent physical properties different. The type D material is made from a blend of virgin, prime virgin and recycled powders, while the type E materials are made from virgin and prime virgin powder only. The recycled powder is made by the attrition of beryllium chips returned from machining operations. The virgin powder is made from vacuum melted ingots of previously hot pressed material, and the prime virgin powder is made from vacuum melted ingots of material having no previous hot pressing history. The powder made from vacuum melted ingots produces material with more uniform particle size and impurity levels. The difference in grain size is due to the use of a –325 mesh screen for the E material versus a –200 mesh screen for the D material.

The S200E and S200F materials differ in that the starting powders are prepared by different methods. The S200F powder is size reduced by impact grinding while the S200E powder is size reduced by attrition milling. The attrition milling produces slightly higher impurity contents, and flat, flakelike particles that result in anisotropic product materials. S200F has increased strength and ductility as well as lower anisotropy when compared with S200E.

S65 is a Be material with higher purity levels than the S200 materials. The oxide content is lower, and the Fe and Al contents are lower and balanced to achieve higher ductility. The powder for the pressed block is impact ground. This material has a minimum ductility of 3% in any direction at room temperature.

1.011 Kawecki Berylco:

Kawecki Berylco Industries Inc. was formed from a merger of The Beryllium Corporation of America (BCA) and Kawecki Chemical Inc. in 1968. The beryllium manufacturing plant was the former BCA plant that operated in Hazelton, PA beginning in 1957. Kawecki Berylco was sold in 1970 to the Cabot Corporation.

Kawicki Berylco manufactured several structural/high strength grades of block material including HIP-50, HP-20, HP-10, HP-40, HP-21, HP-8 and CIP-HIP-1. The HIP-50 and CIP-HIP-1 material are both high strength, high purity material manufactured by the isostatic consolidation of fine particle size powder of electrolytic flake origin. HP-21, HP-20 and HP-10 are both produced by vacuum hot pressing of impact attritioned powder. HP-20 is a standard grade however, while HP-10 was developed to withstand elevated temperatures and thermal cycling.

1.02 Commercial Specifications

1.021 Materion Corporation:

Commercial specifications for several structural grades of Materion Corporation beryllium, specifically grades S200E, S200F, and S65 are given in Figures 1.021a-1.021c.

1.022 Kawecki Berylco:

Commercial specifications for two structural grades of Kawicki Berylco beryllium, specifically grades HIP-50 and HP-21 are given in Figures 1.022a-1.022b.

1.03 Composition

1.031 Materion Corporation:

The composition and starting material characteristics for Materion Corporation S200D, S200E and S200F are given in Figure 1.031a. Micrographs of the Materion S200D, Materion S200E, Materion S200F and S65 materials are given in Figure 1.031b (1,2,3).

1.032 Kawecki Berylco:

The composition and starting material characteristics for Kawicki Berylco HIP-50 and HP-21 are given in Table 1.032.

1.04 Forms and Conditions Available

Materion Corporation sells Be as 1) a mill product which encompasses powder and pressed block; 2) wrought forms which encompass sheets, near net shapes, and extrusions; 3) formed product by mechanical, chemical, electrochemical and electric discharge machining; and as coatings fabricated by electrochemical methods. Kawicki Berylco produced Be as 1) a mill product which encompassed powder and pressed block; 2) wrought forms which encompassed sheets and extrusions; 3) flakes by electrolytic origin. Noncommercially, Be has also been produced by plasma spray deposition. Be is used extensively in alloys.

1.05 Special Considerations

1.051 Health hazards:

The health hazards for Be are as follows: Beryllium exposure can cause Chronic Beryllium Disease (CBD) in those people who are genetically hypersensitive to beryllium. CBD is a lung disease that, once acquired, is incurable, and which has an approximately 30% fatality rate. The incidence of CBD in beryllium machinists has averaged about 15%. If one is in the 85% of the population that is not genetically hypersensitive to beryllium, then there is essentially no problem with beryllium or beryllium oxide exposure. However, if one belongs to the 15% of the population that is hypersensitive to beryllium, a significant health hazard may exist if exposed, even in a minor way, to beryllium or beryllium oxide. It has been reported that secretaries at some beryllium plants acquired CBD, although they never went into the beryllium operational areas. Genetic tests are currently under development to determine genetic hypersensitivity of individuals to beryllium and beryllium oxide (4,5).

1.052 Exposure limits:

The current DOE exposure limit for airborne beryllium particles is 0.2 $\mu g/m^3$ for an eight hour time-weighted average (6).

2. Physical and Chemical Properties

2.01 Structural Properties

2.011 Atomic Bonding:

The atomic bonding in beryllium is highly unusual for a metal (7,8,9). The bonding is metallic in the a-axis basal plane, but has a covalent character to it in the c-axis direction perpendicular to the basal plane. Figure 2.011 shows the density of electronic states curve for beryllium and compares it to that of magnesium. For beryllium, there is a dip in the density of states near the Fermi surface, while for magnesium there is a maximum. This leads to a departure in free electron behavior for beryllium.

2.012 Crystal Structure:

The hexagonal crystal structure of Be is shown in Figure 2.012a. The atoms are situated at the lattice points and at coordinates 2/3, 1/3, 1/2, or alternatively, 1/3, 2/3, 1/2. The environment of the interior atom is different from those of an atom at a corner, and the atomic positions are not translateable. The arrangement is considered a double lattice structure, and contains two atoms per primitive unit cell. The lattice parameters are a = 2.285 Å, c = 3.583 Å with a c/a ratio of 1.568, the smallest of all the elements (10). The effects of temperature on lattice constants are shown in Figure 2.012b (11). The Be unit cell contains four tetrahedral interstices and two octahedral interstices.

2.013 Surface Structure:

The (0001) surfaces of beryllium exhibit an approximately 6% interplanar expansion which is anomalously high for metals (12,13,14). This behavior is shown in Figure 2.013. It is thought to be related to the unusual atomic bonding in beryllium. Any effect that this anomalous expansion may have on the surface properties of beryllium has not been studied.

2.014 Crystallographic textures:

Polycrystalline Be exhibits distinct crystallographic textures, both in the as-fabricated state and after plastic deformation. Figure 2.014a shows (0001) pole figures obtained by neutron diffraction of Materion Corporation vacuum hot pressed beryllium materials (15). Hot pressing made from attrited powder showed strong (0001) textures, while hot pressings made from impact ground powder exhibited weaker (0001) textures. Hot rolling of beryllium (16) produces very strong (0002) and (1010) textures, as shown in Figure 2.014b.

2.02 Thermal Properties

2.021 Melting point:

The melting point of Be between 1289 ± 5°C (17).

2.022 Phase changes:

There is one phase change in cooling Be down from its melting point. From the melting point of 1289°C-1270°C, Be exists in a body centered cubic β-Be crystal structure. Below 1270°C, the crystal structure of Be is the hexagonal α-Be form (17).

2.023 Thermal conductivity and diffusivity:

The thermal conductivity of single crystal Be both perpendicular and parallel have been measured at cryogenic temperatures. The values are listed below (18,19):

Perpendicular to c-axis	Parallel to c-axis
12.2 J•cm/cm^2•sec•°C @ -182.6°C	14.61 J•cm/cm^2•sec•°C @ 181.1°C
14.6 J•cm/cm^2•sec•°C @ -194.2°C	
25.3 J•cm/cm^2•sec•°C @ -250.5°C	

Be is known for its high thermal conductivity to weight ratio. This combination of properties has lead to the use of Be and BeO in the microelectronics industry. The thermal conductivity of Materion S200F is 220 W/m•K at 298K (20). Thermal conductivity as a function of temperature for Materion S200E, S200D and various grades of Be are shown in Figure 2.023a-c (21,22,23,24,25). No anisotropy with pressing direction was found in the S200D material.

Thermal diffusivity (thermal conductivity divided by the density and specific heat at constant pressure) of Be is shown in Figure 2.023d (26).

2.024 Thermal expansion:

The linear thermal expansion of single crystal Be as a function of temperature and direction of measurement (27) is shown in Figure 2.024a (28). The thermal expansion values for polycrystalline Be will depend upon the degree of preferred orientation and the direction of measurement. Figure 2.024b shows linear thermal expansion with temperature for a and c lattice parameters measured within a polycrystalline material (29).

The linear thermal expansion of Materion S200F Be as a function of temperature (27) is shown in Figure 2.024c. Also, the linear thermal expansion of Materion S200F is as follows:

L: 11.39×10^{-6}, T1: 11.57×10^{-6}, T2: 11.45×10^{-6} [5-65°C] (30)

The linear thermal expansion of Materion S200E Be is as follows:

L: 11.39×10^{-6}, T1: 11.76×10^{-6}, T2: 11.82×10^{-6} [5-65°C] (30)

2.03 Other Physical Properties

2.031 Density:

The theoretical density of hexagonal α-Be is 1.8477 g/cm^3 at 298 K (20). The theoretical density of cubic β-Be is 1.42 g/cm^3 at 1773 K (20).

A table of theoretical densities at various temperatures and pressures is given in Figure 2.031 (31).

2.032 Electrical conductivity:

Be is a conductor at room temperature, with conductivity strongly influenced by the presence and form of impurities. Electrical resistivity (inverse of conductivity) for Materion S200D as a function of temperature is shown in Figure 2.032a. The electrical resistivity of other Be materials as a function of temperature (32) are shown in Figure 2.032b.

2.033 Emittance:

The emittance of Be as a function of temperature is shown in Figure 2.033a-b (32,33).

2.034 Reflectance:

The normal spectral reflectance of Be as a function of temperature is shown in Figure 2.034 (32).

2.04 Chemical Properties

2.041 Vapor pressure:

The vapor pressure of Be as a function of temperature is shown in Figure 2.041 (1). A mass spectrometric study on the composition of Be vapor both above and below the melting point, showed that the vapors consist of monatomic Be (34).

2.042 Corrosion resistance:

Galvanically beryllium is an electropositive metal and will corrode in certain galvanic cells. On the emf scale, Be has an electrochemical potential of 1.85 electron volts.

2.0421 Water and aqueous salt solutions:

Be that is clean and free of surface impurities has exceedingly good resistance to attack in low-temperature, high purity water. The corrosion attack in high purity water is typically less than 1 mil/year (35). Be of normal commercial purity, however, is susceptible to attack, primarily in the form of localized pitting, when exposed to impure water (36). A Pourbaix diagram showing potential vs. pH for the Be-H_2O system is shown in Figure 2.0421a (37). The Pourbaix diagram is only valid in the absence of substances with which Be can form soluble complexes (e.g. citric, tartaric, oxalic and fluorine complexes, complexons, and pyro-, meta- and polyphosphoric complexes) or unsoluble compounds (e.g. oxinate and beryllium ammonium phosphate)

Passive current density and corrosion current density as a function of pH for Materion S200D in aqueous solution is shown in Figure 2.0421b. Anodic passivity was observed between pH 2 and 12.5 at potentials <0.6 V vs saturated calomel electrode, but below pH 2, the Be was subject to uniform attack (38). The investigators found that Materion S200F performed the same as the Materion S200D material (39).

Figure 2.0421c shows corrosion rates for Be in various aqueous salt solutions (40). Chloride, fluoride and sulfate ions are notably the most critical contamination in aqueous corrosion. Pitting of Be in aqueous baths containing chloride and sulfate ions has generally been attributed to attack in areas anodic to the bulk of the metal (41). Figure 2.0421d shows pitting potential vs. chloride concentration for Materion S200D. The voltage which corresponded to the onset of pitting was found to decrease logarithmically with increasing chloride concentration (38). Microprobe analysis of pitted Be surfaces has led to the following general conclusions: 1) Pitting corrosion is determined by the distribution of alloy impurities; 2) Sites that have high concentrations of iron, aluminum or silicon (probably in solid solution) tend to form corrosion pits; 3) The corrosion sites are often characterized by the presence of alloy-rich particles which are probably beryllides, although the particles themselves do not appear to be corrosion active; 4) Pitting density is believed to be related to the number of segregated regions in the matrix containing concentrations of iron, aluminum or silicon higher than concentrations present in the surrounding areas. Be_2C inclusions have also been noted for their reactivity with H_2O, resulting in the formation of flowery white corrosion products in air or gelatinous product in an aqueous environment (41).

2.0422 Acids and bases:

Halogen acids react with Be at all concentrations at room temperature. Concentrated sulfuric (H_2SO_4) reacts slowly with Be, while dilute sulfuric reacts rapidly. Dilute nitric acid (HNO_3) does not react with the bulk form, but some reaction does occur with fine powders. Dilute acetic acid (CH_3COOH) reacts slowly with Be (42). Glacial acetic acid (CH_3COOH) does not react with either the bulk form or powder at room temperature. In general, increased temperature will increase the reaction rate of Be with all acids.

Alkali hydroxides in solution vigorously attack Be. Slow reaction occurs in alkali carbonate solutions. No reaction between ammonium hydroxide (NH_4OH) and Be has been observed (42).

2.0423 Organic solvents:

Methyl alcohol in combination with water, freon or perchlorethylene reacts quickly with Be, as does methyl ethyl ketone in combination with freon and water. Other solvents such as trichlorethylene (stabilized) have no observable corrosion (40). A table of Be reaction in various organic solvents is shown in Figure 2.0423 (43).

2.0424 Molten materials:

The resistance of Be to attack by a molten metal is influenced by the amount of oxygen present in the system, since Be reduced most metal oxides. Any BeO formed is apparently nonprotective because flaking occurs which exposes fresh surfaces and results in continuous Be weight loss (42). Be has good corrosion resistance to most molten materials up to at least 650°C. Molten Al, however, reacts readily with Be. Pitting corrosion has been found for molten sulfur and gallium at ~815°C (44).

2.0425 Gases:

When exposed to air, beryllium forms a protective oxide coating, similar to aluminum. The coating contributes to oxidation resistance up to 600-700 °C, with a significant increase in the oxidation rate at ~825°C. Figures 2.0425a-b show weight gain as a function of temperature in an O_2 atmosphere (31,45). The activation energy of the Be-O_2 reaction has been calculated as 50.3 kcal/mole in the temperature range 750-950°C (31).

Be also reacts with N_2, the effects with temperature are shown in Figure 2.0425c. The trends are similar to reactions with O_2, but the rates are slower. The activation energy of the Be-N_2 reaction has been calculated as 75 kcal/mole in the temperature range 725-925°C.

Appreciable reactions between Be and H_2, at a pressure of 2.6 cm Hg have not been observed in the temperature range of 300-780°C (45). However, some evidence that hydrogen can be interstitially absorbed into Be has been observed (31).

The reactions of Be with both wet and dry CO_2 are shown in Figure 2.0425d and were found to be parabolic in the temperature range of 550-720°C (46). At 725°C, an increased rate of reaction occurred after 60-70 hrs. Reaction products were BeO and Be_2C. Be_2C exposed to H_2O created CH_4 as a reaction product. The CH_4 reaction has been proposed as a cause for increased rates of reaction observed between Be and wet CO_2 at extended times (46).

Fluorine reacts with Be at room temperature, while chlorine, bromine, and iodine react at elevated temperatures. HF, HCl, HCN, CO, NO_2, H_2S and CS_2 also react at elevated temperatures (31). Reactions with H_2, N_2, O_2, CO and CO_2 at high temperature are shown in Figure 2.0425e (40).

2.0426 Solids:

The reaction of some solid materials in intimate contact with Be have been measured. Figure 2.0426a lists reaction layer thickness between Be and Fe, Ni, stainless steel, U and UO_2 at several temperatures (47). Minimal or no reaction was observed between Be and Ta, W, Cr plate, Cb, Mo, Ti and Zr-0.5Mo in vacuum or CO_2 atmospheres with <100-ppm H_2O at 1022-1112°F. Be did react with alumel, chromel, Cu, Ni, Nimonic 75, stainless steel, steel, U and Zr (47). The results of similar studies are shown in Figures 2.0426b-c for Be and various metals either in intimate contact or separated by interlayers in evacuated containers (48). Oxide interlayers did not provide adequate protection to prevent interactions between materials (48).

2.04 Nuclear Properties

The principle isotopes and their respective half-lives are ^{6}Be, 0.4 seconds; ^{7}Be, 53 days; ^{8}Be, 10-16 seconds; ^{9}Be, stable; ^{10}Be, 2.5×10^{6} years (20). Be naturally occurs 100% as the isotope Be^{9}.

Beryllium absorbs very little x-ray, gamma, or electromagnetic radiation. It also is an excellent scatterer of neutrons. Nuclear reactions can be produced by neutrons, gamma rays, protons, deuterons and alpha particles (31).

2.051 Neutrons:

Be acts predominantly as a scatterer of neutrons, changing their direction and reducing their energy. Thus, Be has uses as a moderator and reflector material for nuclear fission reactors. The total cross section (absorption + reflection) for low energy neutrons is shown in Figure 2.051a (10,49,50), and for higher energy neutrons in Figure 2.051b (31).

Be readily parts with neutrons, making it useful as a neutron multiplier. Reactions with neutrons are listed as follows:

$$Be^{9}\,(n, \alpha)\, He^{6}$$

In this reaction, the He^{6} produced has a half-life of 0.82 seconds and undergoes radioactive decay to Li^{6}. Each Li^{6} that then captures a neutron produces a helium atom and an atom of

tritium by the reaction Li^6 (n, α) H^3. The He^6 reaction of beryllium occurs at a slow rate, since the neutron cross-section of the reaction is less than 50 mb.

Be^9 (n, γ) Be^{10}

This is a neutron capture reaction. For thermal neutron captures, the initial result of the capture is to form Be^{10} in a state 6.81 MeV above the ground state. This excited state disintegrates practically immediately by either emitting a 6.81 MeV gamma ray or by the emission of two 3.4 MeV gamma rays in succession. The Be^{10} formed by the neutron capture is a very weakly radioactive isotope of beryllium. Its half-life is 2,700,000 years and it decays to B^{10} by the emission of a 0.55 MeV beta ray.

Be^9 (n, 2n) Be^8

This reaction may be a fairly significant source of neutrons.

2.052 Gamma Rays:

Figure 2.052 shows the gamma ray absorption coefficients of Be as a function of gamma ray energy, and compares them to those of aluminum.

2.053 X-Rays:

Beryllium is known for its x-ray transparency, and is often used as a "window" in vacuum environments so that x-rays are allowed to pass but a mechanical seal is still maintained. The mass absorption coefficient of CuK_α radiation (0.0254 cm) for Be is 1.007 cm^2/gm (3).

2.06 Thermodynamic Properties:

2.061 Heat Capacity and Specific Heat:

Heat capacity and specific heat (heat capacity per unit mass) at constant pressure are defined in the following equations:

$$C_p = \left(\frac{dH}{dT}\right)_p \qquad c_p = \frac{C_p}{m}$$

C_p = heat capacity at constant pressure
T = temperature (K)
H = enthalpy
c_p = specific heat at constant pressure
m = mass

Both quantities are given for Be through the equations listed below:

$C_p = (5.068 + 1.361\times10^{-3}T + 0.23\times10^{-6}T^2 - 1.404\times10^{5}T^{-2})$ cal/K•mol
[25-1254°C] (53)

c_p = 1.830 J/g•K @ 298 K, 2.740 J/g•K @ 700 K (20)

The specific heat of Be as a function of temperature is shown in Figures 2.061a (36,51) and 2.061b (52,26) and 2.061d (31). Heat capacity values are also listed in Figure 2.062 (31).

2.062 Enthalpy, Entropy, Free Energy:

Several further thermodynamic properties defined as follows, including enthalpy, entropy, and free energy:

$$H(T) = H_f(298K) + \int_{298}^{T} C_p dT + \sum H_{tr}$$

$$S = S_o(298K) + \int \left(\frac{C_p}{T}\right) dT + \sum \frac{H_{tr}}{T_{tr}}$$

$$G \text{ (or } F) = H - TS$$

T = temperature (K)
H = enthalpy
S = entropy
S_o = entropy at 1 atmosphere pressure
G, F = free energy
$H_f(298K)$ is the enthalpy of formation at 298 K,
H_{tr} is the enthalpy of transformation of the substance
$S_o(298K)$ = entropy at 1 atmosphere pressure and at 298 K
H = 0 for elements in their most stable state at 298 K and 1 atmosphere pressure.

These values as a function of temperature for Be are listed in Figure 2.062 (31).

2.063 Enthalpy of fusion, sublimation, vaporization:

The heat of fusion for Be is 1357 J/g (20,53)

The heat of sublimation for Be is 35.5-36.6 J/g (20,54)

The heat of vaporization for Be is 25.5-34.4 J/g (20,55)

3. Mechanical Properties

3.01 Single Crystal Be

3.011 Elastic Properties:

The elastic modulus and Poisson's ratio for single crystal Be have been determined in both the parallel and perpendicular directions to the basal plane. The data is shown in Figure 3.011a (56).

Elastic constants for Be are listed below:

c_{11} = 2.954, c_{12} = 0.259, c_{13} = -0.01, c_{33} = 3.561, c_{44} = 1.706 (56)

The unusually small value of the c_{13} constant shows minimal coupling of stress between the c-axis and the basal plane. Thus, stress concentrations can easily lead to basal plane cleavage (56). The elastic constants as a function of temperature are shown in Figure 3.011b (57).

3.012 Slip Systems:

The slip planes and slip systems in Be are shown in Figure 3.012a-b (58). Slip can occur in the basal, prismatic and pyramidal planes and is very anisotropic. Figure 3.012c shows the critical slip stress along various planes as a function of temperature (56). At room temperature, the critically resolved slip stress (CRSS) for basal planes is very much lower than other slip planes and therefore, basal slip is by far the dominant slip system in Be. A study of anisotropy of slip, basal plane cleavage and fracture stress in Be has found that increasing the purity (as low as 8 ppm) did not affect these properties, however alloying can substantially increase the CRSS (56). CRSS as a function of impurity content and alloy content is shown in Figure 3.012d-e (56).

3.013 Fracture:

In beryllium, cracks are nucleated by basal plane slip (56), as shown in Figure 3.013a. Stroh proposed the following fracture criterion for the formation of cracks by basal plane splitting (59):

$$\sigma_n = \frac{4\gamma_{(0001)}\mu \cos\chi}{\pi D\tau_s}$$

σ_n = normal stress on the basal plane
χ = angle between the basal plane and specimen axis
μ = shear modulus
D is the specimen diameter
τ_s = effective resolved shear stress
$\gamma_{(0001)}$ = fracture surface energy of the basal planes

In the Stroh expression, the fracture stress increases with increasing basal plane fracture surface energy. Alloying with copper has been observed to have little effect on the crack propagation energy in the basal plane (60), as shown in Figure 3.013b. However, the basal plane fracture surface energy of beryllium exhibits a tendency to increase with increasing temperature (61), as shown in Figure 3.013c.

3.014 Hardness:

Single crystal measurements of Be have given values of Rockwell B-87 along the c-axis and B-35 perpendicular to the c-axis (36). The hardness of beryllium is significantly higher on the basal planes than on the prismatic planes (62), as shown in Figure 3.014a. While no directionality of hardness is evident in the basal plane, significantly periodic maxima and minima occur in the prismatic plane. Figure 3.014b shows beryllium hardness as a function of temperature. Hardness anisotropy persists at temperatures up to 400ºC (62).

3.0. Polycrystalline Be

3.021 Elastic properties:

Elastic moduli, shear moduli, shear rupture moduli and precision elastic limit (the stress required to produce 10^{-6} inch/inch permanent strain) for Materion S200F have been measured at room temperature. The data is presented in Figure 3.021a (30). The elastic modulus of Materion S200E is reported to be 44 mpsi.(30). Elastic moduli and shear moduli as a function of temperature for Materion hot pressed block Be is presented in Figure 3.021b (63). Elastic modulus vs. temperature for two beryllium materials is shown in Figure 3.021c (44).

A Poisson's ratio measured in various directions at room temperature is given for the Materion S200F in Figure 3.021d (64).

3.022 Tensile properties:

A stress vs. strain curve for Materion S200F is given in Figure 3.022a, while further curves for Materion S200E at various strain rates and temperatures for are shown in Figures 3.022b-c. Stress-strain curves for KBI Be blocks at various strain rates are shown in Figure 3.022d (65). Yield stresses increase with increasing strain rates. Effects of biaxial stress loading on the strength of KBI Be is shown in 3.022e (65).

3.0221 Strength:

Tensile properties at various temperatures, orientations and radiation dose are given for Mateiron S200F as well as Materion S200E and Materion S65 in Figure 3.0221a-g (3,30,64,66,67). The properties include ultimate tensile strength, offset yield strength, yield point, reduction in area and elongation.

Both Materion S200 materials have anisotropic tensile properties, but the Materion S200F properties are both greater and less anisotropic when compared with the Materion S200E. The Materion S65 material does not show ultimate strength anisotropy, and the values are roughly comparable with Materion S200E and S200F values.

Higher purity, finer grain size and higher oxide content increase the strength of Be. A small inflection is sometimes observed at the yield point. Figures 3.0221h-i show the effects of grain size and temperature on the tensile yield and ultimate strength of KBI Be block (65). The effects of biaxial stress on the yield strength and ultimate strength for KBI block is shown in Figure 3.0221j (65). The highest values occurs under pure shear loading conditions.

3.0222 Ductility:

The brittleness, or low ductility of Be at temperatures below ~200°C has been a limitation for the material in applications. The preference for slip along the basal planes leads to the low ductility. Ductility values for material having the basal plane aligned with the tensile axis leads to high ductility values (e.g. >20% for sheet) in the tensile direction and low values in the normal direction. Low ductility is inherent to Be, and advances have not resulted in ductility on par with other metals.

Several methods to enhance the ductility have been explored, including minimization of impurities, texturing the material, and controlling grain growth. Tensile elongation values for Materion S200F are given in Figure 3.0221a and for Materion S65 in Figure 3.0221e. Figures 3.0222b-h show the effect of various parameters on tensile elongation, including grain size, impurity content, strain rate and temperature, for Materion S200F, S200E, S65 as well as KBI and other berylliums (1,3,30,65,68,69). The Materion S65 Be has a ductility which is greater than the S200F ductility at room temperature as well as temperatures up to 600+°C.

3.023 Compressive properties:

A compressive stress-strain curve using various strain rates with a KBI Be is shown in Figure 3.023a (65).

Compressive yield strength for Materion S200 material as a function of sample orientation is given in Figure 3.023b. Further compressive properties for a Materion S200 hot pressed material are given in Figure 3.023c (31,64)

3.024 Hardness:

Rockwell B hardness for Materion S200F is reported as 85.5±0.09 and 85.4±1.2 for the longitudinal and transverse directions respectively. This is reported to be comparable to Materion S200E (30).

3.025 Fracture toughness:

Fracture toughness for Be has been found to be primarily dependent on texture and oxide content, and to a less degree on grain size and impurity levels. These properties will depend heavily on the input powder material and the densification process (70).

The average K_{IC} value for Materion S200F has been reported as 8.7±0.3 kpsi•in$^{1/2}$ with a longitudinal stress axis and a radial direction of crack propagation. With a radial stress axis and a longitudinal direction of crack propagation, the average K_{IC} value has been measured as and 9.9±0.3 kpsi•in$^{1/2}$ (64). Another source reports 9.2 kpsi•in$^{1/2}$ in the longitudinal direction and 11.43 kpsi•in$^{1/2}$ in the transverse direction, as well as 9.7 kpsi•in$^{1/2}$ (longitudinal) and 10.2 kpsi•in$^{1/2}$ (transverse) for Materion S200E (70,71) The K_{IC} value for Materion S65 has been reported as 8-11 kpsi•in$^{1/2}$, with no substantial differences between Materion S200F, S200E and S65 (3).

Fracture toughness values, along with some yield and ultimate strength values, are listed in Figures 3.025a-e for Materion S200F, S200E, S200D and S65 Be (64,72,73,73,74). A correlation of Be fracture toughness with tensile properties is shown in Figure 3.025f (72).

Fracture toughness as a function of temperature for Materion S65, KBI CIP-HIP and other grades are shown in Figure 3.025g-i (73,75,76). Fracture toughness tests on a high-yield strength grade of Be block found little effect of sample orientation or temperature to 300°C. Evidence pointed to crack closure, rather than ductility as the source of crack arrest (75). The effects of neutron irradiation and temperature aging on the fracture toughness of Materion S200F and S65 Be are shown in Figure 3.025j (77). A reduction in the beryllium fracture toughness was observed (77).

Effects of BeO content and grain size on hot pressed block are shown in Figures 3.025k (72).

Dynamic fracture toughness values are given in Figure 3.025l (78), and plane strain fracture toughness values are given in Figures 3.025m-n (71).

3.026 Friction:

Coefficients of friction for Be plate against Be rod, and plate Be against 1040 steel rod, have been have been measured by multiple methods and in both wet and dry atmospheres. The values are reported in Tables 3.026a-c (79).

Pin-on-disk sliding friction tests have been conducted with pyroceram pins against Be and anodized Be (51). Friction coefficients obtained are shown in Figure 3.026d.

3.027 Fatigue:

Data, along with graphs of stress vs. cycles to failure are given in Figures 3.027a-d for Materion S200F Be. Smooth fatigue testing gave greater fatigue life in the transverse direction as compared with the longitudinal direction (30). The opposite was true for notch fatigue testing,

however, the authors suspected that a surface etching procedure may have complicated the results (64).

Fatigue life for KBI Be is shown in Figure 3.027e (65).

3.028 Creep:

Creep data for Materion S200F Be block is given in Figure 3.028a (63). Using the Larson-Miller parameter, the time and temperature to produce 0.1%, 0.5% and 1.0% plastic creep at any given stress can be obtained.

Compression creep data as a function of temperature and stress for Be is shown in Figure 3.028b-c (80,81). At low stresses, the creep stress exponent is close to 1, indicating a diffusional flow mechanism. Also, the creep rate is proportional to the inverse of the square of the grain size, and the activation energy for creep is equal to that of self-diffusion in beryllium. At higher stress levels, the stress exponent is 4.5, the activation energy becomes about twice that of self-diffusion, and the creep rate is proportional to the inverse of grain size. This is suggestive of a dislocation glide-climb type of creep mechanism.

3.029 Stress Corrosion Cracking:

Stress-corrosion cracking of Be has been studied most frequently in water and salt conditions. Figure 3.029 shows time to failure as a function of applied stress for Be in seawater (40). The failure of the specimens was not attributed to stress-corrosion cracking, but rather to stress-accelerated corrosion and was closely associated with random pitting. Summarized studies have not found stress corrosion cracking to occur under the conditions of the studies; pitting has been observed as a cause of failure in the presence of salts (40).

4. Fabrication

4.01 Single crystal Be

Single crystal Be has been grown using a zone refinement method (7). The zone refinement method moves a molten zone along the length of a ingot to purify the crystal. The process can be repeated for considerable purification.

4.02 Polycrystalline Be

4.021 Ore reduction:

Beryllium is produced form the ores bertrandite ($Be_4Si_2O_7(OH)_2$) and beryl ($3BeO•Al_2O_3•6SiO_2$). The Be is strongly bonded to the oxygen in these ores and therefore a combination of chemical and mechanical processes are used to extract the metal from the ore. Primary Be is a “pebble” product from the magnesium reduction of anhydrous beryllium

fluoride. The pebbles are vacuum melted to eliminate impurities, and poured into molds to form ingots. This cast material has poor machining and mechanical properties.

The mechanical properties of Be are greatly affected by grain size, as governed by the Hall-Petch relationship. The smaller the grain size, the larger the strength and ductility of the beryllium. Since cast products contain large grains, powder metallurgy techniques are used in forming structural beryllium, which are capable of producing grains similar in size to the starting powder.

4.022 Powder production:

The first step in producing the powder is lathing the ingots into machining swarf. Beyond this step, the powder production methods vary, including attrition milling, impact grinding, ball milling and gas atomization. The method used will impact the properties of the final densified body, particularly if when the processing results in a powder with an anisotropic shape.

During attrition milling, swarf is fed into a mill via a hopper. The mill consists of two Be disks with radial grooves. One of the disks is stationary while the other is rotated by a fixed-speed motor. Heat buildup during the attrition process requires that the disks be water cooled, a procedure that must be carefully performed to minimize oxide formation. Impurities are removed from the attrited material magnetically, and the powder is then screened to –325 mesh ($\leq$44 μm). Powder $\geq$44 μm is returned to the attrition mill and the process repeated. Size reduction proceeds primarily by basal plane cleavage, and therefore in flat particles result. These flat particles tend to align during packing processes which results in a textured billed after consolidation.

Impact grinding requires a feed that is finer than the machining swarf and therefore a pregrind operation is completed. Once preground, the material is placed into a gas stream and impacted against a Be target. The impacted particles are separated by air into coarse and $\leq$44 μm particles. The coarse powder is sent through the grinding process again. Impact grinding results in a relatively lower impurity content and a more isotropic particle morphology.

Ball milling is accomplished by placing machining swarf into a cylindrical drum with a liquid medium and balls for attrition. The cylindrical drum is rotated continuously until the desired particle size ($\leq$10 μm) is reached. Ball milling can lead to higher contamination levels from the containers and balls as well as from the liquid medium.

4.023 Powder consolidation:

Beryllium powder may be consolidated into forms by various powder metallurgy techniques. These include vacuum hot pressing (VHP), hot isostatic pressing (HIP), cold isostatic pressing (CIP), cold pressing (CP) and sintering (S), and various combinations of these techniques. Further processes include coining and plasma spraying. Most commonly used are VHP and HIP; hot pressed block describes material produced by either of these methods.

For VHP, powder is contained is a leak-tight die. A vacuum is pulled while heat and pressure are applied uniaxially. Vacuum hot pressing occurs between 1000-1100°C, a temperature range

just below the temperature at which extensive grain growth occurs. Resultant grain sizes are approximately equivalent to starting particle sizes. VHP pressures depend largely upon the die material; graphite dies typically require relatively low pressures, ~1200 psi. VHP densification depends upon evaporation-condensation, surface diffusion, volume diffusion and creep mechanisms. Each of these mechanisms is time and temperature dependent, showing increased rates at higher temperatures. Pressings may last for many hours.

During the HIP process, a leak-tight container is filled with Be powder. The container is then heated and a vacuum pulled to remove gases. The container is then sealed while under vacuum, followed by application of temperature and isostatic pressure simultaneously. HIP uses relatively high pressures and a range of temperatures. Thus, densification occurs much more quickly, and properties are more easily tailored.

4.024 Machining:

Generally, Be is considered to be easily machinable into intricate shapes with close tolerances. Machining practices are similar to those for cast iron. Be has a machinability factor of 55% (with 1113 steel as 100%). Be is relatively soft, but also abrasive so that carbide cutting tools are generally used.

Be suffers surface damage from machining operations, commonly forming microcracks and twins. The depth of the damage depends on the severity of the machining process, e.g. the sharpness of the tool, the rigidity of the setup, as well as the grain size of the material.

4.025 Treatments for removal of machine damage:

Machining can serious degrade the mechanical properties of Be. There are three approaches to eliminating machine damage: 1) tight control of the machine process, 2) temperature annealing of the machined part, and 3) chemical removal of the machined surface. A study was completed on Materion S200E which compared the effectiveness of using the temperature anneal and chemical etching techniques on mechanical properties. Results of these studies are shown in Figures 4.025a-b (39). Temperature annealing was found not only to return surface damaged properties to bulk values, but also to affect other previously unaffected properties. Chemical etching of 25-50 μm was found to remove the effects of machining damage on mechanical properties, although damage was still noted visually in micrographs (39). Materion recommended procedures for etching Be surfaces are given in Figure 4.025c.

4.026 Heat treatment:

A heat treatment may be completed after consolidation to achieve desired properties. The heat treatment ensures that all low melting point aluminum impurities are contained in the higher melting point beryllium compound $AlFeBe_4$. The heat treatment may also be used to relieve residual stresses induced during processing and machining. Heat treatment above ~900°C can cause grain growths which results in generally lower strengths and slightly higher ductilities.

4.027 Joining:

Adhesive bonding may be used to join Be to itself or to other materials. The surfaces to be bonded must be exceptionally clean. Adhesive bonded joints are generally not as strong as brazed joints (63).

Brazing may also be used to join Be to itself or to other materials. The autogenous brazing of beryllium (i.e. the brazing of beryllium directly to beryllium) is not generally practical due to the extensive fusion zone cracking that occurs in autogenous joints (83,84). The cause of this cracking is associated with the presence of low melting point impurities, particularly aluminum.

Braze materials are typically silver, zinc, or aluminum based alloys, each having particular strength and thermal capabilities. Brazing is considered to be the most reliable metallurgical joint for Be (63). Figures 4.027a-b are tables of Be joint properties fabricated by braze-welding and furnace brazing techniques (42). The primary difficulties of brazing beryllium are hot cracking, cracking at defects, and ductility limitation or thermally induced cracking. Joining can be improved by control of the Fe/Al ratio in the base metal to reduce hot cracking, minimization of the BeO content, control of grain size to limit cracks at defects and ductility limitation cracks, and optimization of the welding process (84).

Electron beam welding, diffusion bonding and the pressurized inert gas metal arc (PIGMA) process are joining techniques that have been used successfully with Be. The PIGMA process uses an Al-12 wt% Si filler in the weld zone (85). Fusion welding is not recommended because of a cast grain structure that develops in the fusion zone (63).

4.028 Coatings:

Coatings may be applied to Be to protect the material from hostile environments or to add different surface characteristics. Chemical conversion or passivation coatings may be applied by dipping the material in solution. These coatings have been found to have a beneficial effect on the resistance of Be to corrosive attack during normal handling and storage. Furthermore, the coatings have been shown to provide significant protection against high humidity, salt atmospheres and immersion in water (41).

Coatings are commonly applied electrochemically to Be. Anodized coatings are used for corrosion protection, typically for corrosive aqueous protection or air oxidation at elevated temperatures. Plated coatings are used on to provide specific capabilities, such as electrical contact or wear resistance (41).

Organic paint coatings provide electrical insulation between Be and another metal. The insulation protects against galvanic attack in the presence of water (41).

4.03 Alloys

The solid solubility of alloying elements in beryllium is relatively limited (86). In the hcp beryllium structure, only copper, nickel, cobalt, silver, and palladium show a solid solubility of

more than 1 atomic %, as shown in Figure 4.029a. Because of the small atomic radius of beryllium and its electronegativity value, no element can form an extensive solid solution with beryllium, as shown in Figure 4.029b (86)

The phase diagrams of Be-Cu, Be-Ni, and Be-Al are shown in Figures 4.029c-e respectively. Information on ternary beryllide compounds is given in Figure 4.029f (86). Ternary beryllium compounds with nonmetals are shown in Figure 4.029g (86).

Bibliography

Abeln, S., P. Kyed, "Summary of beryllium specifications, current and historical," RFP-4283, Rocky Flats Plant, Golden CO (1990).

Beryllium Science and Technology, Volume 1 and Volume 2, eds. D. Webster, G. London, Plenum Press, New York NY (1979).

Brush Wellman, Designing With Beryllium, Brush Wellman Inc., Cleveland OH, 1999.

Dombrowski, D., "Manufacture of beryllium for fusion energy applications," Fusion Engineering and Design, 37, pp. 229-242 (1997).

Reactor Handbook: Volume I, Materials, ed. C. Tipton, Interscience Publishers, New York NY (1960).

Stonehouse, A., "Physics and Chemistry of Beryllium", Journal of Vacuum Science and Technology A, 4, 1163-1170 (1986).

Schierloh, F., S. Babcock, "Tensile properties of beryllium at high strain rates and temperatures," Technical Report AFML-TR-69-273, General Motors Corporation, General Motors Technical Center, Warren, MI (1969).

Walsh, Kenneth A.; Vidal, Edgar E.; Goldberg, Alfred; Dalder, Edward N.C.; Olson, David L.; Mishra, Brajendra, "ASM- Beryllium and Beryllium Alloys," Cleveland OH, American Society of Metals International (2010).

The Metal Beryllium, ed. D. White, J. Burke, Cleveland OH, American Society of Metals (1955).

References

1. Schierloh, F., S. Babcock, "Tensile properties of beryllium at high strain rates and temperatures," General Motors Technical Center, AFML-TR-69-27 (1969).

2. Hanafee, J., "Effect of annealing and etching on machining damage in structural beryllium," Journal of Applied Metal Working, 1, *3*, pp. 41-51 (1980).

3. Marder, J., "Beryllium in stress critical environments," Journal of Materials for Energy Systems, 8, *1,* pp. 17-26 (1986).

4. Pavlova, M., P. Wambach, D. Harvey, "Communicating health risks working safely with beryllium", Oak Ridge National Laboratory Report (1998).

5. Wang, Z., P. White, M. Petrovic, O. Tatum, L. Newman, L. Maier, B. Marrone, "Differential susceptibilities to chronic beryllium disease contributed by different Glu^{69} HLA-DPB1 and –DPA1 Alleles", Journal of Immunology, 163, pp. 1647-1653 (1999).

6. Department of Energy Final Rule 10 CRF 850, "Chronic beryllium disease prevention program (CBDPP)" (1999).

7. Silversmith, D., B. Averbach, "Pressure dependence of the elastic constants of beryllium and beryllium-copper alloys", Physical Review B, 1, pp. 567-571 (1970).

8. Chatterjee, S., P. Sinha, "Energy band structure of beryllium and magnesium", Journal of Physics F: Metal Physics, 5, pp. 2089-2097 (1975).

9. Chou, M. P. Lam, and M. Cohen, "Ab initio study of structural and electronic properties of Beryllium," Physical Review B, 28, pp. 4179-4185 (1983).

10. Hughes, D., Pile Neutron Research, pp. 292-301, Addison Wesley (1953).

11. Gordon, P., "Some measurements of the thermal coefficients of expansion of beryllium," AECD 2426 (1948).

12. Davis, H., J. Hannon, K. Ray, and E. Plummer, "Anomalous interplanar expansion at the (0001) surface of Be", Physical Review Letters, 68, pp. 2632-2635 (1992).

13. Plummer, E., J. Hannon, "The surfaces of beryllium", Progress in Surface Science, 46, pp. 149-158 (1994).

14. Stumpf, R., J. Hannon, P. Feibelman, E. Plummer, "The unusual properties of beryllium surfaces", Sandia National Laboratories Report SAND94-3025C (1994).

15. Bennett, K., R. Varma, and R. Von Dreele, "Texture development in S200-D, -E and P31664 beryllium blocks from neutron diffraction spectra", Scripta Materialia, 40, pp. 825-830 (1999).

16. Moment, R., "The elastic anisotropy of rolled beryllium", Transactions of the Metallurgical Society of AIME, 239, pp. 542-546 (1967).

17. ASM Handbook: Alloy Phase Diagrams, 3, ed. H, Baker, ASM International, 1986.

18. Gruneisen, E., H. Erfling, Annalen der Physick., 38, p. 399 (1940).

19. Erfling, H., E. Gruneisen, Annalen der Physick, 41, p. 89 (1942).

20. Encyclopedia of Chemical Technology, Bearing Materials to Carbon, Volume 4, ed. Kroschwitz, M. Howe-Grant, John Wiley & Sons, New York NY (1991).

21. Dynatech, "Thermal conductivity of hot pressed beryllium between 4 and 600K," Reference TEX-6, 1976.

22. Tye, R., J. Quinn, "The thermal conductivity of hot pressed beryllium block" in Symposium on Thermophysical Properties, ed. J. Moszynski, Society of Mechanical Engineers, New York NY, pp. 144-149 (1968).

23. Military Standards Assn. Handbook—Metallic Materials and Elements for Aerospace Vehicle Structures, MIL-HDBK-5B, Chapter 7 (1973).

24. Brown, W., B. King, Aerospace Structural Metals Handbook, Code 100, Mechanical Properties Data Center Report No. AFML-TR-68-115 (1974).

25. Powell, R., "The thermal and electrical conductivities of beryllium," Philosophical Magazine 44, *353*, pp. 645-663 (1953).

26. Lagedrost, J., "Thermal Conductivity Studies of Beryllium Samples," Battelle Columbus Report (1972).

27. Haws, W., "Thermal expansion of S-200F beryllium from 100K to 450K" Brush Wellman Technical Memo-894 (1988).

28. Meyerhoff,, R., J. Smith, "Anisotropic expansion of single crystals of thallium, yttrium, beryllium and zinc at low temperatures," Journal of Applied Physics, 33, *1*, pp. 219-224 (1962).

29. Amonenko, V., V. Ivanov, G. Tikhinsky, V. Finkel, I. Shpagin, "High temperature polymorphism of beryllium," The Physics of Metal and Metallography., 12, *77* (1962).

30. Haws, W., "Characterization of beryllium structural grade S-200F" Brush Wellman Technical Memo-778 (1975).

31. The Metal Beryllium, ed. D. White, J. Burke, The American Society for Metals, Cleveland OH, pp. 71-101 (1955).

32. Touloukian, Y., "Thermophysical properties of high temperature solid materials," in The Elements,Volume 1, Macmillan Co., New York NY (1967).

33. R. Blickensderfer, D. Deardorff, and R. Lincoln, "Normal Total Emittance at 400-850 ^{o}K and Normal Spectral Reflectance at Room Temperature of Be, Hf, Nb, Ta, Ti, V and Zr", Journal of Less-Common Metals, 51, pp. 13-23 (1977).

34. Nikitin, O., L. Gorokhov, Zhurnal Neorganicheskoikhimii, 6, p. 224 (1961).

35. Wanklyn, J., P. Jones, "The aqueous corrosion of reactor metals," The Journal of Nuclear Materials, 6, *3*, pp. 291-329 (1962).

36. Lillie, D., "The physical and mechanical properties of beryllium metal," in The Metal Beryllium, Cleveland OH, American Society of Metals (1955).

37. Pourbaix, M., Atlas of Electrochemical Equilibria in Aqueous Solutions, Pergamon Press, New York, NY, p. 135 (1966).

38. Hill, M., D. Butt, R. Lillard, "The passivity and breakdown of beryllium in aqueous solutions," Journal of the Electrochemical Society, 145, *8*, pp. 2799-2805 (1998).

39. Hill, M., private communication (2002).

40. Miller, P., W. Boyd, "Corrosion of beryllium," Defense Metals Information Center, Columbus OH, Report DMIS-242 (1967).

41. Mueller, J., D. Adolphson, "Corrosion", pp. 417-433 in Beryllium Science and Technology, Volume 2, eds. D. Floyd and J. Lowe, Plenum Press, New York NY (1979).

42. Reactor Handbook: Volume I, Materials, ed. C. Tipton, Interscience Publishers, New York NY (1960).

43. Steele, J. "General problems in the corrosion of beryllium," National Association of Corrosion Engineers Conference, New York NY (1961).

44. Aerospace Structural Metals Handbook (1990).

45. Gulbransen, E., K. Andrew, "The kinetics of the reactions of beryllium with oxygen and nitrogen and the effect of oxide and nitride on its vapor pressure," Journal of the Electrochemical Society, 97, *11*, pp. 383-395 (1950).

46. Werner, W., H. Inouye, "The reactions of beryllium with wet carbon dioxide," Oak Ridge National Laboratory paper at Institute of Metals Conference on Metallurgy of Beryllium, London England (1961).

47. Lampert, H., Sturn, J., "Corrosion resistance and wear characteristics of beryllium," Brush Beryllium Company, Metallurgical Test Report No. 36.

48. Baird, J., G. Geach, H. Knapton, K. West, "Compatibility of beryllium with other metals used in reactors," Proceedings of the Second United Nations Conference on the Peaceful Uses of Atomic Energy, Geneva Switzerland, 5, pp. 328-330 (1958).

49. Hughes, D., "Neutron cross sections, "AEC document AECU-2040 including supplements n. 1, 2 and 3, Office of Technical Services, US Dept. of Commerce, (1952,1953,1954).

50. Palevsky, H., R. Smith, "Low energy cross-section measurements with the Brookhaven slow neutron chopper," Physical Review, 86, p. 604 (1952).

51. Saka, N., V. Tran, E. Rabinowicz, "Effects of plasma-polymerized coatings on the frictional behavior of beryllium surfaces", Tribology Transactions, 35, pp. 651-658 (1992).

52. Stull, D., H. Prophet, JANAF Thermochemical Tables, U.S. Govt. Printing Office, Washington D.C. (1971).

53. Kubaschewski, O., E. Evans, Metallurgical Thermochemistry, Pergamon Press (1956).

54. Holden, R., R. Speiser, H. Johnston, "The vapor pressures of inorganic substances, I. beryllium," Journal of the American Chemical Society, 70, p. 3897 (1948).

55. Baur, E., R. Brunner, Dampfdruckmessungen and hochsiedenden Metallen, Helvetica Chimica Acta , 17, pp. 958-969, 1934.

56. F. Aldinger, "Flow and Fracture of Single Crystals", pp. 7-107 in Beryllium Science and Technology, Volume 1, eds. D. Webster and G. London, Plenum Press, New York NY (1979).

57. Rowland, W., J.White, "The Determination of the elastic constants of beryllium in the temperature range 25 to 300°C", Journal of Physics F: Metal Physics, 2, pp. 231-236 (1972).

58. Saxton, H., G. London, "Flow and fracture of polycrystalline beryllium", pp. 115-143 in Beryllium Science and Technology, Volume 1, eds. D. Webster and G. London, Plenum Press, New York NY (1979).

59. Stroh, A., "The cleavage of metal single crystals", Philosophical Magazine, 3, pp. 597-606 (1958).

60. Wilhelm, M., F. Aldinger, "Low temperature basal cleavage in single crystals of beryllium and beryllium alloys with copper", Zeitschrift fur Metallkunde, 66, pp. 323-328 (1975).

61 Govila, R., M. Kamdar, "Cleavage in beryllium monocrystals", Metallurgical Transactions, 1, pp. 1011-1018 (1970).

62. Tsuya, K., "The Effect of Temperature on the Hardness Anisotropy of Beryllium Single Crystals", Journal of Nuclear Materials, 22, 148-157 (1967).

63. Brush Wellman, Designing With Beryllium, Brush Wellman Inc., Cleveland Ohio (1999).

64 Haws, W., "Characterization of beryllium structural grade S-200F Supplemental Data" Brush Wellman Technical Memo-890 (1988).

65. Pinto, N., "Properties", pp. 319-350 in Beryllium Science and Technology, Volume 2, eds. D. Floyd and J. Lowe, Plenum Press, New York NY (1979).

66. Shogan, R., "Irradiation effects on the mechanical properties of S200 grade beryllium and Lockalloy at cryogenic temperatures," Westinghouse Astronuclear Laboratory, WANL-TME-1659 (1967).

67. Stonehouse, A., "Physics and Chemistry of Beryllium", Journal of Vacuum Science and. Technology A, 4, pp. 1163-1170 (1986).

68. Brush Wellman, unpublished data.

69. Beaver, W., A. Stonehouse, K. Wikle, F. Vinci, "A study of the factors relating to the consistency of mechanical properties in extruded beryllium," USAEC Report NYO-1120 (1953).

70. Grensing, F., D. Hashigushi, J. Marder, "Fracture toughness of vacuum hot pressed beryllium powder," Advances in Powder Metallurgy, Volume 2, Metal Powder Industries Federation, Princeton NJ, pp. 27-36 (1980).

71. Lemon, D., W. Brown, "Fracture toughness of hot-pressed beryllium," 24th AIAA/ASME/ASCE/AHS Structures, Structural Dynamics and Materials Conference (1983).

72. Conrad, H., J. Hurd, D. Woodard, "The fracture toughness of beryllium," Journal of Testing and Evaluation, 1, 88-99 (1973).

73. Brush Wellman, data from W. Haws (2002).

74. Lemon, D., W. Brown, "Fracture toughness of hot-pressed beryllium", Journal of Testing and Evaluation, 13, 152-161 (1985).

75. Perra, M., I. Finne, "Fracture toughness of a high-strength beryllium at room temperature and 300°C," Journal of Materials Science, 12, pp. 1519-1526 (1977).

76. Barker, L., A. Jones, and S. Chou, "Fracture toughness of CIP-HIP beryllium at elevated temperatures", Theoretical and Applied Fracture Mechanics, 7, pp. 45-49 (1987).

77. Tye, R., J. Quinn, "The thermal conductivity of hot pressed beryllium block" in Symposium on Thermophysical Properties, 4th, College Park MD, 1968, ed. J. Moszynski, Society of Mechanical Engineers, New York NY, pp. 144-149 (1968).

78. Shabbits, W., W. Logsdon, "S200 grade beryllium fracture toughness properties," Journal of Testing and Evaluation, 1, *2*, pp. 110-118 (1973).

79. Morrison, R., "The determination of static friction of beryllium to beryllium and beryllium to 1040 steel," Lawrence Livermore Laboratory, UCID-19687 (1983).

80. Greene, R., G. Pinkerton, "Beryllium improvement program," Lockheed Missiles & Space Co., AFML-TR-73-12 (1973).

81. Borch, N., "Elevated Temperature Behavior", pp. 307-329 in Beryllium Science and Technology, Volume 1, eds. D. Webster and G. London, Plenum Press, New York NY (1979).

82. "Recommended etching procedures/solutions," Brush Wellman Inc. Elmore, OH.

83. Cotton J., R. Field, "Microstructural features of cracking in autogenous beryllium weldments", Metallurgical and Materials Transactions A, 28A, pp. 673-680 (1997).

84. Hill, M., B. Damkroger, R. Dixon, E. Robertson, "Beryllium weldability", Proceedings, Materials Weldability Symposium, ASM Materials Week 1990, Detroit MI, (Los Alamos National Laboratory Report LAUR-90-2516).

85. Heiple, C., R. Merlini, R. Adams, "Investigation of fracture in pressurized gas metal arc welded beryllium", Rockwell International Rocky Flats Plant Report RFP-2463 (1976).

86. Aldinger, F., G. Petzow, "Constitution of beryllium and its alloys", pp. 235-305 in Beryllium Science and Technology, Volume 1, eds. D. Webster and G. London, Plenum Press, New York NY (1979).

BRUSHWELLMAN

ENGINEERED MATERIALS

Brush Wellman Inc. • Elmore, OH 43416 • Phone 419/862-2745 • TWX 810/490-2300

SPECIFICATION SHEET

BERYLLIUM BLOCK
STANDARD GRADE S-200-E

Effective February 20, 1984
Supersedes previous Specification 5/8/72

1. Scope

1.1 This specification defines the requirements for standard Beryllium designated as S-200E.

This standard grade is produced by hot pressing beryllium powder. This specification covers parts and shapes that are machined from hot pressed material.

2. Chemical Composition

2.1 Chemical composition shall conform to the following:

	S-200-E
Beryllium Assay, % min.	98.0
Beryllium Oxide, % max.	2.0
Aluminum, % max.	0.16
Carbon, % max.	0.15
Iron, % max.	0.18
Magnesium, % max.	0.08
Silicon, % max.	0.08
Other Metallic Impurities % each, max., as determined by normal spectrographic methods.	0.04

2.2 Detailed analytical procedures used by Brush Wellman Inc. are available on request.

3. Density

3.1 The minimum bulk density shall be 99% of the theoretical density. Theoretical density shall be established by the formula:

$$\text{Theoretical Density} = \frac{100}{\frac{100 - \%\,BeO}{1.8477\ gm/cc} + \frac{\%\,BeO}{3.009\ gm/cc}}$$

3.2 Density shall be determined by using the water displacement method.

4. Tensile Properties

4.1 Minimum tensile properties at room temperature shall be:

	S-200-E
Ultimate Tensile Strength, psi, minimum	40,000
Yield Strength (0.2% offset) psi, minimum	30,000
Elongation (% in 1 inch) minimum	1%

Page 1 of 3

Figure 1.021a: Commercial specifications for Materion Corporation S200E standard grade beryllium block.

4.2 Federal test method standard No. 151 is applicable. Detailed test procedures used by Brush Wellman Inc. are available on request.

5. Penetrant Inspection

5.1 Liquid penetrant inspection of machined surfaces shall reveal no porosity or cracks.

5.2 Liquid penetrant inspection shall be performed in accordance with MIL-1-6866 A, Type 1 using penetrants and a dry developer conforming to MIL-1-25135 Group V. Personnel performing this inspection shall be certified in accordance with MIL-STD-410.

6. Radiographic Inspection

6.1 Radiographic indications (voids and/or inclusions) shall conform to the requirements as established and defined below:

6.1.1 Requirements:

Material shall conform to the requirements defined in 6.1.2 as follows:

Type	Maximum Dimension	Maximum Average Dimension	Total Combined Volume Per Cubic Inch
Type I	0.030 inch	0.020 inch	Sphere 0.050 inch diameter
Type II	0.030 inch	0.020 inch	Sphere 0.032 inch diameter

6.1.2 Definitions:

6.1.2.1 **Maximum Dimensions of any Indication.** Any dimension of any indication measured in the plane of the radiograph shall not exceed 0.030 inch.

6.1.2.2 **Maximum Average Dimension of any Indication.** The average dimensions of an indication shall not exceed 0.020 inch. The average dimension of an indication shall be the arithmetic average of the maximum and minimum dimensions measured in the plane of the radiograph.

6.1.2.3 **Total Combined Volume Per Cubic Inch of all Indications.** The total combined volume per cubic inch of all indications with an average dimension larger than 0.001 inch shall not exceed the volume of a sphere of the indicated diameter.

6.2 Radiographic inspection to a penetrameter sensitivity of 2% shall be performed in accordance with MIL-STD-453.

7. Grain Size

7.1 The average grain size shall not exceed 25 microns.

Page 2 of 3

Figure 1.021a: Commercial specifications for Materion Corporation S200E standard grade beryllium block.

7.2 The average grain size shall be determined in accordance with ASTM E-112, Section 7b.

8. Tolerances

8.1 Material furnished under this specification shall conform to the dimensions and dimensional tolerances established by the purchase order and applicable drawings. If tolerances are not specified by the purchase order the following standard tolerances shall apply.

Diameter, Width or Thickness, Inches	Tol. Inch
Up to 3, inclusive	-0 + 1/64
Over 3 to 20, inclusive	-0 + 1/16
Over 20	-0 + 1/4
Length, Inches	
Up to 20, inclusive	-0 + 1/8
Over 20	-0 + 1/4

9. Surface Finish

9.1 The material shall be furnished with a machined surface. The standard surface finish shall be 125 microinches rms maximum.

10. Reports

10.1 Certification of compliance with this specification will be furnished on request and, when specified, actual test results will be certified. Testing in accordance with individual customer instructions will be performed if mutually acceptable and actual test results will be certified.

11. Marking

11.1 Each part, surface area permitting, will be legibly marked to give the following information:

Specification Number
Lot and/or Part Number
Manufacturer's Identification

Figure 1.021a: Commercial specifications for Materion Corporation S200E standard grade beryllium block.

BRUSHWELLMAN

ENGINEERED MATERIALS

Brush Wellman Inc. Elmore, Ohio 43416 419/862-2745 FAX: 419/862-4174

S-200-F STANDARD GRADE BERYLLIUM BLOCK

Effective: April 1, 1987 Revision A

1. SCOPE

1.1 This specification defines the requirements for a standard grade of beryllium designated as

This standard grade is to be produced through the consolidation of beryllium powder by vacuum hot pressing. Parts and shapes are machined from the vacuum hot pressed material.

2. CHEMICAL COMPOSITION

2.1. The chemical composition shall conform to the following:

Beryllium Assay, % minimum (1)	98.5
Beryllium Oxide, % maximum (2)	1.5
Aluminum, % maximum (3)	0.10
Carbon, % maximum (3)	0.15
Iron, % maximum (4)	0.13
Magnesium, % maximum (3)	0.08
Silicon, % maximum (3)	0.06
Other Metallic Impurities, % maximum (3)	0.04

Note: (1) Difference (i.e. 100% - other elements)
(2) Leco Inert Gas Fusion
(3) DC Plasma Emission Spectrometry
(4) Leco Combustion

3. DENSITY

The minimum bulk density shall be 99.0% Theoretical Density.

The theoretical density is to be calculated using the following formula:

$$\text{Theoretical Density} = \frac{100}{\frac{100-\%\ \text{BeO}}{1.8477} + \frac{\%\ \text{BeO}}{3.009}}\ \%$$

3.3. Density shall be determined using the water displacement method.

4. TENSILE PROPERTIES

4.1. Minimum tensile properties for the material at room temperature, as determined per ASTM E-8, and MAB-205 M shall be:

Ultimate Tensile Strength, psi, minimum	47,000
Yield Strength (0.2% offset), psi, minimum	35,000
Elongation (% in 4 diameters), minimum	2.0

Federal Test Method Standard No. 151 is applicable.

Figure 1.021b: Commercial specifications for Materion Corporation S200F standard grade beryllium block.

Federal Test Method Standard No. 151 is applicable.

5. PENETRANT INSPECTION

Penetrant and Visual Acceptance Criteria

A. Cracks are not permissible.

B. Pores (as determined by penetrant):

1. The size of an individual pore on the surface may not exceed 0.050".

2. A maximum of 3 pores (of the size 0.003" to 0.050") per square inch of the surface is acceptable.

3. No restrictions to size or number if they do not hold Zyglo.

5.2. Penetrant inspection shall be performed per MIL-STD-6866, using penetrants and a dry developer conforming to MIL-I-25135, Type I, Level 2, Method B, Form A. Personnel performing this inspection shall be certified in accordance with MIL-STD-410.

6. PENETRANT INSPECTION

6.1. Radiographic inspection to a penetrameter sensitivity of 2% shall be performed in accordance with MIL-STD-453, however exceptions are taken to the penetrameter contrast requirement and applicable area of penetrameter density rages of +30% or -15% from the density at penetrameter location(s).

Note: Due to the nature of radiographic inspection, it is pointed out that the sensitivity of the inspection method decreases with increasing material thickness.

Radiographic indication (voids and/or inclusions) shall conform to the requirements as established and defined below.

6.2.1 Requirements

Material shall conform to the following requirements, as defined in 6.2.2.

	Maximum Dimension	Maximum Average Dimension	Total Combined Volume per Cubic Inch
Type I	0.030 inch	0.020 inch	Sphere 0.050 inch diameter
Type II	0.030 inch	0.020 inch	Sphere 0.032 inch diameter

6.2.2. Dimensions:

6.2.2.1. Maximum Dimension of any Indication.

Any dimension of any indication measured in the plane of the radiograph shall not exceed 0.030 inch.

6.2.2.2. Maximum Average Dimension of any Indication.

Figure 1.021b: Commercial specifications for Materion Corporation S200F standard grade beryllium block.

The average dimension of an indication shall be the arithmetic average of the maximum and minimum dimensions measured in the plane of the radiograph. The average dimension of an indication shall not exceed 0.020 inch.

6.2.2.3. Total Combined Volume Per Cubic Inch of all Indications

The total combined volume per cubic inch of all indications with an average dimension larger than 0.001 inch shall not exceed the volume of a sphere of the indicated volume.

6.2.2.4. The minimum detectable size of voids and inclusions will increase as the section thickness increases, due to the decrease sensitivity referred to in paragraph 6.1.

6.2.2.5. Part Density Uniformity.

The terms variable density areas, banding or striations shall denote relatively large areas of a radiograph, which vary in density as compared to the surrounding area. These areas shall not vary in radiographic density by more than 5% as compared to the surrounding area of comparable section thickness.

6.2.2.6. Light high density indications or areas in material 1.000" thick or less, which are 5% or less in radiographic density compared to the surrounding material, are radiographically acceptable.

7. GRAIN SIZE

7.1 The average grain size shall be determined in accordance with ASTM E-112, using the intercept method at 500 magnification.

7.2. the average grain size shall not exceed 20 microns

8. TOLERANCES

8.1 Materials furnished under this specification shall conform to the dimensions and dimensional tolerances as established by the purchase order and applicable drawings. If tolerances are not specified by purchase order, the following standard tolerances shall apply employing ANSI Y 14.5M:

Diameter, Width or Thickness, Inches	Tolerance
Up to 3, inclusive	-0 + 1/64
Over 3 to 20, inclusive	-0 + 1/16
Over 20	-0 + 1/4

Length, Inches	Tolerance
Up to 20, inclusive	-0 + 1/8
Over 20	-0 + 1/4

9. SURFACE FINISH

9.1 The materials shall be furnished with a machined surface. The standard surface finish shall be 125 microinches rms. (Approximately = 110 Ra) maximum, employing ANSI/ASME B46.1.

Figure 1.021b: Commercial specifications for Materion Corporation S200F standard grade beryllium block.

10. REPORTS

10.1. Certification of Compliance with this specification will be furnished on request and, when specified, actual test results will be certified. Testing in accordance with individual customer instructions will be performed, if mutually acceptable and actual test results will be certified.

11. MARKING

Surface area permitting, each part will be legibly marked employing an electroetching technique or tagging if insufficient area is available.

Marking is to include the following:

Brush Wellman Inc. (BWI)
Lot and/or Part Number
Serial Number
Specification Number
X-Ray number
Purchase Order Number
Warning Beryllium

12. PROCEDURES

Detailed analytical and test procedures used by Brush Wellman Inc. are available upon request.

Figure 1.021b: Commercial specifications for Materion Corporation S200F Standard Grade Beryllium Block.

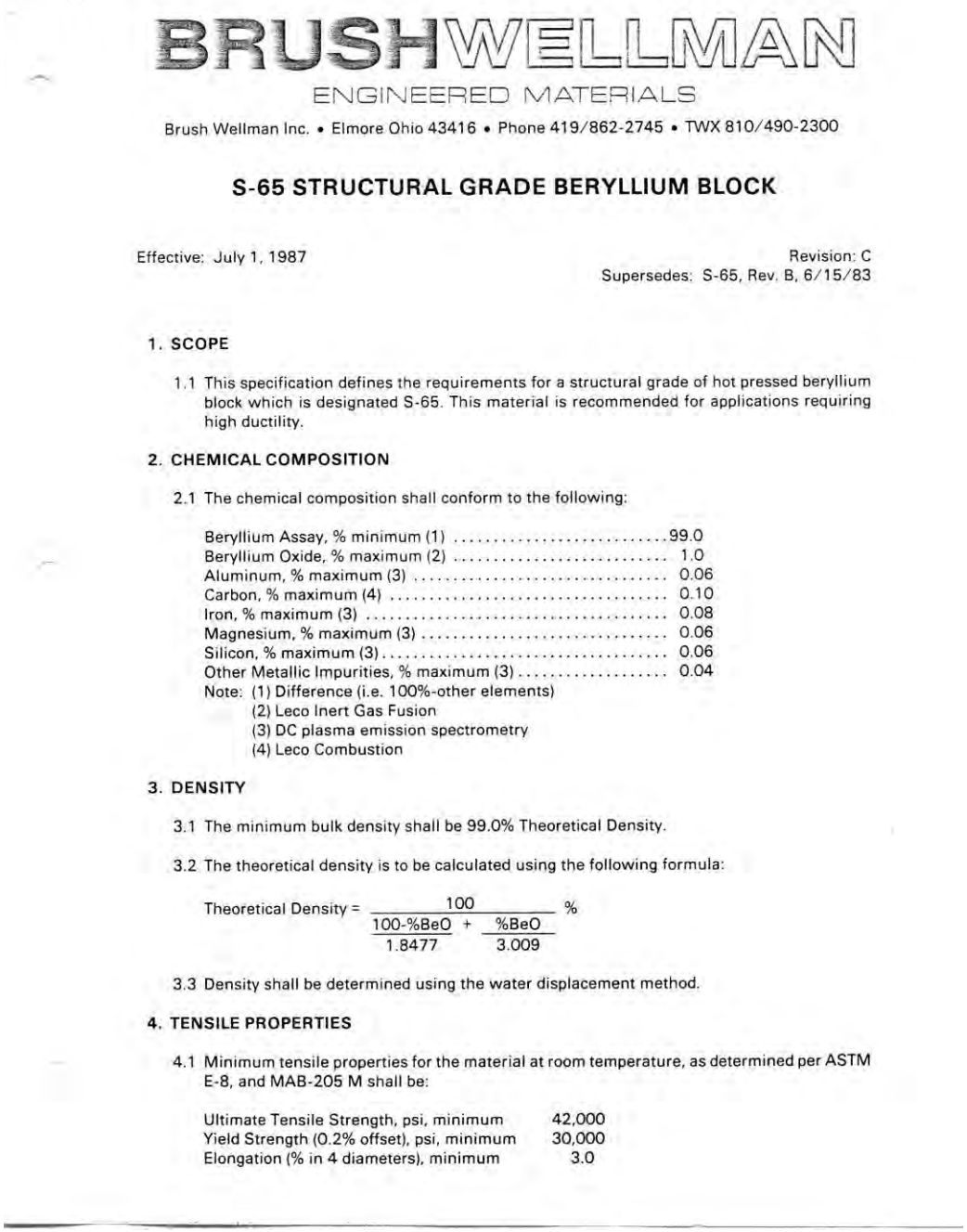

BRUSHWELLMAN

ENGINEERED MATERIALS

Brush Wellman Inc. • Elmore Ohio 43416 • Phone 419/862-2745 • TWX 810/490-2300

S-65 STRUCTURAL GRADE BERYLLIUM BLOCK

Effective: July 1, 1987

Revision: C
Supersedes: S-65, Rev. B, 6/15/83

1. SCOPE

1.1 This specification defines the requirements for a structural grade of hot pressed beryllium block which is designated S-65. This material is recommended for applications requiring high ductility.

2. CHEMICAL COMPOSITION

2.1 The chemical composition shall conform to the following:

Beryllium Assay, % minimum (1)	99.0
Beryllium Oxide, % maximum (2)	1.0
Aluminum, % maximum (3)	0.06
Carbon, % maximum (4)	0.10
Iron, % maximum (3)	0.08
Magnesium, % maximum (3)	0.06
Silicon, % maximum (3)	0.06
Other Metallic Impurities, % maximum (3)	0.04

Note: (1) Difference (i.e. 100%-other elements)
(2) Leco Inert Gas Fusion
(3) DC plasma emission spectrometry
(4) Leco Combustion

3. DENSITY

3.1 The minimum bulk density shall be 99.0% Theoretical Density.

3.2 The theoretical density is to be calculated using the following formula:

$$\text{Theoretical Density} = \frac{100}{\frac{100-\%BeO}{1.8477} + \frac{\%BeO}{3.009}} \%$$

3.3 Density shall be determined using the water displacement method.

4. TENSILE PROPERTIES

4.1 Minimum tensile properties for the material at room temperature, as determined per ASTM E-8, and MAB-205 M shall be:

Ultimate Tensile Strength, psi, minimum	42,000
Yield Strength (0.2% offset), psi, minimum	30,000
Elongation (% in 4 diameters), minimum	3.0

Figure 1.021c: Commercial specifications for Materion Corporation S65 Grade Beryllium Block.

4.2 Federal Test Method Standard No. 151 is applicable.

5. PENETRANT INSPECTION

5.1 Penetrant and Visual Acceptance Criteria

A. Cracks are not permissible.

B. Pores (as determined by penetrant):

1. The size of an individual pore on the surface may not exceed 0.050".

2. A maximum of 3 pores (of the size 0.003" to 0.050") per square inch of the surface is acceptable.

3. No restrictions to size or number if they do not hold Zyglo.

5.2 Penetrant inspection shall be performed per MIL-STD-6866, using penetrants and a dry developer conforming to MIL-I-25135, Type I, Level 2, Method B, Form A. Personnel performing this inspection shall be certified in accordance with MIL-STD-410.

6. RADIOGRAPHIC INSPECTION

6.1 Radiographic inspection to a penetrameter sensitivity of 2% shall be performed in accordance with MIL-STD-453, however exceptions are taken to the penetrameter contrast requirement and applicable area of penetrameter density ranges of + 30% or -15% from the density at penetrameter location(s).

Note: Due to the nature of radiographic inspection, it is pointed out that the sensitivity of the inspection method decreases with increasing material thickness.

6.2 Radiographic indications (voids and/or inclusions) shall conform to the requirements as established and defined below.

6.2.1 Requirements.

Material shall conform to the following requirements, as defined in 6.2.2

Maximum Dimension	Maximum Average Dimension	Total Combined Volume per Cubic Inch
0.030 inch	0.020 inch	Sphere 0.050 inch diameter

6.2.2 Dimensions:

6.2.2.1 Maximum Dimension of any Indication.

Any dimension of any indication measured in the plane of the radiograph shall not exceed 0.030 inch.

-2-

Figure 1.021c: Commercial specifications for Materion Corporation S65 Grade Beryllium Block.

6.2.2.2 Maximum Average Dimension of any Indication.

The average dimension of an indication shall be the arithmetic average of the maximum and minimum dimensions measured in the plane of the radiograph. The average dimension of an indication shall not exceed 0.020 inch.

6.2.2.3 Total Combined Volume Per Cubic Inch of all Indications.

The total combined volume per cubic inch of all indications with an average dimension larger than 0.001 inch shall not exceed the volume of a sphere of the indicated volume.

6.2.2.4 The minimum detectable size of voids and inclusions will increase as the section thickness increases, due to the decrease sensitivity referred to in paragraph 6.1.

6.2.2.5 Part Density Uniformity.

The terms variable density areas, banding or striations shall denote relatively large areas of a radiograph, which vary in density as compared to the surrounding area. These areas shall not vary in radiographic density by more than 5% as compared to the surrounding area of comparable section thickness.

6.2.2.6 Light high density indications or areas in material 1.000" thick or less, which are 5% or less in radiographic density compared to the surrounding material, are radiographically acceptable.

7. GRAIN SIZE

7.1 The average grain size shall be determined in accordance with ASTM E-112, using the intercept method at 500 magnification.

7.2 The average grain size shall not exceed 20 microns.

8. TOLERANCES

8.1 Materials furnished under this specification shall conform to the dimensions and dimensional tolerances as established by the purchase order and applicable drawings. If tolerances are not specified by purchase order, the following standard tolerances shall apply employing ANSI Y 14.5M:

Diameter, Width or Thickness, Inches	Tolerance
Up to 3, inclusive	-0 + 1/64
Over 3 to 20, inclusive	-0 + 1/16
Over 20	-0 + 1/4

Length, Inches	Tolerance
Up to 20, inclusive	-0 + 1/8
Over 20	-0 + 1/4

9. SURFACE FINISH

9.1 The materials shall be furnished with a machined surface. The standard surface finish shall be 125 microinches rms. (Approximately = 110 Ra) maximum, employing ANSI/ASME 846.1.

-3-

10. REPORTS

10.1 Certification of Compliance with this specification will be furnished on request and, when specified, actual test results will be certified. Testing in accordance with individual customer instructions will be performed, if mutually acceptable and actual test results will be certified.

11. MARKING

11.1 Surface area permitting, each part will be legibly marked employing an electroetching technique or tagging if insufficient area is available.

11.2 Marking is to include the following:

Brush Wellman Inc. (BWI)
Lot and/or Part Number
Serial Number
Specification Number
X-Ray Number
Purchase Order Number
Warning Beryllium

12. PROCEDURES

12.1 Detailed analytical and test procedures used by Brush Wellman Inc. are available upon request.

Figure 1.021c: Commercial specifications for Materion Corporation S65 Grade Beryllium Block.

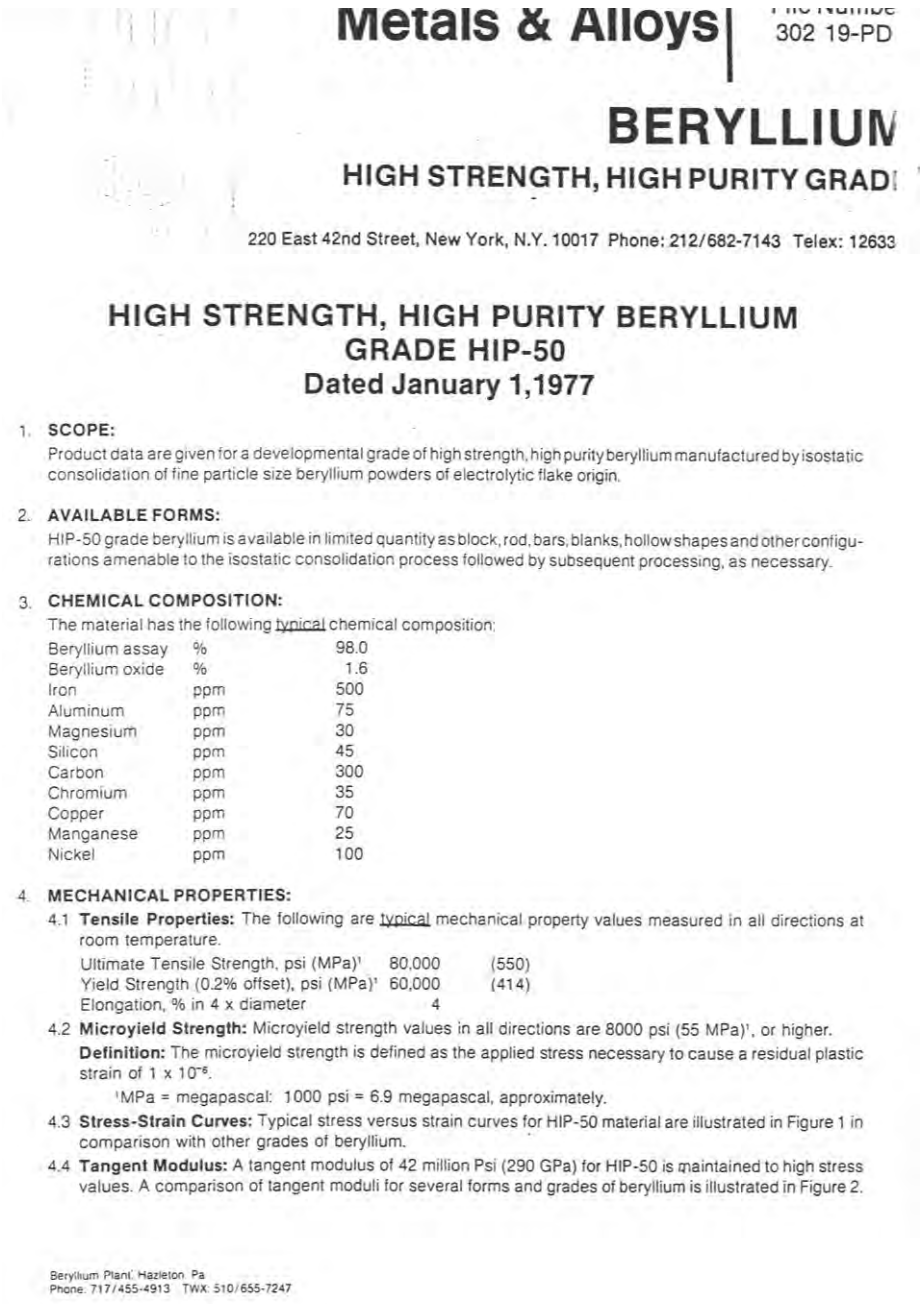

Metals & Alloys | File Number 302 19-PD

BERYLLIUM

HIGH STRENGTH, HIGH PURITY GRADE

220 East 42nd Street, New York, N.Y. 10017 Phone: 212/682-7143 Telex: 12633

HIGH STRENGTH, HIGH PURITY BERYLLIUM GRADE HIP-50 Dated January 1,1977

1. **SCOPE:**
Product data are given for a developmental grade of high strength, high purity beryllium manufactured by isostatic consolidation of fine particle size beryllium powders of electrolytic flake origin.

2. **AVAILABLE FORMS:**
HIP-50 grade beryllium is available in limited quantity as block, rod, bars, blanks, hollow shapes and other configurations amenable to the isostatic consolidation process followed by subsequent processing, as necessary.

3. **CHEMICAL COMPOSITION:**
The material has the following typical chemical composition:

Beryllium assay	%	98.0
Beryllium oxide	%	1.6
Iron	ppm	500
Aluminum	ppm	75
Magnesium	ppm	30
Silicon	ppm	45
Carbon	ppm	300
Chromium	ppm	35
Copper	ppm	70
Manganese	ppm	25
Nickel	ppm	100

4. **MECHANICAL PROPERTIES:**

4.1 **Tensile Properties:** The following are typical mechanical property values measured in all directions at room temperature.

Ultimate Tensile Strength, psi (MPa)[1]	80,000	(550)
Yield Strength (0.2% offset), psi (MPa)[1]	60,000	(414)
Elongation, % in 4 x diameter	4	

4.2 **Microyield Strength:** Microyield strength values in all directions are 8000 psi (55 MPa)[1], or higher.
Definition: The microyield strength is defined as the applied stress necessary to cause a residual plastic strain of 1×10^{-6}.

[1]MPa = megapascal: 1000 psi = 6.9 megapascal, approximately.

4.3 **Stress-Strain Curves:** Typical stress versus strain curves for HIP-50 material are illustrated in Figure 1 in comparison with other grades of beryllium.

4.4 **Tangent Modulus:** A tangent modulus of 42 million Psi (290 GPa) for HIP-50 is maintained to high stress values. A comparison of tangent moduli for several forms and grades of beryllium is illustrated in Figure 2.

Beryllium Plant, Hazleton, Pa
Phone: 717/455-4913 TWX: 510/655-7247

Figure 1.022a: Commercial specifications for Kawicki Berylco HIP-50 structural grade beryllium block.

5. **GRAIN SIZE:**
Typical grain size for this material is 3.5 - 5 microns (micrometers).

6. **GENERAL:**
Additional data are available from KBI upon request.

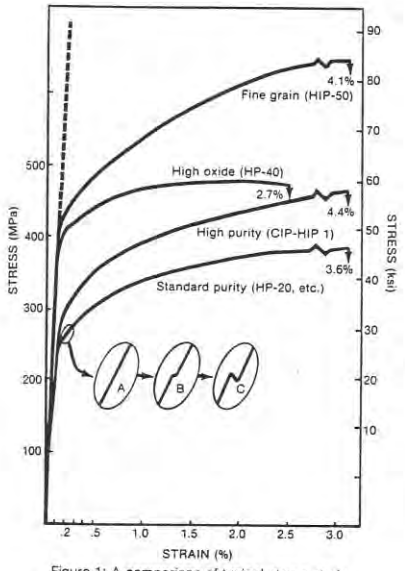

Figure 1: A comparison of typical stress strain curves for HIP-50 material and other grades of beryllium.

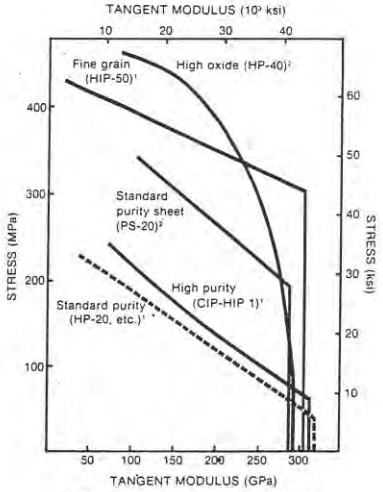

Figure 2: A comparison of tensile and compressive tangent moduli of several forms and grades of beryllium.
(¹ in Tension, ² in Compression)

KAWECKI BERYLCO INDUSTRIES, INC.
General Sales Office: 220 East 42nd Street, New York, N.Y. 10017
212/682-7143 Telex: 126332

OI 6/77 Printed in USA

Figure 1.022a: Commercial specifications for Kawicki Berylco HIP-50 structural grade beryllium block.

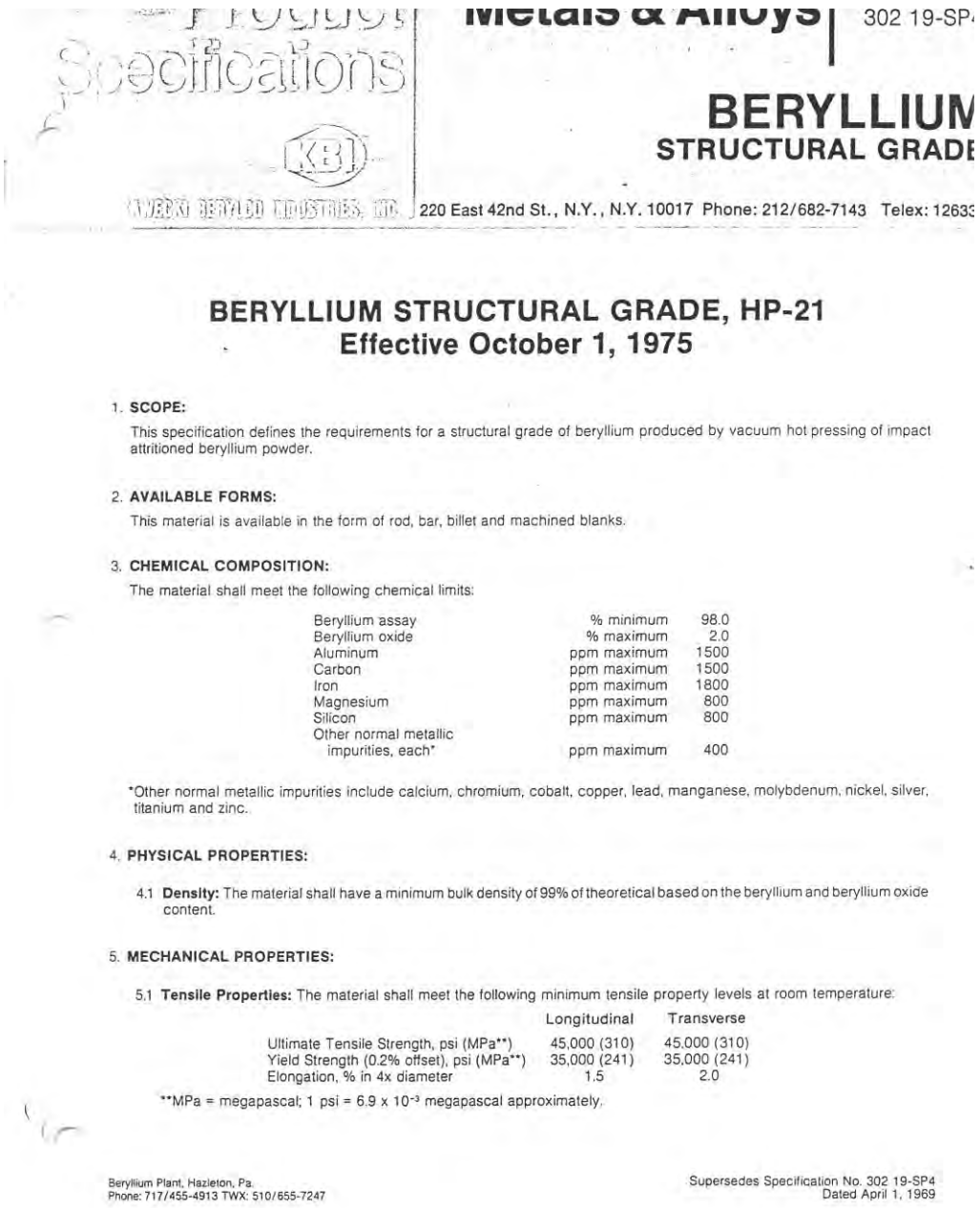

Specifications

Metals & Alloys | 302 19-SP4

BERYLLIUM
STRUCTURAL GRADE

KAWECKI BERYLCO INDUSTRIES, INC. 220 East 42nd St., N.Y., N.Y. 10017 Phone: 212/682-7143 Telex: 12633

BERYLLIUM STRUCTURAL GRADE, HP-21
Effective October 1, 1975

1. **SCOPE:**

This specification defines the requirements for a structural grade of beryllium produced by vacuum hot pressing of impact attritioned beryllium powder.

2. **AVAILABLE FORMS:**

This material is available in the form of rod, bar, billet and machined blanks.

3. **CHEMICAL COMPOSITION:**

The material shall meet the following chemical limits:

Beryllium assay	% minimum	98.0
Beryllium oxide	% maximum	2.0
Aluminum	ppm maximum	1500
Carbon	ppm maximum	1500
Iron	ppm maximum	1800
Magnesium	ppm maximum	800
Silicon	ppm maximum	800
Other normal metallic impurities, each*	ppm maximum	400

*Other normal metallic impurities include calcium, chromium, cobalt, copper, lead, manganese, molybdenum, nickel, silver, titanium and zinc.

4. **PHYSICAL PROPERTIES:**

4.1 **Density:** The material shall have a minimum bulk density of 99% of theoretical based on the beryllium and beryllium oxide content.

5. **MECHANICAL PROPERTIES:**

5.1 **Tensile Properties:** The material shall meet the following minimum tensile property levels at room temperature:

	Longitudinal	Transverse
Ultimate Tensile Strength, psi (MPa**)	45,000 (310)	45,000 (310)
Yield Strength (0.2% offset), psi (MPa**)	35,000 (241)	35,000 (241)
Elongation, % in 4x diameter	1.5	2.0

**MPa = megapascal; 1 psi = 6.9 x 10^{-3} megapascal approximately.

Beryllium Plant, Hazleton, Pa.
Phone: 717/455-4913 TWX: 510/655-7247

Supersedes Specification No. 302 19-SP4
Dated April 1, 1969

Figure 1.022b: Commercial specifications for Kawicki Berylco HP-21 structural grade beryllium block.

BERYLLIUM STRUCTURAL GRADE, HP-21
Effective October 1, 1975

10. **SAMPLING AND TEST PROCEDURES:**

Individual tests will be performed as required by the specification or as required per specific customer instructions. Testing w be in accordance with Military, Federal and/or ASTM Standards, where applicable.

10.1 **Chemical Analysis:** Analysis for beryllium oxide and other insolubles will be determined by the 6% bromine-absolu methanol dissolution method or other acceptable procedures.

10.2 **Density:**

10.2.1 Bulk density will be determined by the water displacement method or by the geometric method.

10.2.2 The theoretical density is to be determined using the following formula:

$$\text{Theoretical density} = \frac{100}{\frac{100 - \%\,BeO}{1.8477} + \frac{\%\,BeO}{3.009}} \text{ gram per cubic centimeter}$$

10.3 **Mechanical Properties:** Mechanical properties will be measured on tensile test specimens removed from the material two mutually perpendicular directions, one direction to be the primary axis of the pressing. Test specimens will b prepared in accordance with accepted beryllium machining and etching procedures.

Tensile testing will be performed according to ASTM E8, Federal Test Method 151 and MAB-205M recommended te procedure for beryllium.

10.4 **Radiographic Inspection:** Radiographic inspection will be performed in accordance with MIL-STD-453 (Quality Lev 2-2T).

10.5 **Penetrant Inspection:** Liquid penetrant inspection will be performed in accordance with MIL-I-6866, Type 1, Group Personnel performing this inspection will be certified in accordance with MIL-STD-410.

10.6 **Grain Size:** The average grain size will be determined by the intercept method in accordance with ASTM E112, Meth 7b.

11. **GENERAL:**

11.1 A certificate of compliance with this specification will be provided. In addition, certified results will be reported of tes conducted in accordance with specific customer instructions.

11.2 Material will be appropriately packaged and labeled to comply with applicable government regulations and/or standa procedures of Kawecki Berylco Industries, Inc.

11.3 The International System of Units (SI) are given in accordance with recommendations of the ASTM Standard E370. conversion of U.S. units to SI, values have been rounded to an appropriate minimum number of significant digits. In tho instances where correspondence of values is not exact because of rounding, U.S. units will apply.

Figure 1.022b: Commercial specifications for Kawicki Berylco HP-21 structural grade beryllium block.

BERYLLIUM STRUCTURAL GRADE, HP-21
Effective October 1, 1975

6. **MATERIAL QUALITY:**

6.1 **Radiographic Inspection:** The material shall be radiographically inspected for conformance to Type 1 or Type 2 quality with regard to radiographic indications (voids and/or inclusions).

Definition of Type 1 and Type 2 Quality:

Maximum Dimension of Radiographic Indications: The largest dimension of an indication measured in the plane of the radiograph shall not exceed 0.030 inch (0.76 millimeter).

Maximum Average Dimension of Radiographic Indications: The arithmetic average of the maximum and the minimum dimensions of an indication measured in the plane of a radiograph shall not exceed 0.020 inch (0.51 millimeter).

Total Combined Volume of Radiographic Indications: In any one cubic inch (1.64 x 10^{1} cubic millimeter) of material, the total combined volume of all indications larger than 0.001 inch (0.025 millimeter) shall not exceed the volume of spheres of the following diameters:

Quality	Diameter of Sphere Inch (Millimeter)	Volume Cubic Inch x 10^{-6} (Cubic Millimeter)
Type 1	0.050 (1.27)	66 (1.07)
Type 2	0.032 (0.81)	17 (0.28)

The volume of the indications shall be calculated on the basis of an assumed sphere, the diameter of which is equal to the maximum average dimension of the indication.

6.2 **Penetrant Inspection:** The surface of the material in the machined or machined and etched condition shall be free of porosity or cracks as detected by liquid penetrant inspection.

7. **GRAIN SIZE:**

The material shall have an average grain size not exceeding 25 microns (25 micrometers).

8. **DIMENSIONAL TOLERANCES:**

Block, rod or bar shall be machined to the following standard tolerances:

Diameter or Thickness, Inches (Millimeters)	Tolerance, Inch (Millimeters)
Up to 3 (76), inclusive	-0 + 1/64 (0.4)
Over 3 (76) to 20 (508), inclusive	-0 + 1/16 (1.6)
Over 20 (508)	-0 + 1/4 (6.4)
Length, Inches (Millimeters)	
Up to 3 (76), inclusive	-0 + 1/64 (0.4)
Over 3 (76) to 20 (508), inclusive	-0 + 1/8 (3.2)
Over 20 (508)	-0 + 1/4 (6.4)

Dimensional tolerances on machined shapes shall be agreed upon.

9. **SURFACE FINISH:**

The surface finish of machined or machined and etched material shall be 125 microinches (3175 nanometer) rms or finer, unless otherwise agreed upon.

Figure 1.022b: Commercial specifications for Kawicki Berylco HP-21 structural grade beryllium block.

Material	Materion S200D	Materion S200E	Materion S200F	Materion S65
Date		-1987	1987+	1987
Form	block	block	block	block
Grain Size (μm)	block	≤25	≤20	≤20
Chemistry of Block			*see manufacturers' specifications for measurement details	
Be, minimum wt.%	98.0	98.0	98.0	99.0
BeO, maximum wt.%	2.0	2.0	1.5	1.0
Al, maximum wt.%	1.6	1.6	0.13	0.06
C, maximum wt.%	1.5	1.5	0.10	0.10
Fe, maximum wt.%	1.8	1.8	0.15	0.08
Mg, maximum wt.%	0.08	0.08	0.08	0.06
Si, maximum wt.%	0.08	0.08	0.06	0.06
other metallic, maximum wt%	0.04	0.04	0.04	0.04
Particle Characteristics				
Grind Method	attrition	attrition	impact	impact
Average Particle Diameter (before pressing) (μm)	27.0	13.4	11.4	
Maximum Particle Diameter (before pressing) (μm)	80	56	50	

Figure 1.031a: Chemistry and starting particulate characteristics for Materion Corporation beryllium.

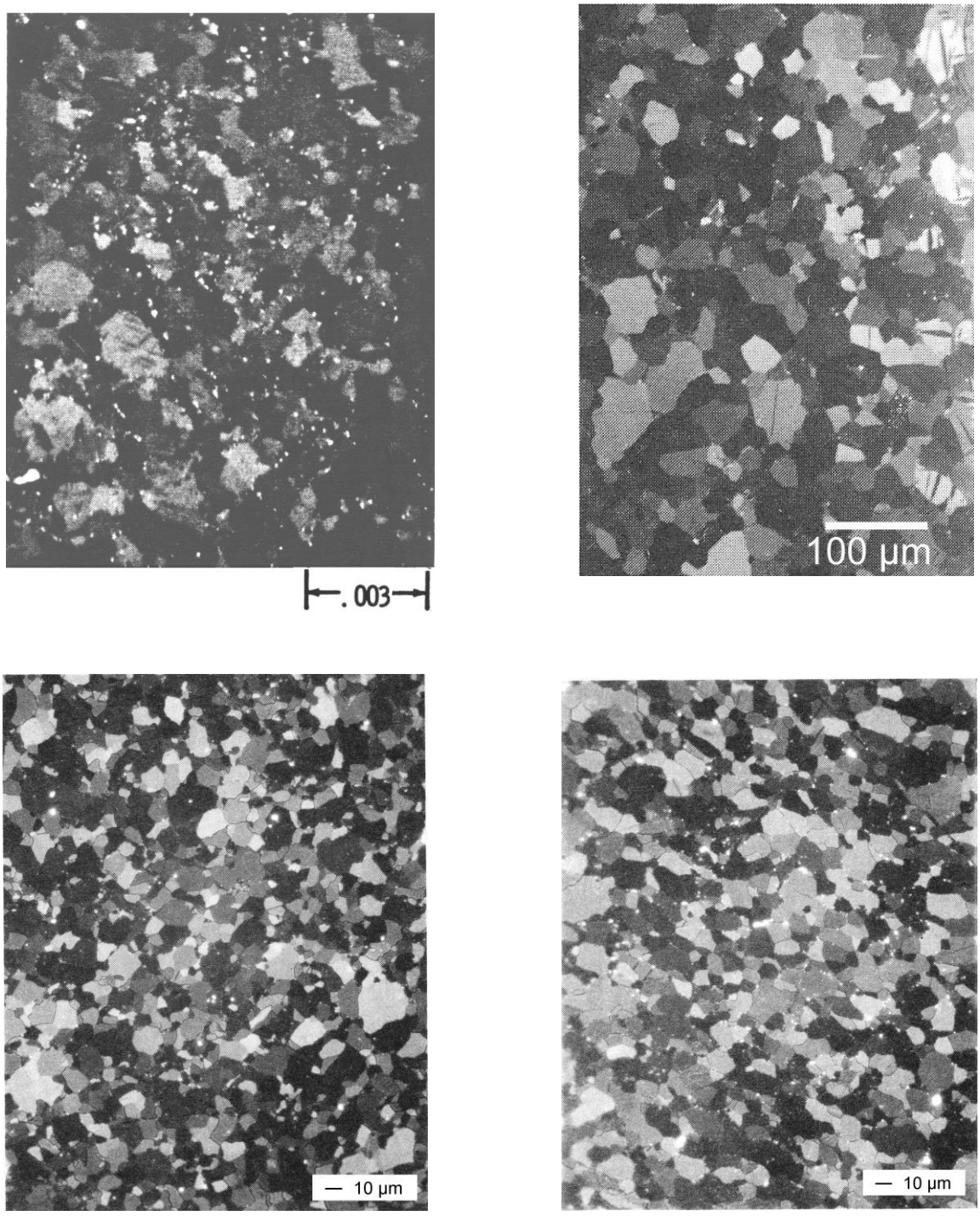

Figure 1.031b: Micrograph of Materion S200D (upper left) (1), Materion S200E (upper right) (2), Materion S200F (lower left) (3) and Materion S65 (lower right) (3).

Material	HIP-50	HP-21	HP-20	HP-10	HP-40	HP-8	CIP-HIP-1
Date	1977	1969	1968	1970	1968	1968	1974
Form	block	block	block	block	block	block	block
Grain Size (μm)	3.5-5		≤25 μm	≤25 μm	≤10 μm		≤15 μm
Chemistry of Block	*see manufacturers' specifications for measurement details						
Be, minimum wt.%	98.0	98.0	98.0	98.5	94.0	99.0	99.0
BeO, maximum wt.%	1.6	2.0	2.0	1.2	4.25 (min)	0.9	1.2
Al, maximum wt.%	0.0075	1.5	1.5	0.08	0.16	0.07	0.01
C, maximum wt.%	0.03	1.5	1.5	0.10	0.25	0.10	0.03
Fe, maximum wt.%	0.05	1.8	1.8	0.15	0.25	0.075	0.03
Mg, maximum wt.%	0.003	0.08	0.08	0.08	0.08	0.06	0.006
Si, maximum wt.%	0.0045	0.08	0.08	0.08	0.15	0.06	0.01
other metal, each wt%	≤0.001	0.04	0.04	0.04	0.10	≤0.02	≤0.02
Particle Characteristics							
Grind Method	electrolytic flake	impact	impact	impact			electrolytic flake/ impact

Figure 1.032: Chemistry and starting particulate characteristics for various Kawicki Berylco berylliums.

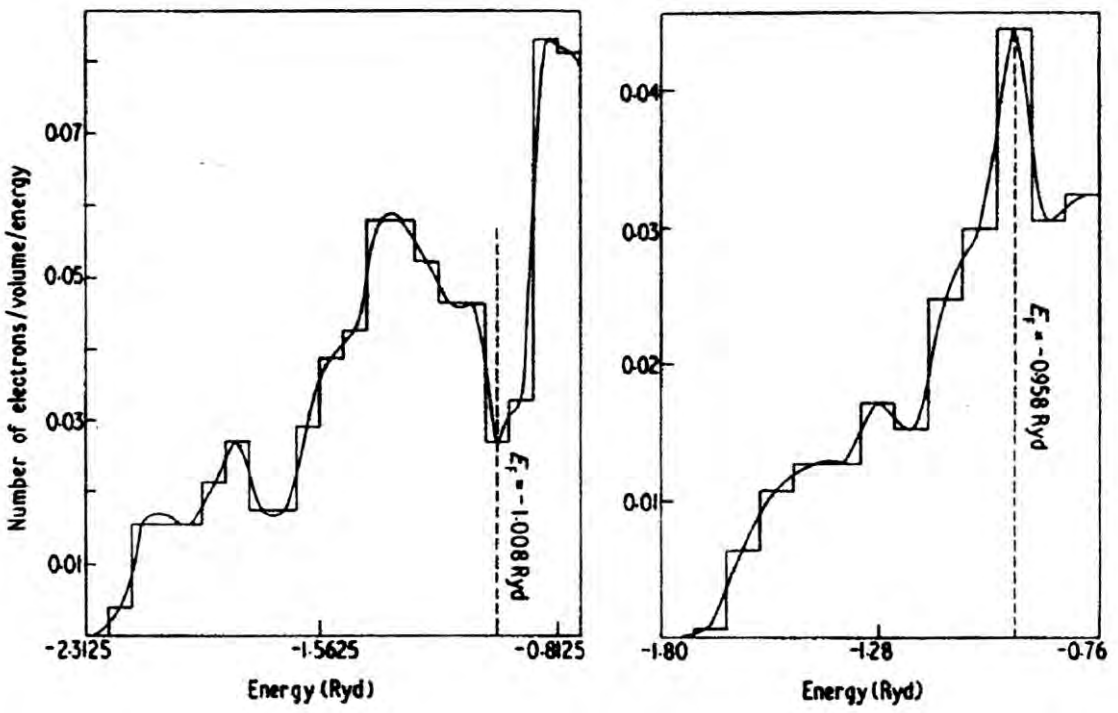

Figure 2.011: Density of states curves for beryllium and magnesium (8). E_F = Fermi energy.

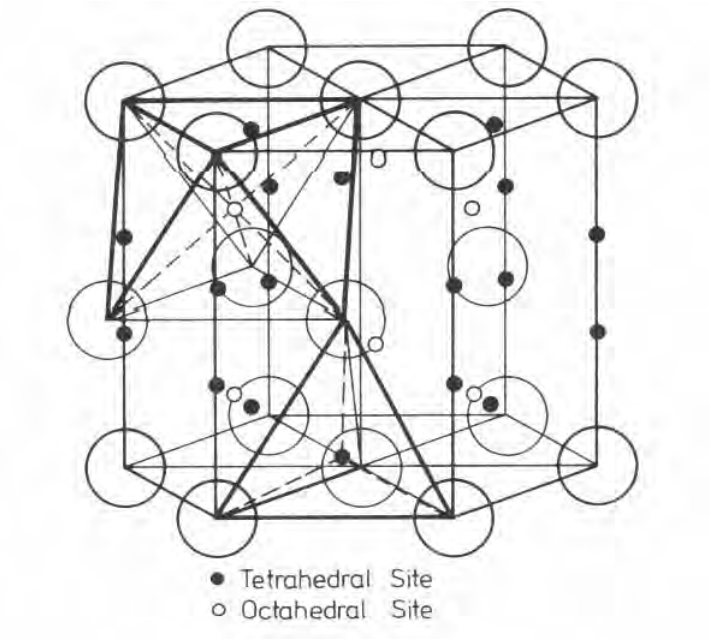

Figure 2.012a: Hexagonal crystal structure of Be (54).

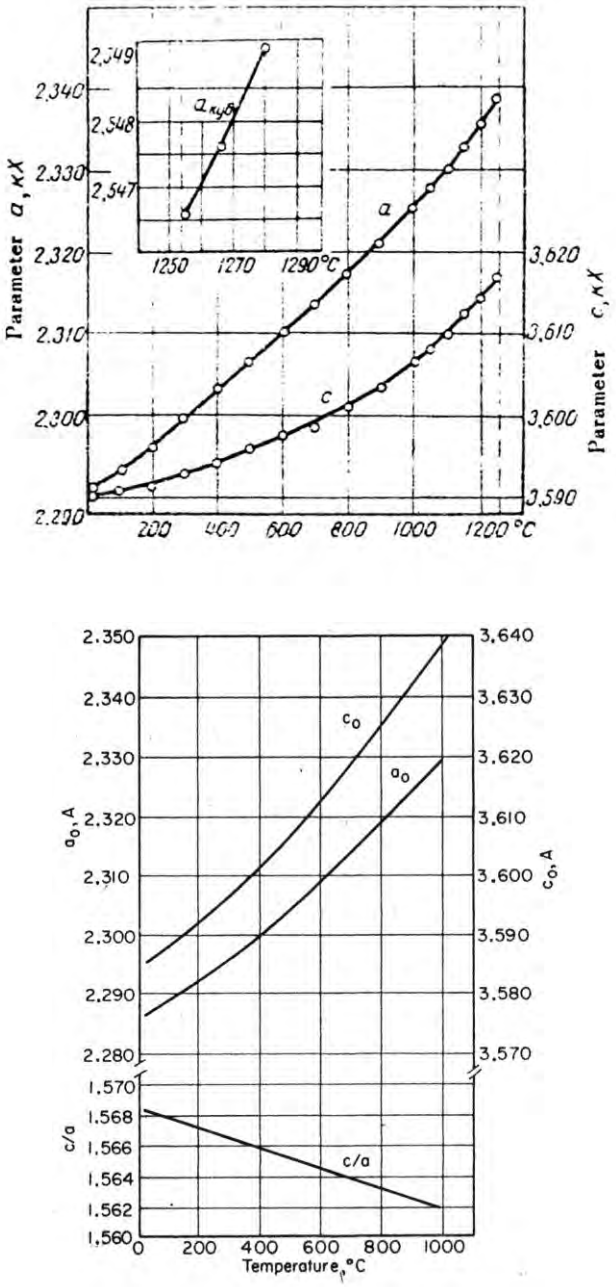

Figure 2.012b: Be lattice parameters as a function of temperature; upper figure (29), lower figure (11).

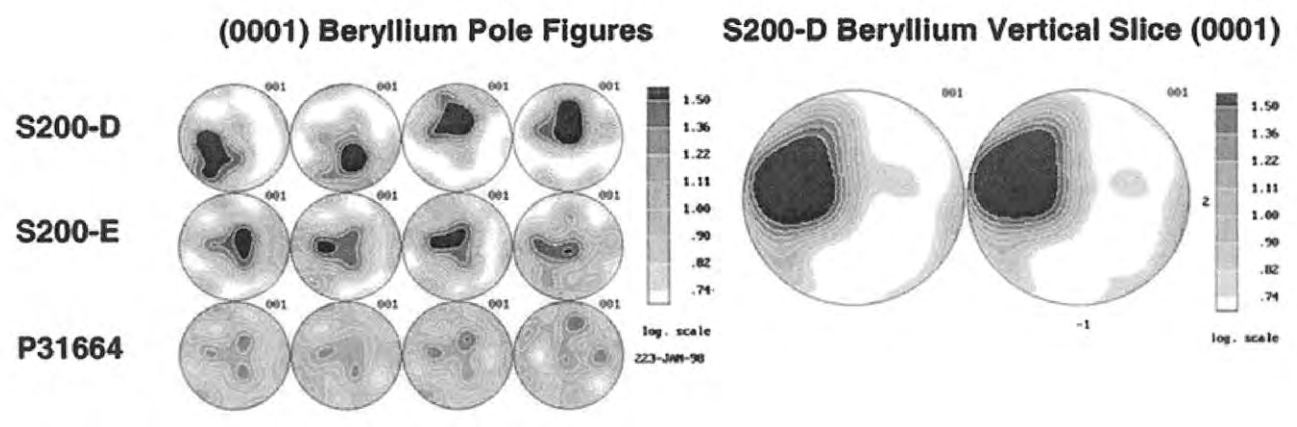

Figure 2.014a: (0001) texture neutron diffraction pole figures obtained on Materion vacuum hot pressed beryllium (15). Grades S200D and S200E were pressed from Braun-type attrited powders and showed strong (0001) textures. Grade P31664 was hot pressed from impact ground powder and exhibited a weaker and broader (0001) texture. Four different samples with the hot pressing (longitudinal) direction normal to the page (left), and two different samples with the transverse direction normal to the page.

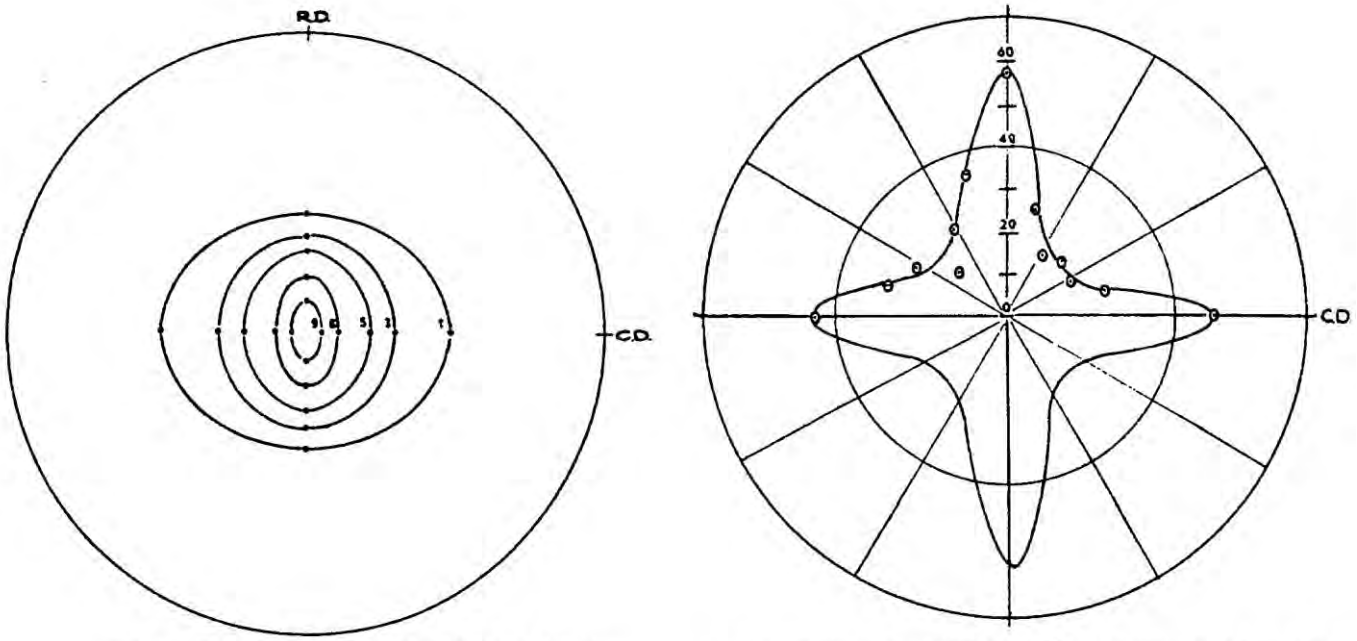

—(0002) pole figure for cross-rolled beryllium.

—Relative intensities of $(10\bar{1}0)$ reflections as a function of orientation for cross-rolled beryllium.

Figure 2.014b: Crystallographic textures produced by the hot rolling of beryllium (16). R.D. = rolled direction, C.D. = cross direction.

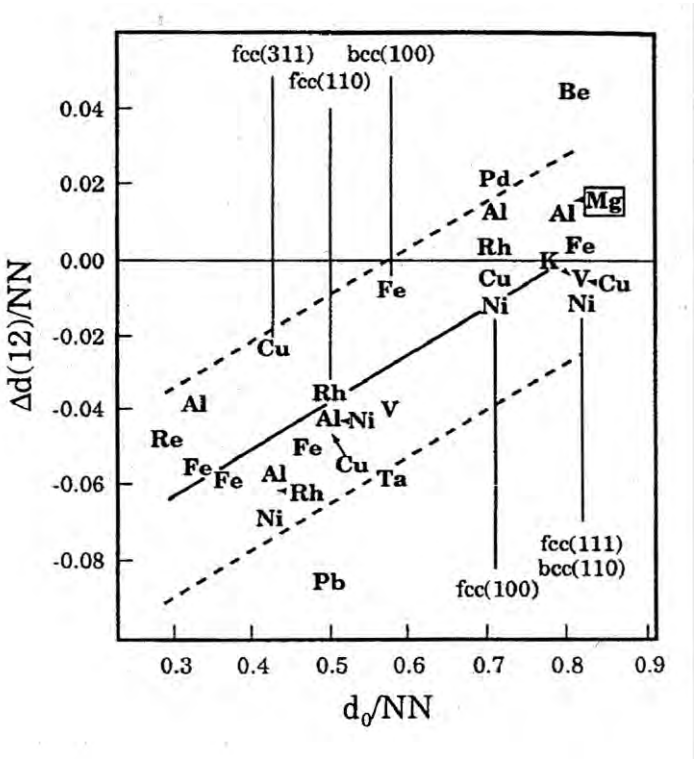

Figure 2.013: Anomalously high increase in the (0001) interplanar spacing at the surface of beryllium (13). Δd = change in interplanar spacing, d_0 = bulk interplanar spacing, NN = nearest neighbor.

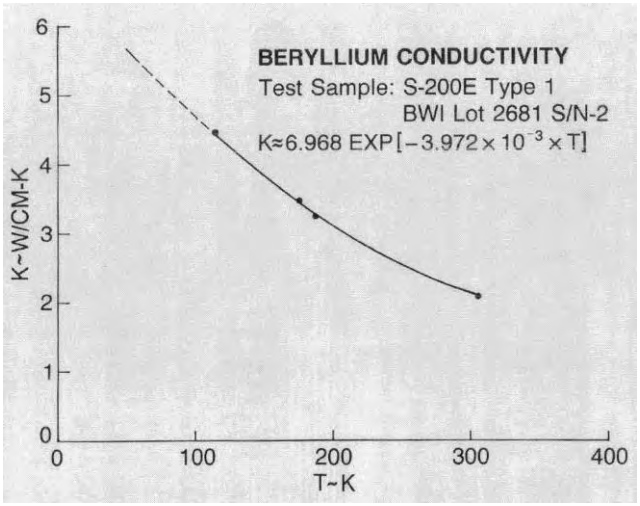

Figure 2.023a: Thermal conductivity of Materion 200E Be as a function of temperature (21).

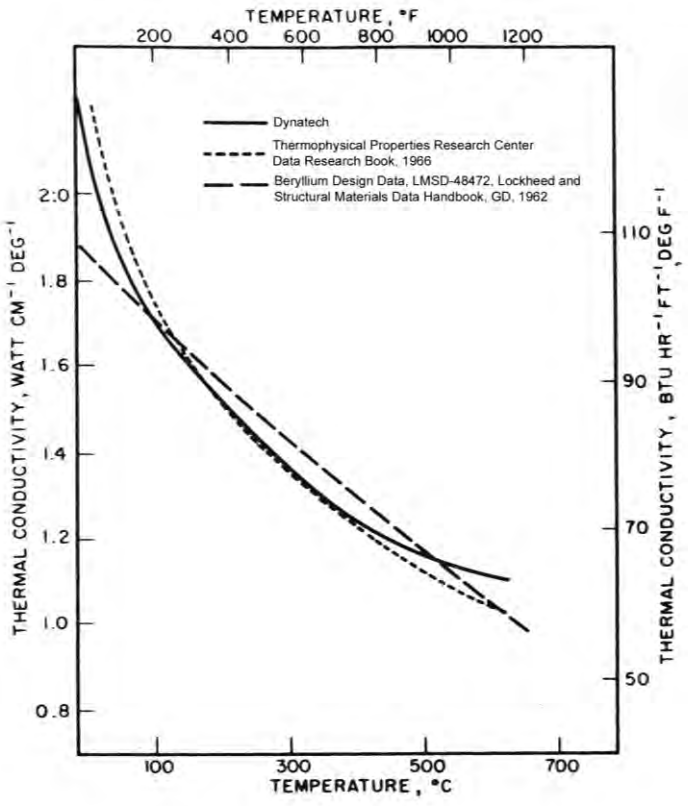

Sample Number	Mean Temperature °C	Thermal Conductivity Watt cm^{-1} deg^{-1}	Mean Temperature °C
1	184	1.56	20*
	258	1.42	20
	323	1.33	168
	112	1.65	188
	248	1.42	258
	397	1.25	277
	483	1.2	586
	592	1.12	131
	322	1.33	110
			20
2	57	1.79	20*
	94	1.74	20
	141	1.60	94
	204	1.51	193
	341	1.30	209
	368	1.25	341
	520	1.19	368
	611	1.11	597
	247	1.44	535
			443
			390
			297
			20
3	24	1.94	21*
	159	1.57	20
	369	1.23	159.5
	288	1.40	289
	445	1.17	445
	534	1.11	534
	174	1.54	369
			174
5	30,5	1.87	21*
	130	1.57	20
	209	1.49	30.5
	485	1.13	355
	552	1.09	401
	580	1.07	482
	355	1.26	552

Figure 2.023b: Thermal conductivity of four Materion S200D Be samples (Dynatech), and other Be as a function of temperature (22).

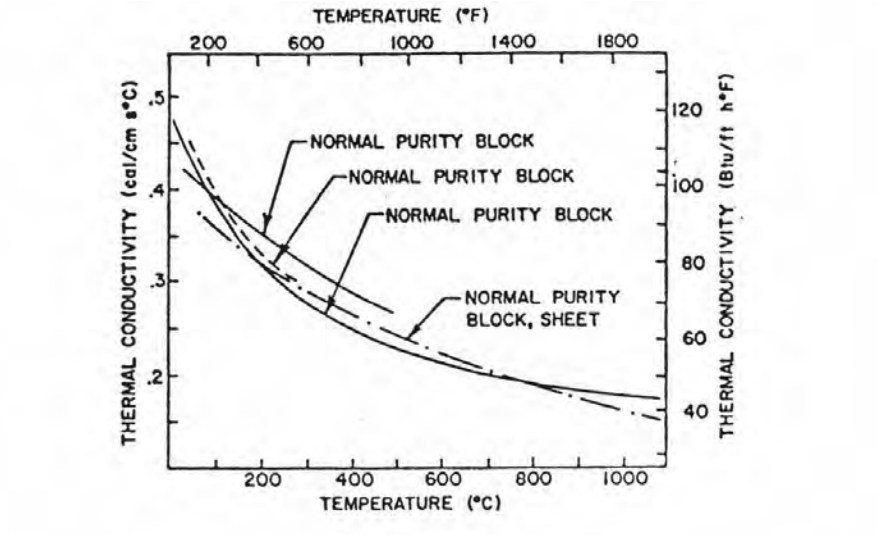

Figure 2.023c: Thermal conductivity of various grades of Be as a function of temperature (23,24,22,25).

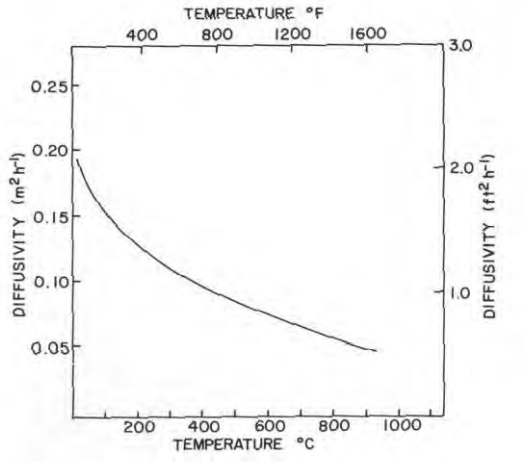

Figure 2.023d: Thermal diffusivity of Be as a function of temperature (26).

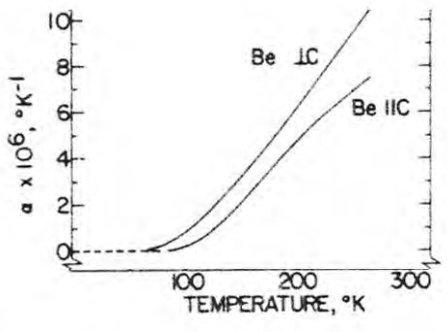

Figure 2.024a: Thermal expansion of single crystal Be as a function of temperature (28).

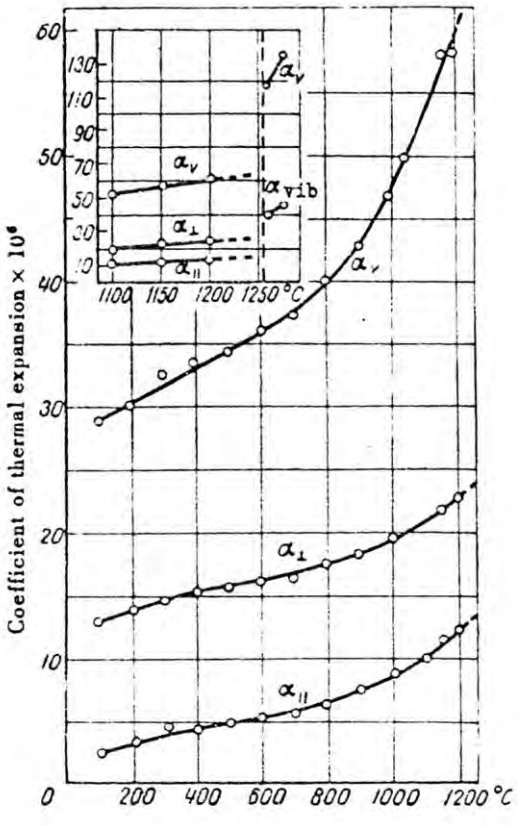

Figure 2.024b: Thermal expansion of α and β Be as a function of temperature (29). $\alpha_{//}$ = coefficient of linear expansion along the hexagonal axis; $\alpha_{\perp}$ = coefficient of linear expansion perpendicular to the hexagonal axis; a_{vib} = coefficient of linear expansion of β Be; a_v = coefficient of volume expansion.

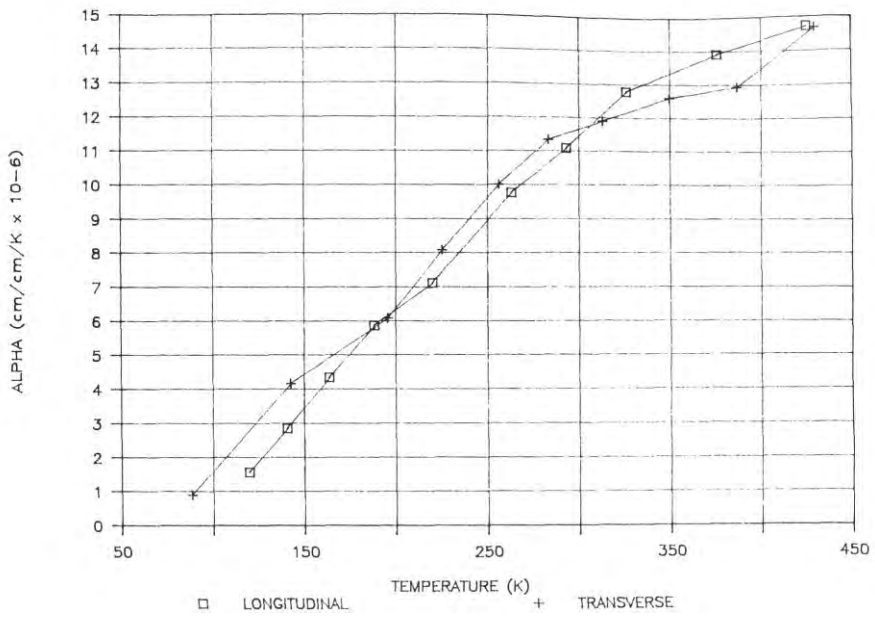

Average Temperature (K)	Coefficient Thermal Expansion (10^{-6} cm/cm/K)	Average Temperature (K)	Coefficient Thermal Expansion (10^{-6} cm/cm/K)	Comments
Longitudinal Orientation Specimen		Transverse Orientation Specimen AX-1401		
119.6	1.6	88.8	0.9	New data
140.6	2.9	103.8	3.5	Suspect data point
163.9	4.3	107.6	3.7	Suspect data point
188.4	5.9	113.1	3.3	Suspect data point
219.8	7.1	124.6	4.1	Suspect data point
263.0	7.8	142.9	4.6	Suspect data point
293.0	11.1	142.4 (167.9)	4.2 (4.1)	Recalculated(1)
326.1	12.8	195.8	6.1	
375.6	13.9	225.3	8.1	
425.1	14.7	256.1	10.0	
		283.3	11.3	
		312.9	11.9	
		349.8	12.6	
		386.8	12.9	
		429.6	14.7	

(1) Recalculated by eliminating the suspect data points. Original data are in parenthesis.

Figure 2.024c: Thermal expansion of Materion S200F Be as a function of temperature (27).

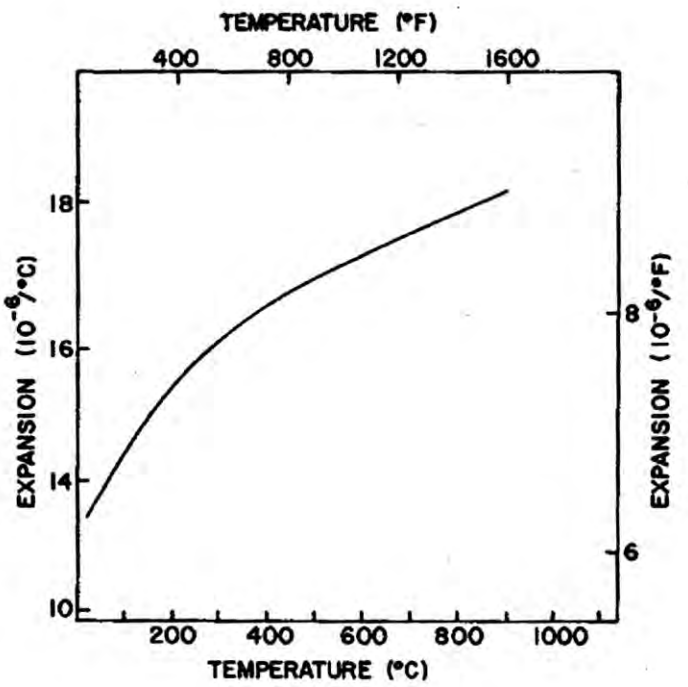

Figure 2.024d: Thermal expansion coefficient of Be block and sheet (65).

DENSITY (g/cm³), @ TEMPERATURE (°C)	VALUE
25	1.8477±0.0007
200	1.837
400	1.820
600	1.800
800	1.779
1000	1.756
DENSITY (g/cm³), @ 25°C and PRESSURE (kg/cm²)	**VALUE**
40,000	1.912
100,000	1.955

Figure 2.031: Theoretical density values for Be at various temperatures and pressures (31).

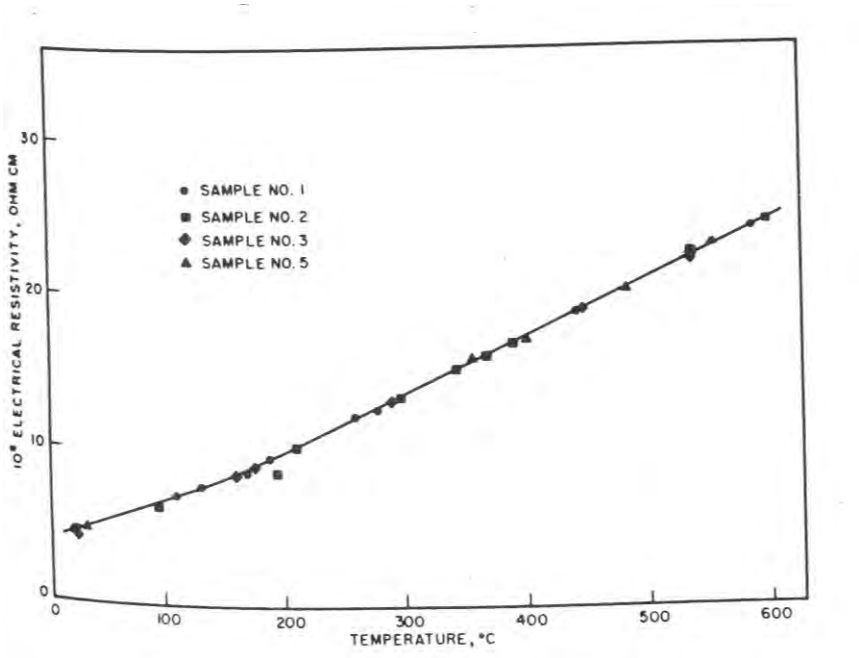

Figure 2.032a: Electrical resistivity of Materion S200D Be as a function of temperature (22).

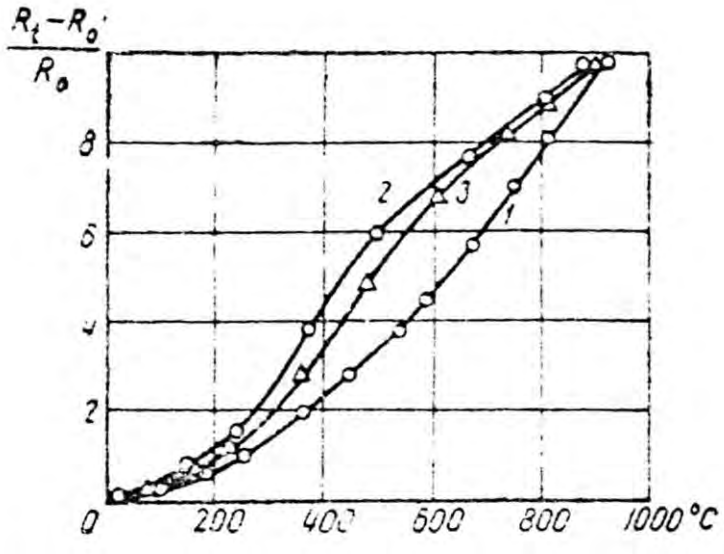

Figure 2.032b: Electrical resistivity of Be as a function of temperature (32). R_t = resistivity at temperature , R_0 = resistivity at room temperature, 1 = 99.97% purity, 2 = 98% purity, 3 = 99.97% purity after 10% deformation and annealing at 900°C for 1.5 hr.

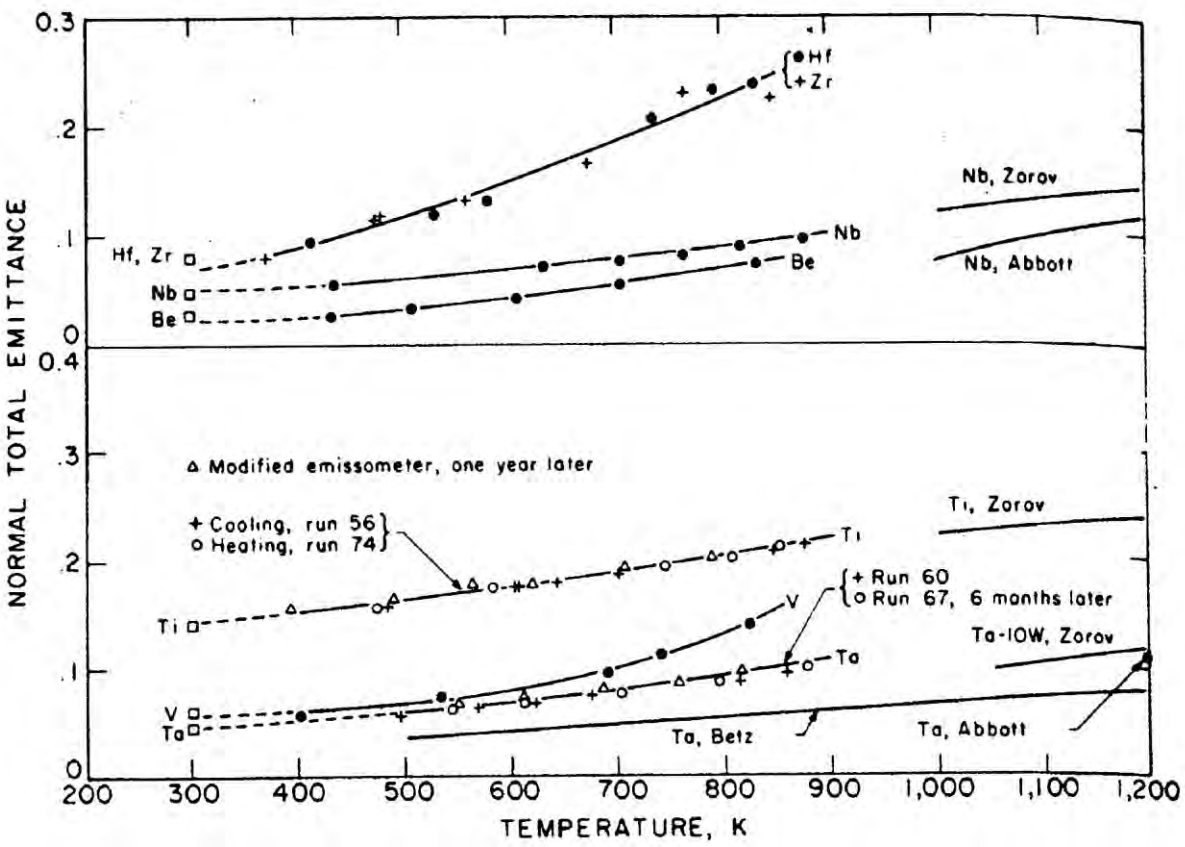

Figure 2.033a: Emittance of Be as a function of temperature (33).

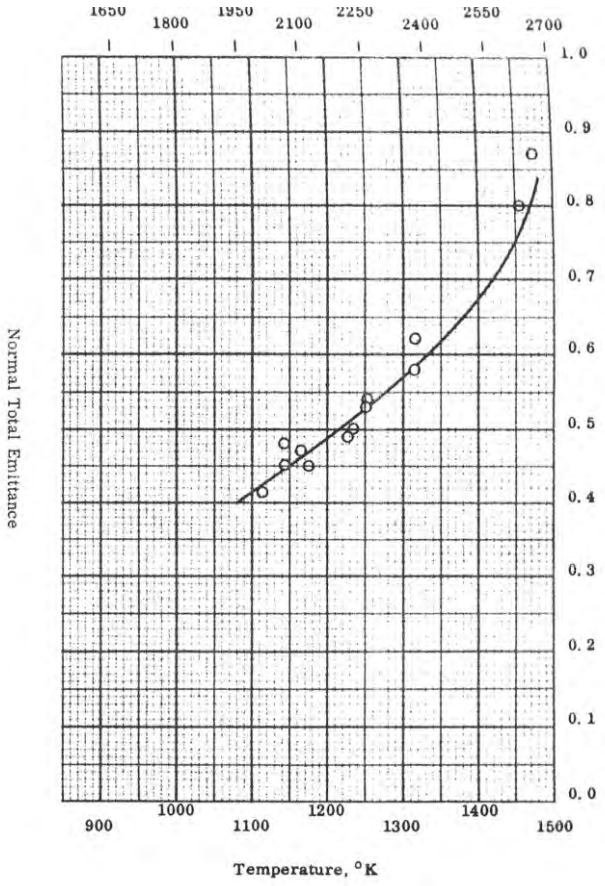

Figure 2.033b: Emittance of Be from 1116-1473 ºK (32).

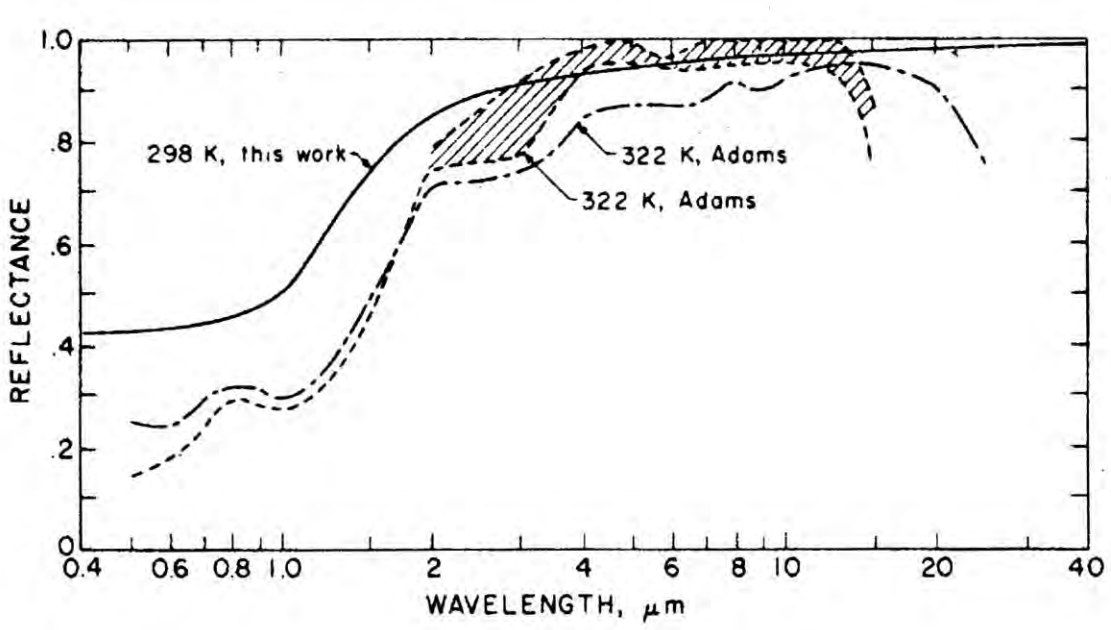

Figure 2.034: Normal spectral reflectance of Be as a function of wavelength (33).

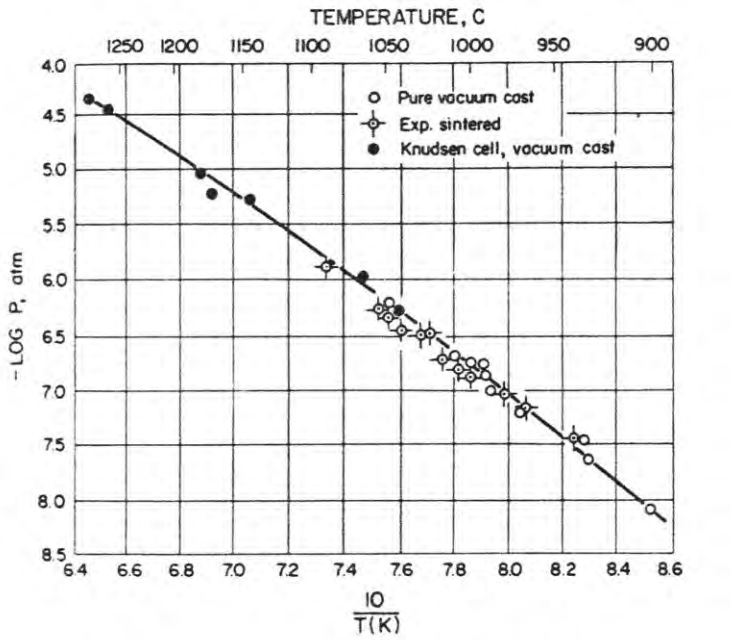

Figure 2.041: Vapor pressure of Be from 1172-1572 ºK (1).

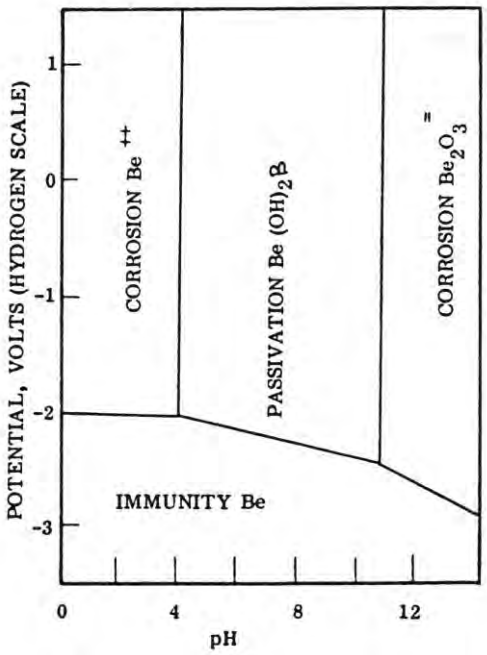

Figure 2.0421a: Pourbaix diagram for Be (37).

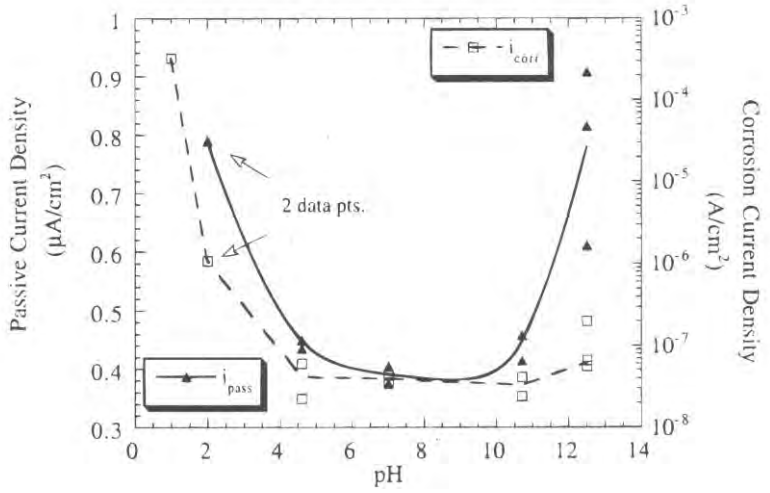

Figure 2.0421b: Passive and corrosion current density as a function of pH in aqueous solution pH for Materion S200D (38)

Source	(19)	
Alloy	Be	
Form	SR 200 Sheet	
Environment	Corrosion Rate (mils per year)(a)	Maximum Pit Depth (mils)
Distilled H_2O	0.8	0.8 (b)
Synthetic sea H_2O	13.7	4.6
Natural sea H_2O	18.4	4.6
3 percent NaCl Sol.	21.5	-
3.5 percent NaCl Sol.	33.4	6.8 (c)
(a) 30 days exposure (b) 18 days exposure (c) 8 days exposure		

Figure 2.0421c: Corrosion rates for Be in aqueous and aqueous salt solutions (40).

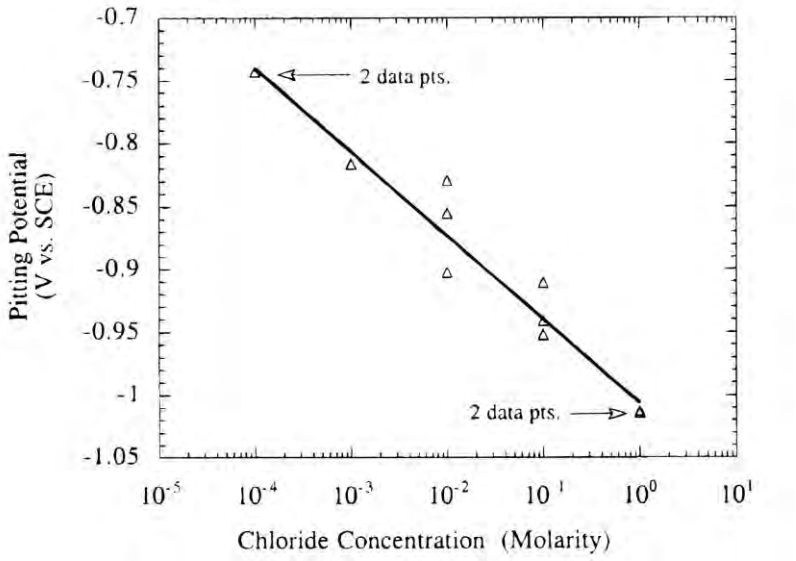

Figure 2.0421d: Pitting potential as a function of chloride concentration in aqueous salt solutions for Materion S200D (38).

Methyl alcohol and water (distilled)	Immediate chemical reaction
Methyl alcohol and Freon	Strong chemical reaction
Methyl alcohol and perchlorethylene	Chemical reaction
Methyl ethyl ketone and Freon	Chemical reaction in 3 minutes
Methyl ethyl ketone and water (distilled)	Reaction starts immediately
Perchlorethylene	No reaction
Freon (TF)	No reaction
Varsol	No reaction
Methyl alcohol	No reaction
Ethyl alcohol	No reaction
Acetone	No reaction
Water (distilled)	No reaction
Perchlorethylene and water (distilled)	No reaction
Freon and water (distilled)	No reaction
Acetone and water (distilled)	No reaction
Varsol and Freon	No reaction
Varsol and acetone	No reaction
Varsol and perchlorethylene	No reaction
Varsol and methyl alcohol	No reaction
Varsol and water (distilled)	No reaction
Methyl ethyl ketone	No reaction
Methyl ethyl ketone and Varsol	No reaction
Methyl ethyl ketone and acetone	No reaction
Methyl ethyl ketone and methyl alcohol	No reaction
Oakite No. 61	No reaction
Oakite No. 61 and acetone	No reaction
Oakite No. 61 and water (distilled)	No reaction

Figure 2.0423: Reaction of Be in various organics (43).

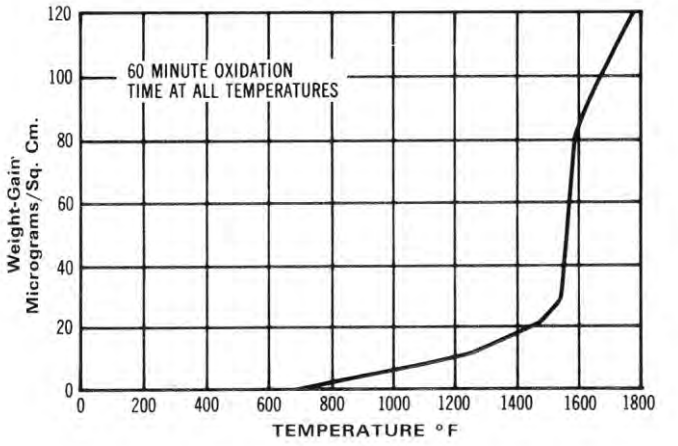

Figure 2.0425a: Reaction of Be in O_2 as a function of temperature (31).

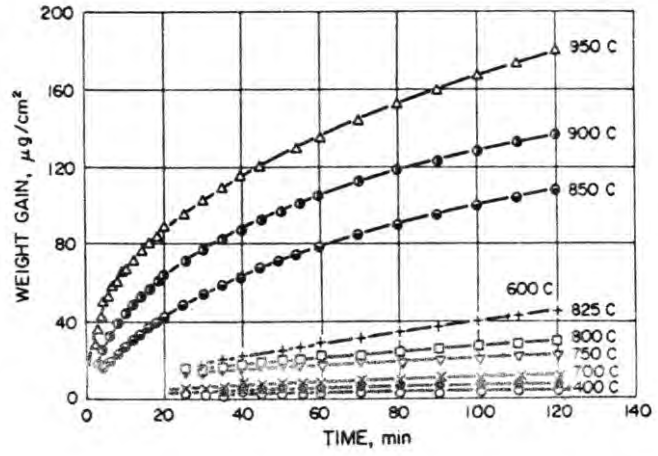

Figure 2.0425b: Reaction of Be in O_2 as a function of temperature and time (45).

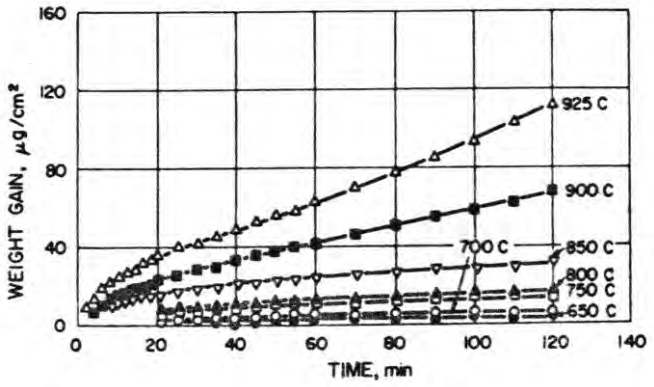

Figure 2.0425c: Reaction of Be in N_2 as a function of temperature and time (45).

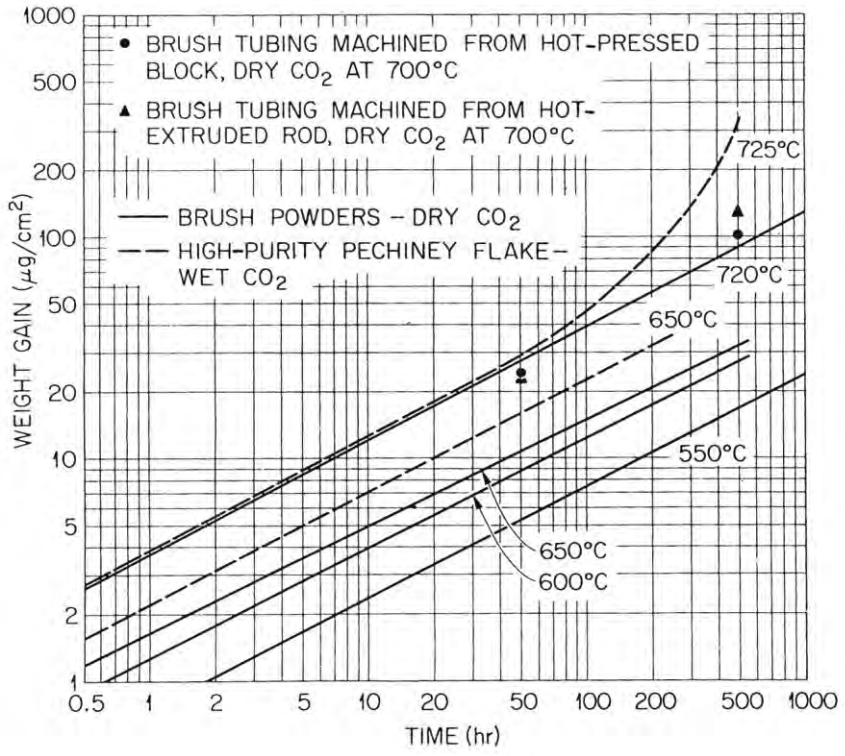

Figure 2.0425d: Reaction of Be in wet and dry CO_2 at elevated temperatures (46).

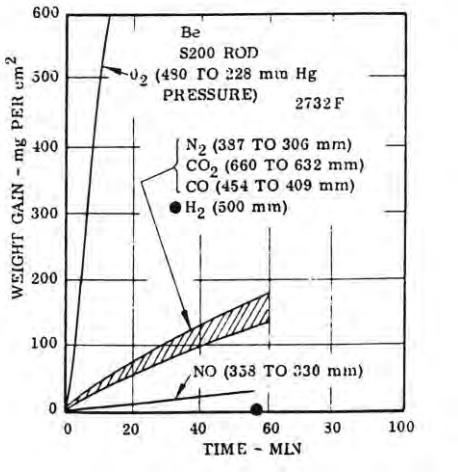

Figure 2.0425e: Reaction of Be in several gases at high temperature (40).

Material	Time, days	Reaction-Layer Thickness, μ 932 F	1112 F	1292 F
Beryllium-iron	7	None observed	10	48
	14	8	10	80
	28	12	30	228
	56	24	40	240
	112	24	80	312
Beryllium-nickel	7	64	44	256
	14	120	60	350
	28	206	84	802
	56	210	124	1120
	112	180	280	1260
Beryllium-stainless steel	7	None observed	12	70
	14	14	35	90
	28	21	50	140
	56	30	66	184
	112	56	92	288
Beryllium-uranium	14	--	5	12
	28	4	10	--
	56	2	10	32
	112	4	14	40
	224	--	--	60
	254	--	20	--
		1112 F	1292 F	1472 F
Beryllium-UO_2[a]	14	None observed	4	20
	28	2	8	20
	56	2	10	80
	112	None observed	80	90
	224	36	110	140

(a) Also 7 days, 1832 F; 160 μ

Other studies showed that beryllium does not react or reacts only slightly with Ta, W, Cr plate, Cb, Mo, Ti, or Zr-0.5Mo in vacuum or CO_2 atmospheres with <10-ppm water at 1022

Figure 2.0426a: Reaction of Be with various solids (47).

Material	Temperature, F	Time, days	Thickness of Reaction Product	Remarks
Aluminum	1112	8.5	No reaction	Compatible
Antimony	1292	5 hr	No reaction	Compatible
Carbon	932	18.5	No reaction	Compatible
	1112	8.5	No reaction	Compatible
Chromium	932	28	No reaction	Compatible
	1112	14	No reaction	Compatible
Copper	932	29	18μ	Incompatible
Iron	932	29	8μ	Incompatible
Magnesium	932	8.5	No reaction	Compatible
Nickel	932	31	40μ	Incompatible
	1112	30	170μ	Incompatible
Columbium	932	31	5μ (irregular)	Incompatible
Tantalum	932	31	8μ (irregular)	Incompatible
Titanium	932	31	No reaction	Compatible
	1112	30	3μ	Incompatible
Uranium	932	28	4μ (irregular)	Incompatible
with cast beryllium	1112	28	10μ	Incompatible
Uranium	932	28	No reaction	Compatible (?)
	932	56	Very occasional 2μ spots	Compatible (?)
	1112	14	5μ	Incompatible
	1112	56	6μ with 10μ spots	Incompatible
	1292	14	12μ	Incompatible
Uranium/UC Cermet 1	1112	14	3μ	Incompatible
0.251% carbon	1292	14	33μ	Incompatible
Uranium/UC Cermet 2	1112	14	6μ	Incompatible
0.5% carbon	1292	14	33μ	Incompatible
Uranium/UC Cermet 3 1.0% carbon	1292	14	16μ	Incompatible
UC Cermet 4	1112	14	3μ (irregular)	Incompatible
4.71% carbon	1292	14	43μ	Incompatible
Zirconium	932	31	30μ	Incompatible
Zircaloy	932	29	34μ	Incompatible

Figure 2.0426b: Reaction of Be with various solids (48).

Material	Temperature, F	Time, days	Thickness of Reaction Product	Remarks
Beryllium-iron (beryllium oxidized 2 hr in oxygen at 1472 F)	1112	14	6μ	Incompatible
	1292	14	10μ	Incompatible
Beryllium-18/8 stainless steel (beryllium oxidized as in beryllium-iron)	1112	14	12μ	Incompatible
	1292	14	70μ	Incompatible
Beryllium-nickel (beryllium oxidized as in beryllium-iron)	1112	14	24μ	Incompatible
	1292	14	130μ	Incompatible
Beryllium-uranium (beryllium oxidized as in beryllium-iron)	932	28	No reaction	Compatible
	1112	14	2μ	Incompatible
	1292	14	6μ	Incompatible
Beryllium-uranium (natural oxide film on beryllium)	1112	28	8μ	Incompatible
Beryllium-uranium (natural oxide film on uranium)	1112	28	8μ	Incompatible
Beryllium-uranium (uranium oxidized for 2-1/2 hr in wet argon)	1112	14	Occasional large spots 6 to 12μ thick	Incompatible
Beryllium-uranium (uranium oxidized for 1 hr at 1202 F in poor vacuum)	932	14	None	Compatible
	1112	14	Traces	Incompatible
	1292	14	14μ	
Beryllium (oxidized as in beryllium-iron and uranium)	1112	14	Occasional spot 2μ thick	Incompatible
(oxidized in wet argon)	1292	14	16μ	Incompatible
Beryllium-uranium (in presence of Aquadag layer)	1112	14	3 to 4μ	Incompatible
	1292	14	20 to 30μ	Incompatible

Figure 2.0426c: Reaction of Be with various solids (48).

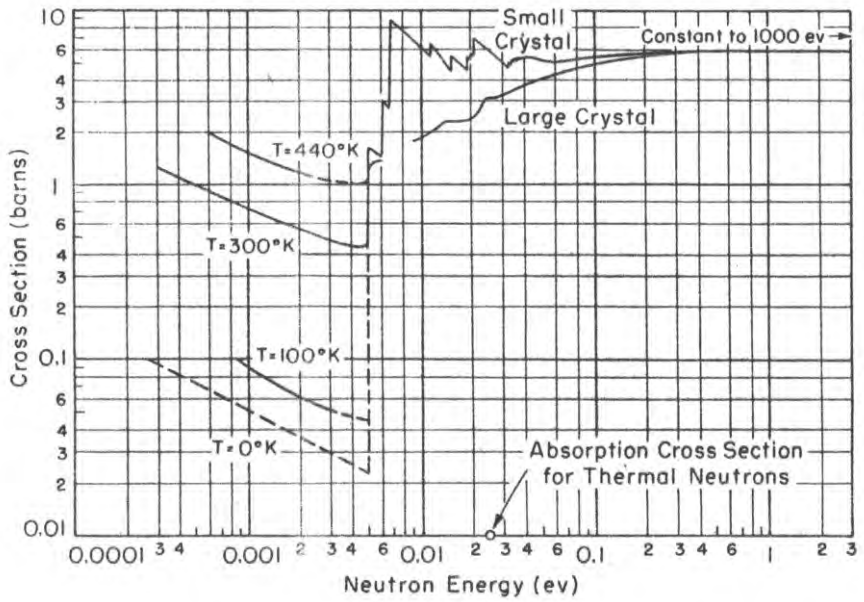

Figure 2.051a: Slow neutron cross sections for Be (10,49,50). The dashed data for the 0K temperature data represents theoretical data. Dashed portions of other curves represent interpolations.

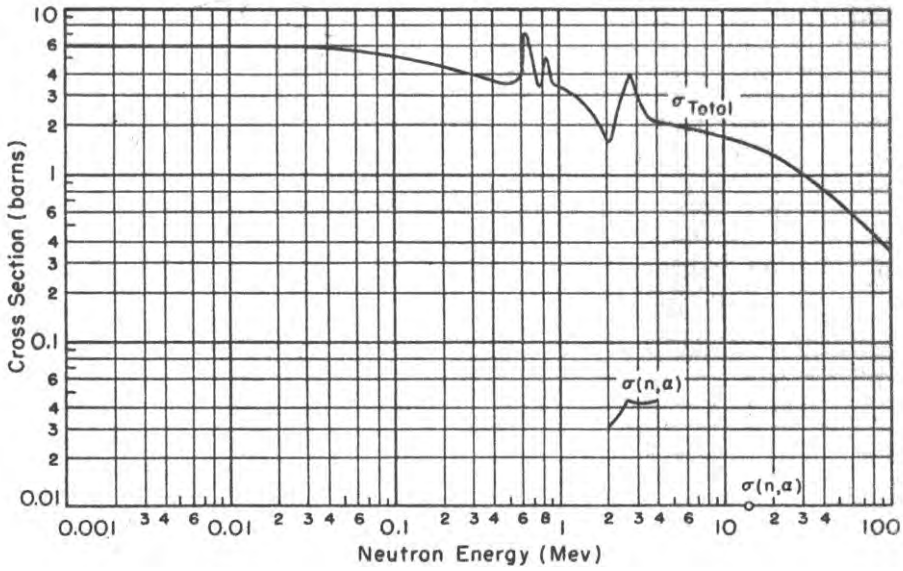

Figure 2.051b: Fast neutron cross sections for Be (31).

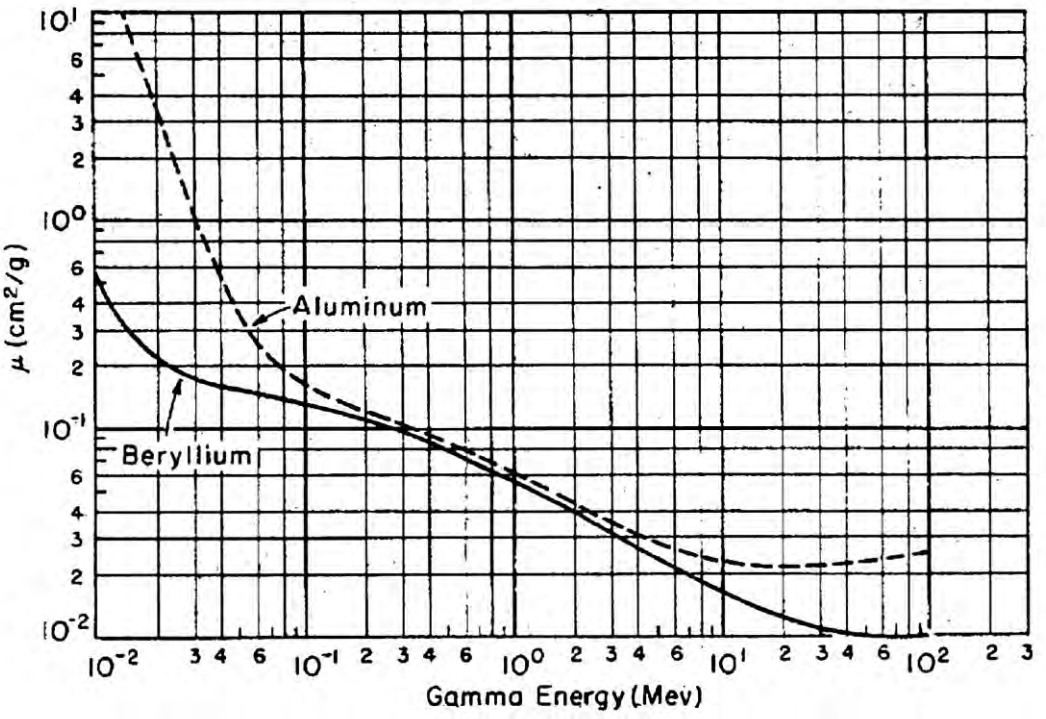

Figure 2.052: Gamma ray absorption coefficients for Be as a function of gamma ray energy (15).

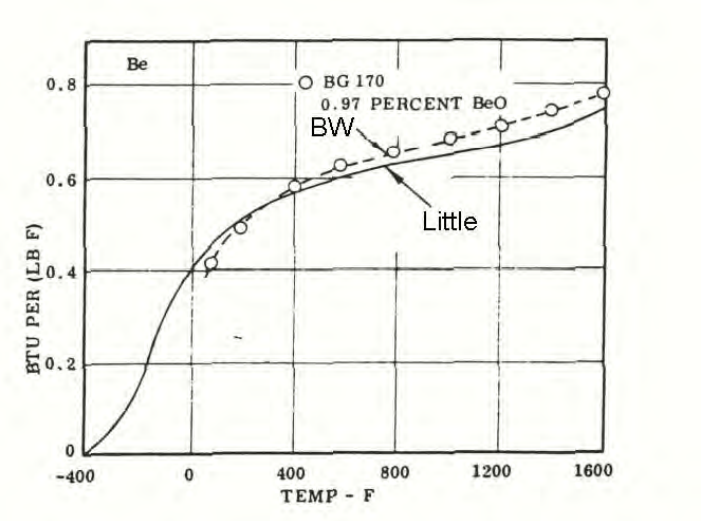

Figure 2.061a: Specific heat of Be (36,51).

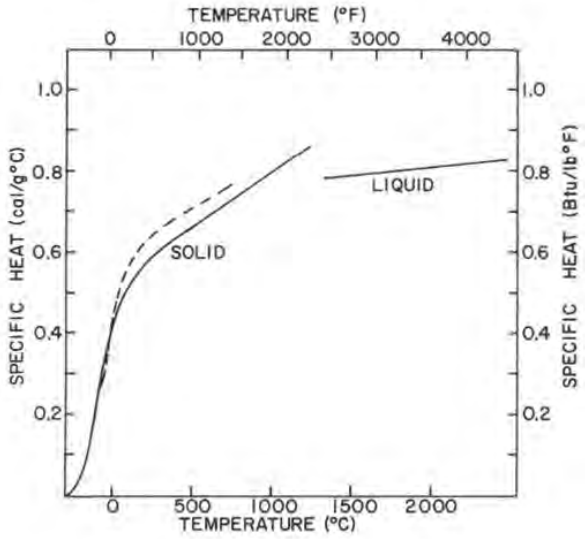

Figure 2.061b: Specific heat of Be (52,26).

.

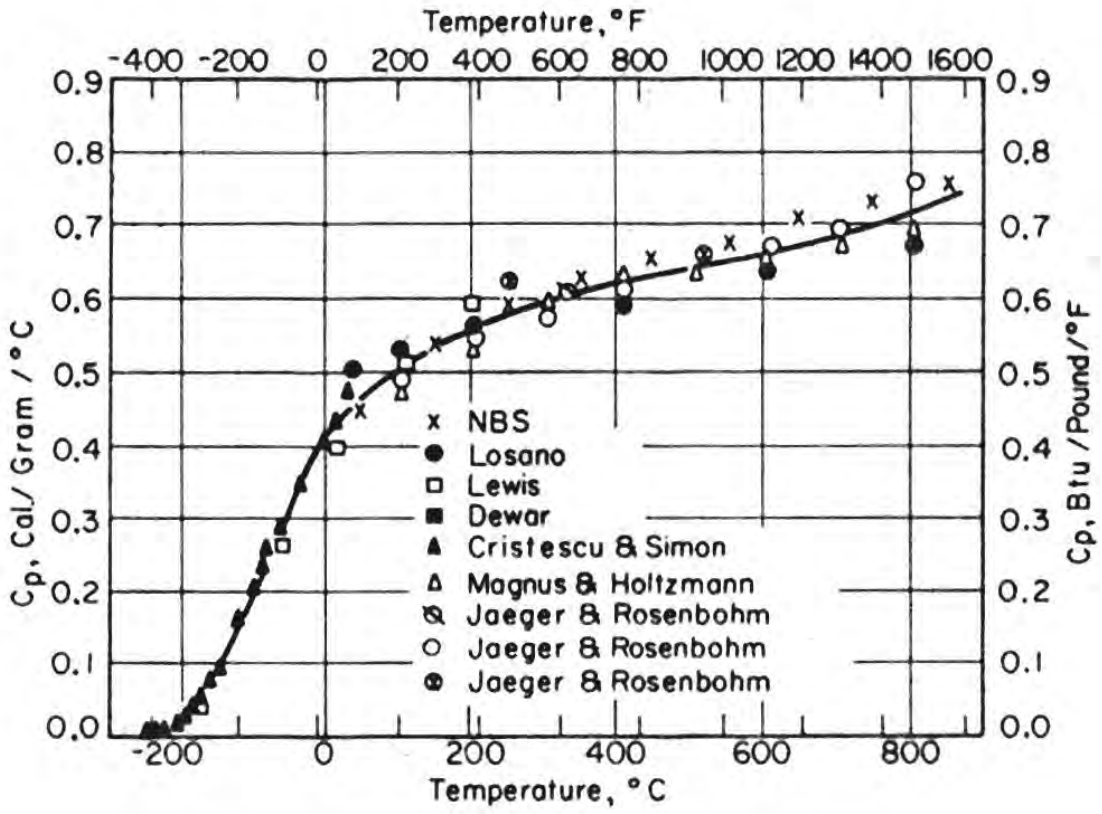

Figure 2.061c: Specific heat of Be (31).

Temp., °K	Heat capacity, C_p, cal/mole/°K		Enthalpy, $H_T - H_0$, cal/mole		Entropy, S_T cal/mole/°K		Free energy function $[(F_0-H_0)/T]$, cal/mole/°K	
	Condensed	Vapor	Condensed	Vapor	Condensed	Vapor	Condensed	Vapor
298.16	4.26	4.97	465	1481	2.28 ± 0.02	32.56 ± 0.01	0.72	27.60
400	4.56	—	880	—	3.48	—	1.28	—
500	4.85	4.97	1,365	2484	4.56	35.13	1.83	30.16
600	5.14	—	1,880	—	5.50	—	2.42	—
700	5.43	—	2,430	—	6.34	—	2.87	—
800	5.72	—	3,000	—	7.10	—	3.35	—
900	6.01	—	3,600	—	7.81	—	3.81	—
1000	6.30	4.97	4,210	4971	8.45	38.57	4.24	33.61
1100	6.59	—	4,830	—	9.04	—	4.65	34.08
1200	6.88	—	5,455	—	9.59	—	5.04	34.50
1300	7.17	—	6,080	—	10.09	—	5.41	34.90
1400	7.46	—	6,740	—	10.56	—	5.75	35.27
1500	7.75	4.97	7,465	7451	11.05	40.59	6.07	35.62
1588 (solid)	8.00	—	8,080	—	11.40	—	6.31	—
1588 (liquid)	5.27	—	11,415	—	12.87	—	6.31	—
2000	5.27	4.97	13,565	9931	13.98	42.02	7.20	37.05

Figure 2.062: Thermodynamic properties of Be as a function of temperature (31).
C_p = heat capacity at constant pressure
H_T = enthalpy at constant temperature
H_o = enthalpy at 1 atmosphere pressure
F_o = free energy at 1 atmosphere pressure
T = temperature

Bulk Modulus (10^{12} dyne cm^{-2})	Shear Modulus (10^{12} dyne cm^{-2})	Elastic Modulus (10^{12} dyne cm^{-2})	Poisson's Ratio
1.1158	1.5736	3.2112	0.020

Figure 3.0111a: Elastic properties of single crystal Be at room temperature (56).

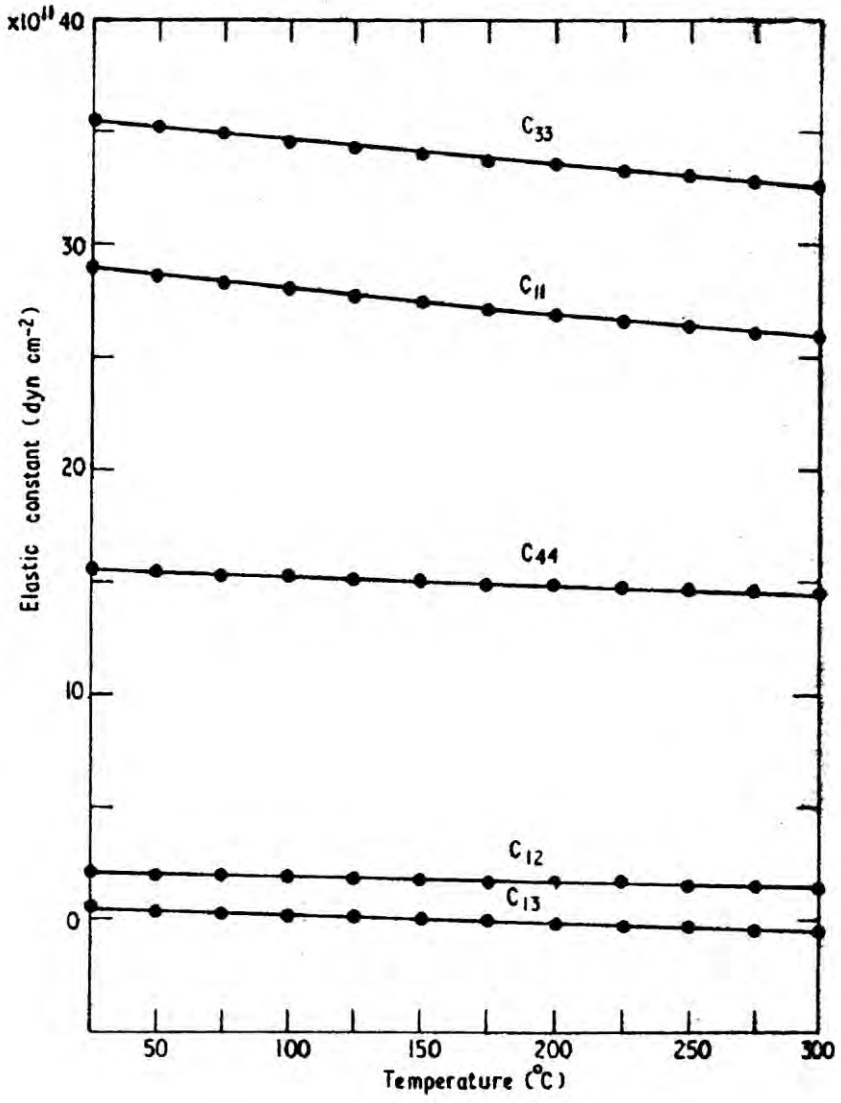

Figure 3.011b: Elastic properties of Materion S200F Be at room temperature (57).

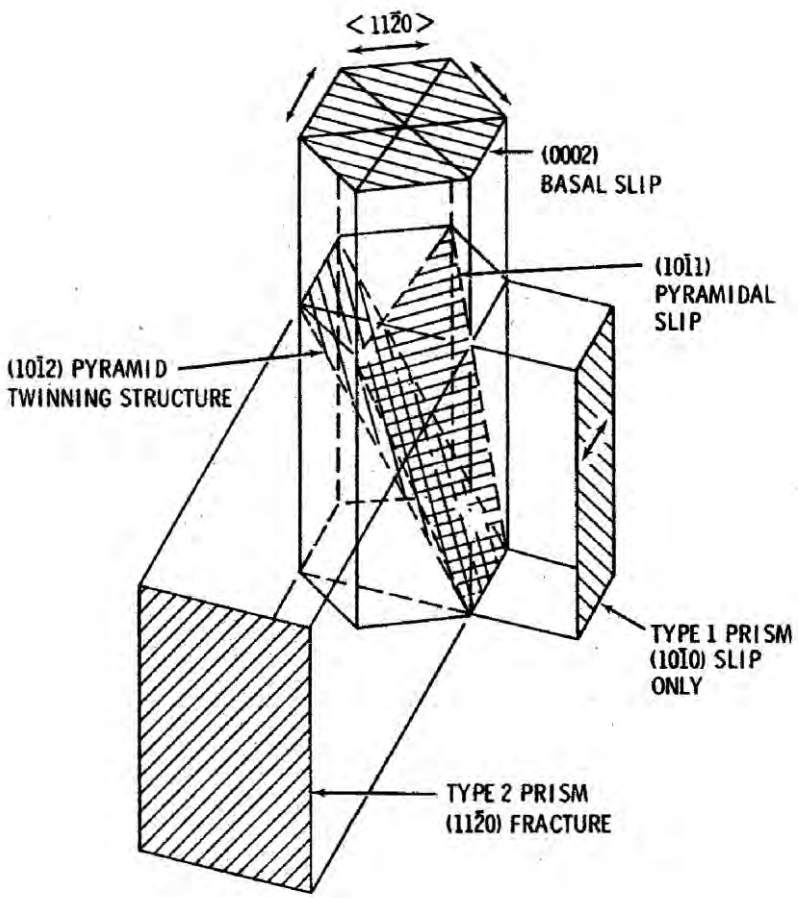

Figure 3.012a: Slip planes in Be (58).

Type	Indices	Number of independent slip systems
Basal	$\{0001\}\langle\bar{2}110\rangle$	2
Prismatic	$\{10\bar{1}0\}\langle\bar{2}110\rangle$	2
Pyramidal	$\{10\bar{1}1\}\langle\bar{2}110\rangle$	4
$(c + a)$	$\{11\bar{2}2\}\langle\bar{1}\bar{1}23\rangle$	5

Figure 3.012b: Slip systems in Be (58).

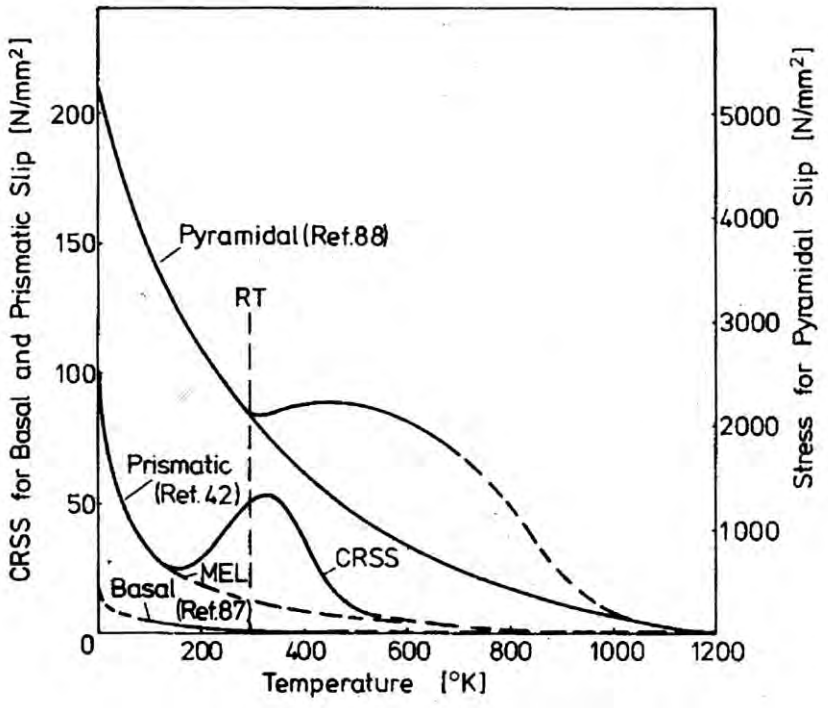

Figure 3.012c: Critical resolved shear stress for plane slip as a function of temperature (56).

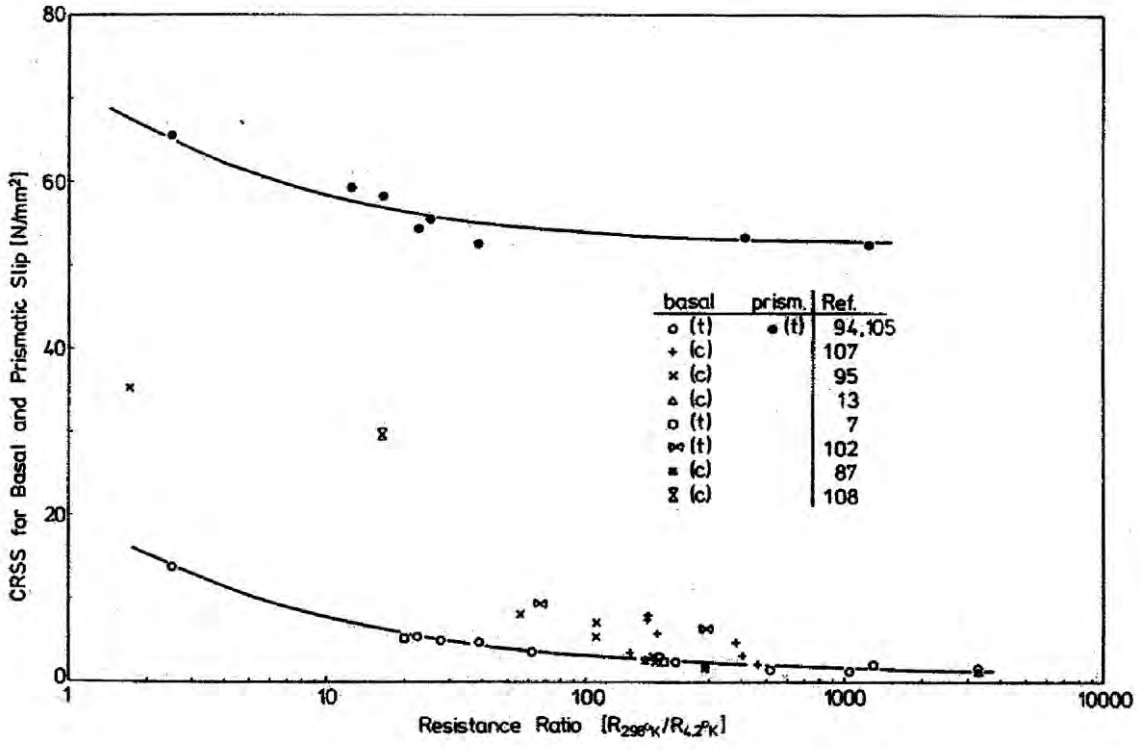

Figure 3.012d: Effects of purity on the critical resolved shear stresses for basal and prismatic slip in Be (56). The purity is demonstrated by the electrical resistance ratio.

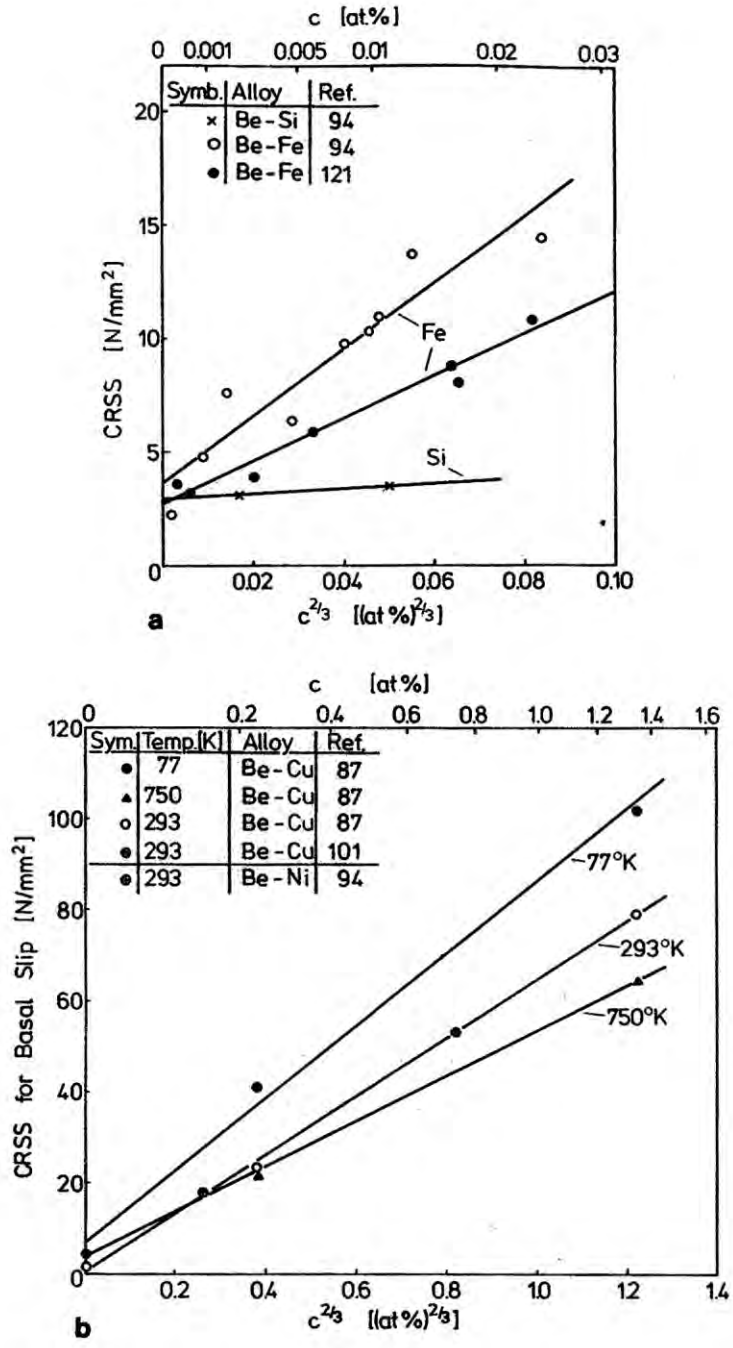

Figure 3.012e: Effect of solid solution alloying on the critical resolved shear stress of basal slip in Be (56).

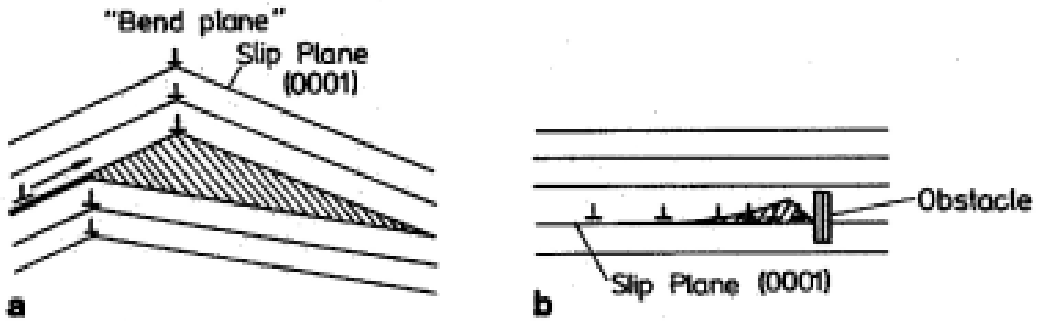

Figure 3.013a: Nucleation of basal cleavage cracks in single crystal Be by (a) bend plane splitting and (b) dislocation pileup (56).

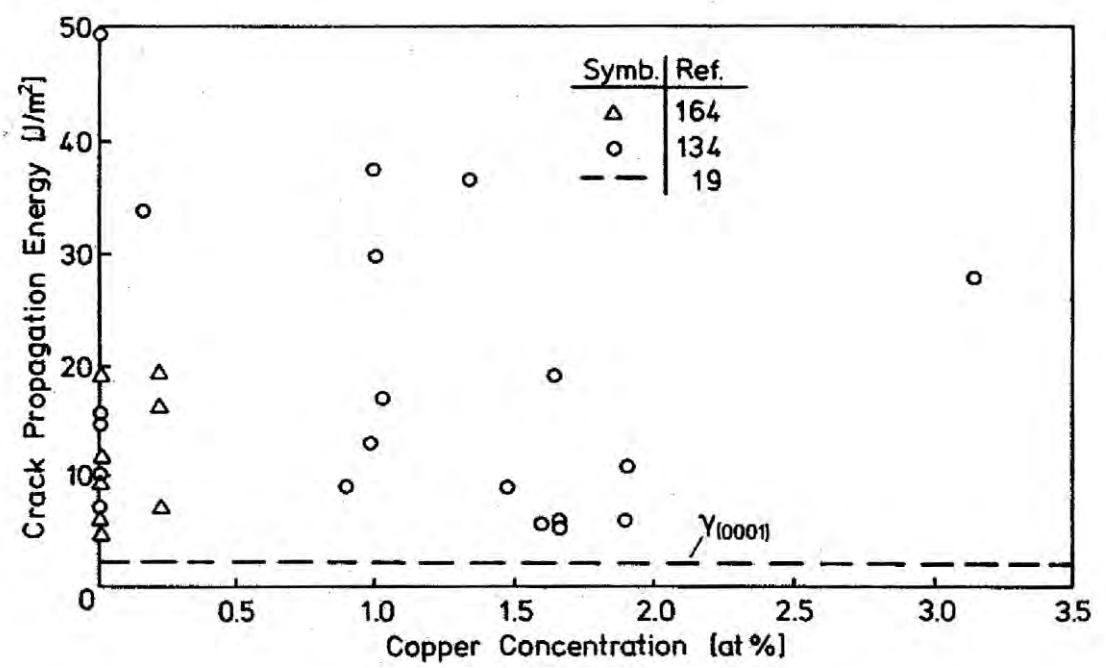

Figure 3.013b: Effect of alloying with copper on the basal plane crack propagation energy of single crystal Be (60).

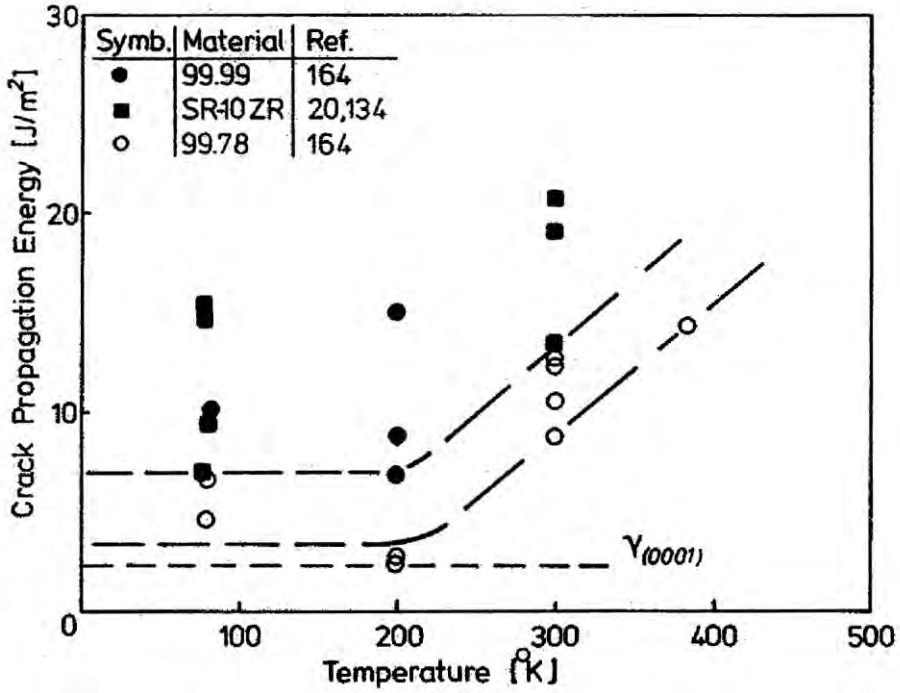

Figure 3.013c: Basal plane cleavage energy of single crystal Be as a function of temperature (61).

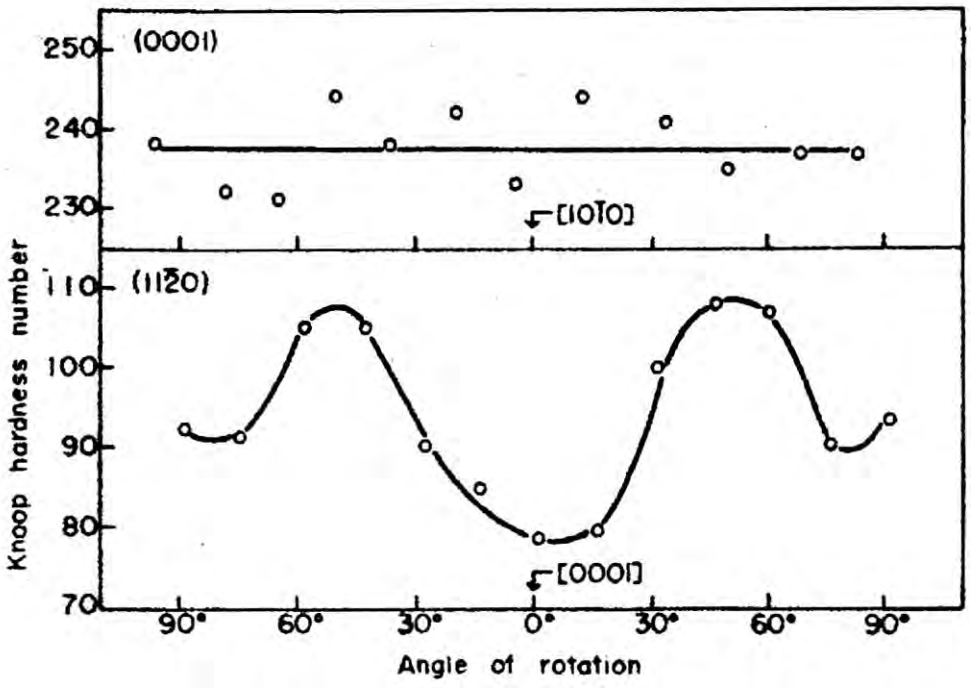

Figure 3.014a: Variation of Knoop hardness with indenter orientation (62).

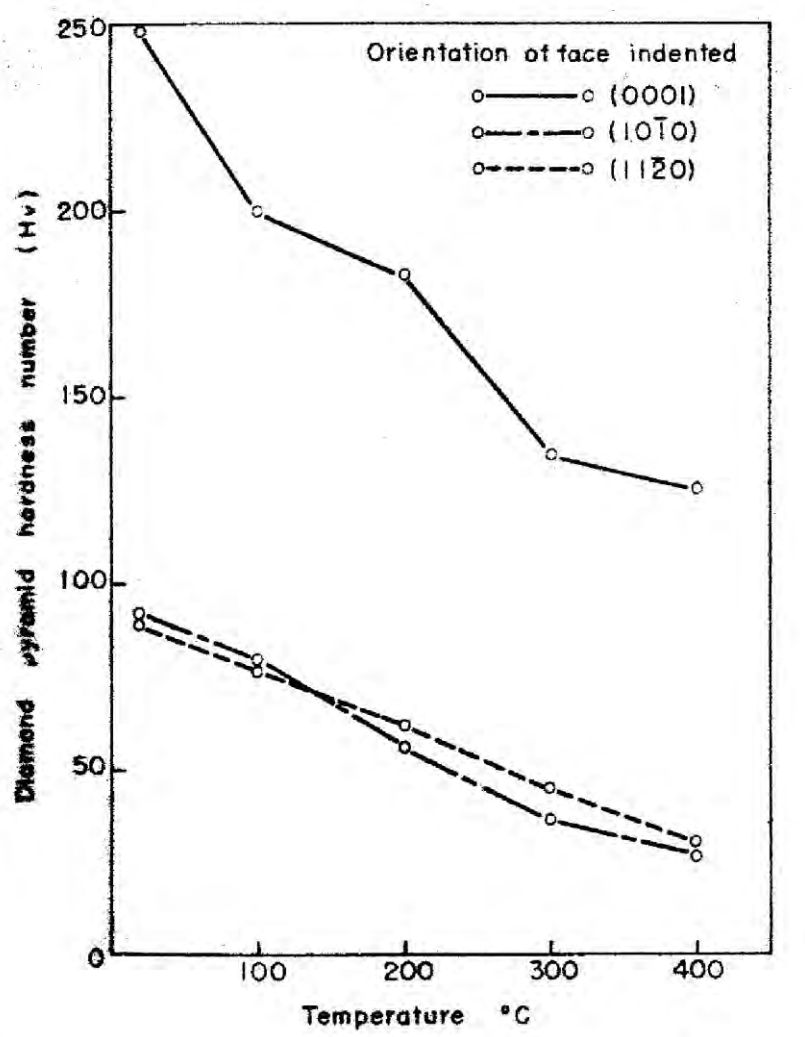

Figure 3.0114b: Hardness as a function of temperature for Be single crystal (62).

DIRECTION	ELASTIC MODULUS (mpsi)	SHEAR MODULUS (mpsi)	SHEAR RUPTURE MODULUS (kpsi)	PRECISION ELASTIC LIMIT (kpsi)
longitudinal	45.1±1.0	19.5±0.7	43.1±1.9	4.7±0.4
transverse	44.9±0.7	19.4±0.4	44.8±1.2	5.0±0.3

Figure 3.021a: Elastic properties of Materion S200F Be at room temperature (30,64).

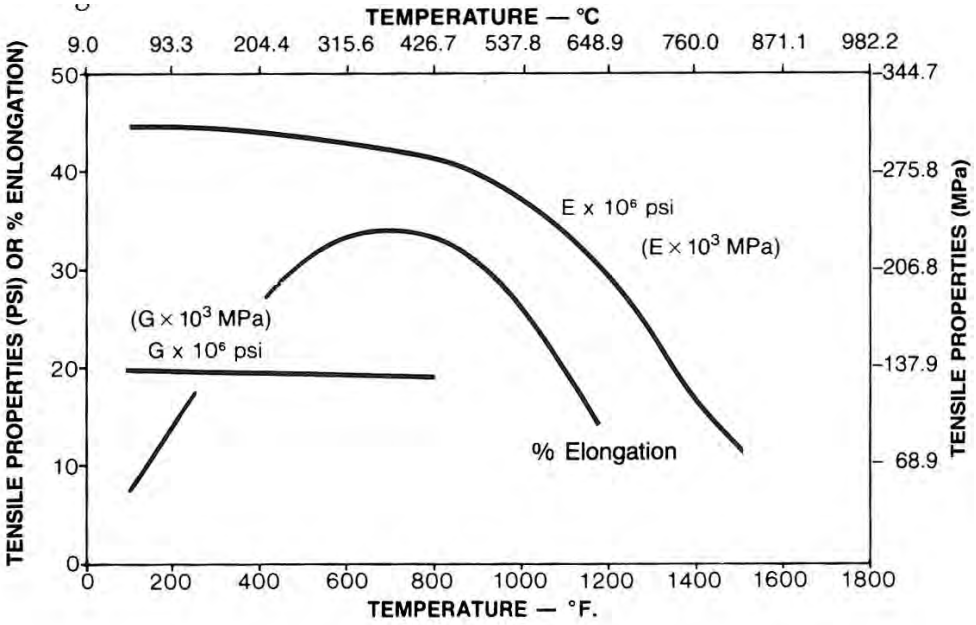

Figure 3.021b: Elastic modulus (E) and shear modulus (G) of Materion S200F with temperature (63).

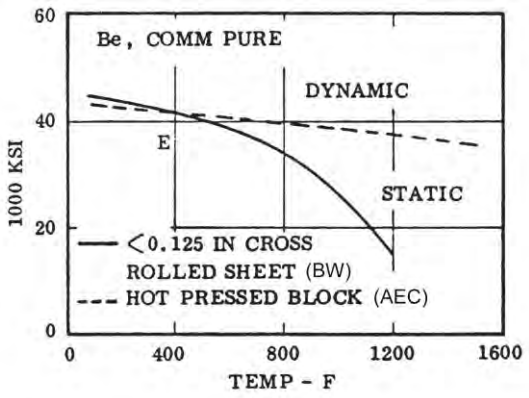

Figure 3.021c: Elastic modulus of Be in tension as a function of temperature (44).

Specimen ID	Orientation	Poisson's Ratio
B-102	LC	0.102
B-137	LC	0.064
H-319	LC	0.072
B-102	LR	0.102
B-137	LR	0.080
B-319	LR	0.105
AH-707	TL	0.069
N-403	TL	0.071
S-506	TL	0.108
AH-707	TR	0.102
N-403	TR	0.058
S-506	TR	0.066

Figure 3.021d: Room temperature Poisson's ratio for Materion S200F Be (64)
L = longitudinal stress axis of specimen, C = circumferential direction of orthogonal strain
L = longitudinal stress axis of specimen, R = radial direction of orthogonal strain
T = transverse stress axis of specimen, C = circumferential direction of orthogonal strain
T = longitudinal stress axis of specimen, R = radial direction of orthogonal strain

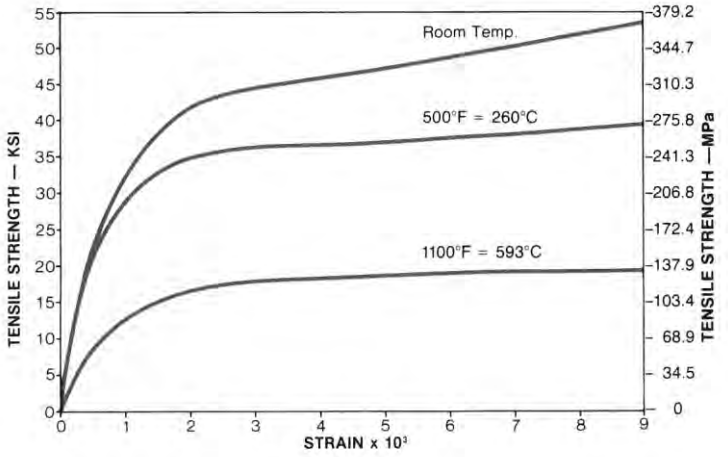

Figure 3.022a: Stress as a function of strain for Materion S200F (63).

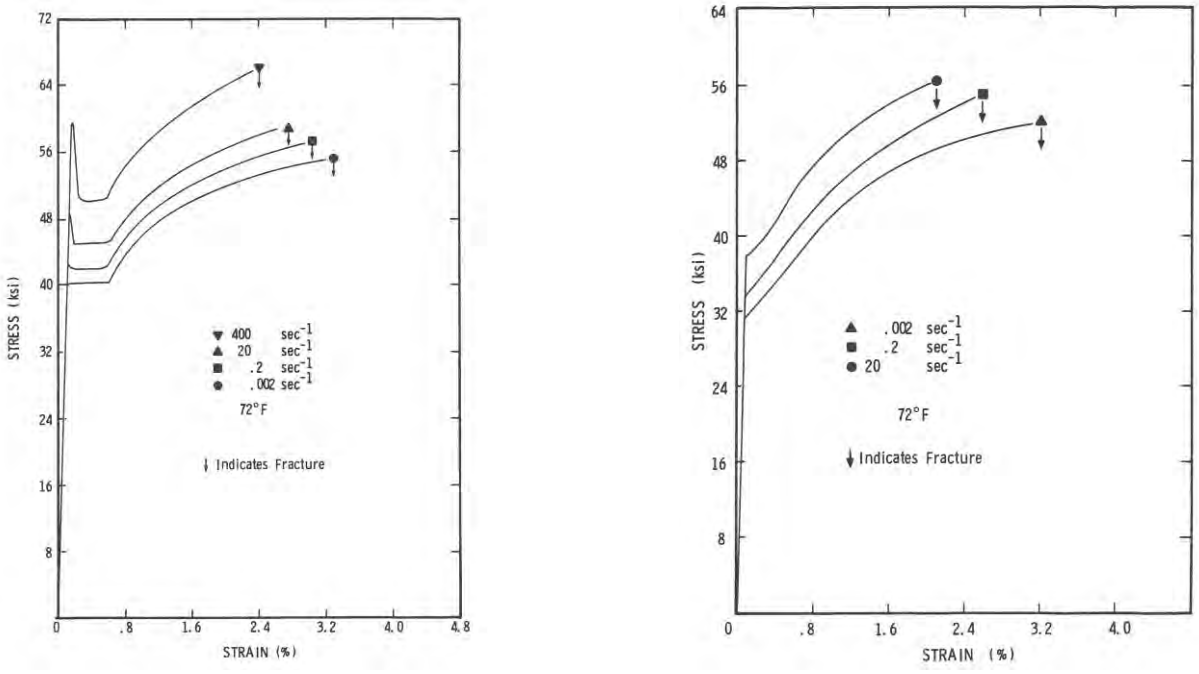

Figure 3.022b: Stress as a function of strain at various strain rates and room temperature for Materion S200E (1).

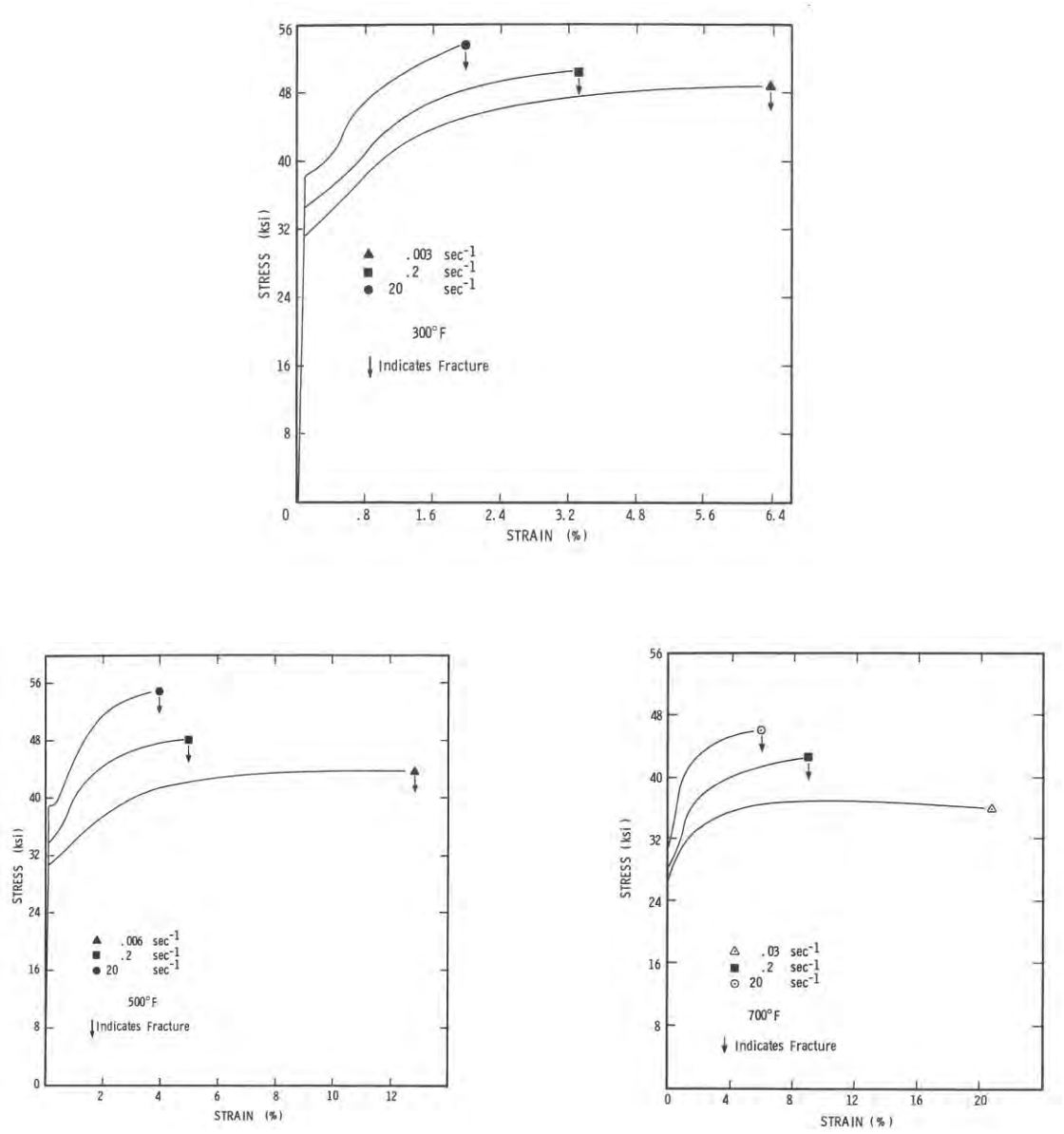

Figure 3.022c: Stress as a function of strain at various strain rates and 300°F (upper), 500°F (left) and 700°F (right) for Materion S200E (1).

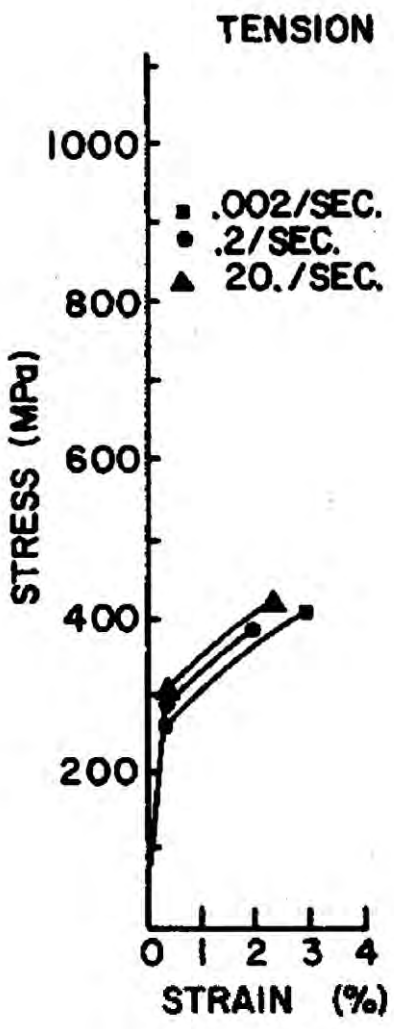

Figure 3.022d: Stress as a function of tensile strain at various strain rates and room temperature for KBI Be block (65).

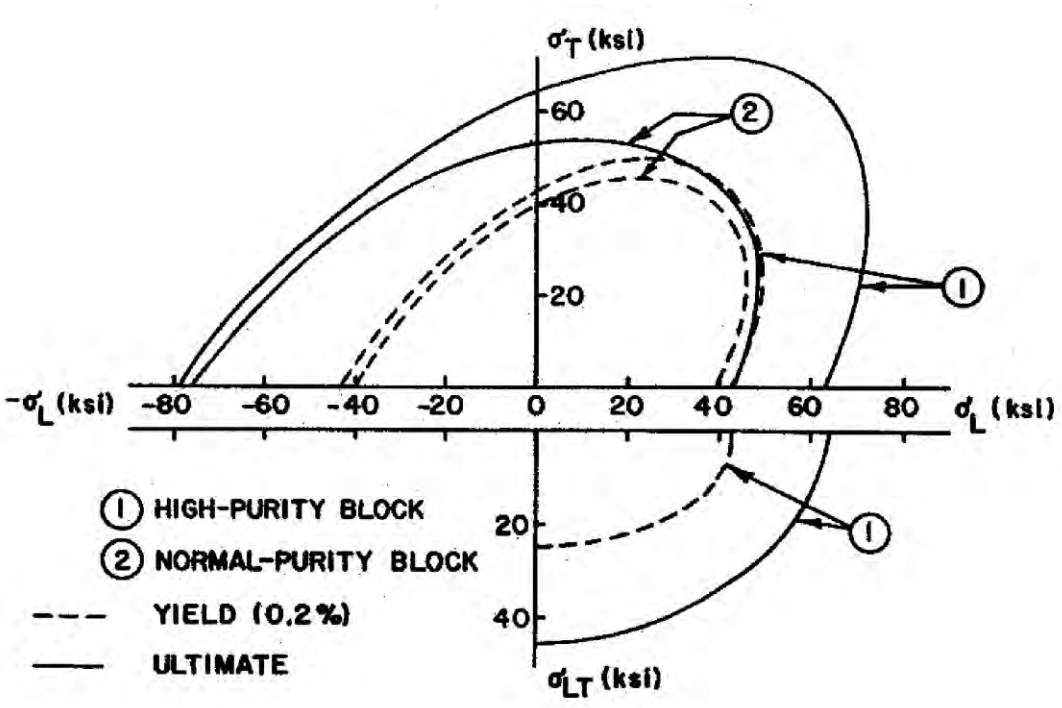

Figure 3.022e: The effect of biaxial stress on yield and ultimate strengths for KBI Be (65).

Temp. (F)	Orient.	Ultimate Tensile Strength (ksi)	Yield Strength 0.2% Offset (ksi)	Yield Point Upper (ksi)	Yield Point Lower (ksi)	Elong. (%)	Reduction In Area (%)
RT	L	55.4 ±0.3	38.2 ±0.5	38.9 ±0.3	38.1 ±0.3	3.4 ±0.3	3.3 ±0.3
	T	59.1 ±0.7	38.0 ±0.1	39.6 ±0.5	38.0 ±0.1	6.1 ±0.5	5.9 ±0.2
400	L	48.1 ±0.5	37.1 ±0.7	37.7 ±0.1	37.0 ±0.6	12.0 ±1.3	11.2 ±1.4
	T	48.4 ±0.3	37.7 ±0.5	38.0 ±0.2	37.1 ±0.1	29.5 ±4.1	25.9 ±3.3
800	L	35.4 ±0.4	29.4 ±0.8	29.6 ±0.7	28.5 ±0.5	30.4 ±2.4	52.5 ±1.2
	T	34.2 ±0.9	27.2 ±0.7	27.6 ±0.8	26.5 ±0.7	33.8 ±0.2	54.0 ±0.2
1000	L	28.9 ±0.1	20.8 ±0.1	--(2)	--(2)	22.4 ±0.8	29.4 ±2.2
	T	28.4 ±0.1	20.9 ±0.7	21.2 ±0.5	20.9 ±0.7	25.7 ±0.6	33.9 ±1.7
1200	L	15.7 ±0.3	13.0 ±0.5	13.5 ±0.9	12.5 ±0.4	8.8 ±1.4	7.3 ±0.4
	T(1)	15.5 ±0.6	13.8 ±0.5	--(2)	--(2)	10.9 ±2.1	9.7 ±2.0

(1) Average of 4 specimens
(2) Did not have a yield point

Figure 3.0221a: Tensile properties of Materion S200F Be as a function of temperature and sample orientation (30). L= longitudinal, T = transverse.

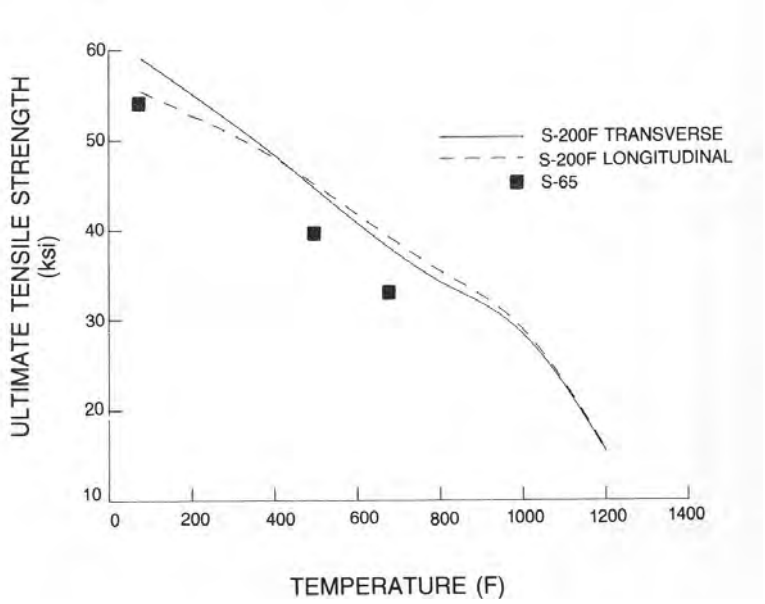

Figure 3.0221b: Ultimate tensile strength of Materion S200F and S65 Be as a function of temperature and sample orientation (3).

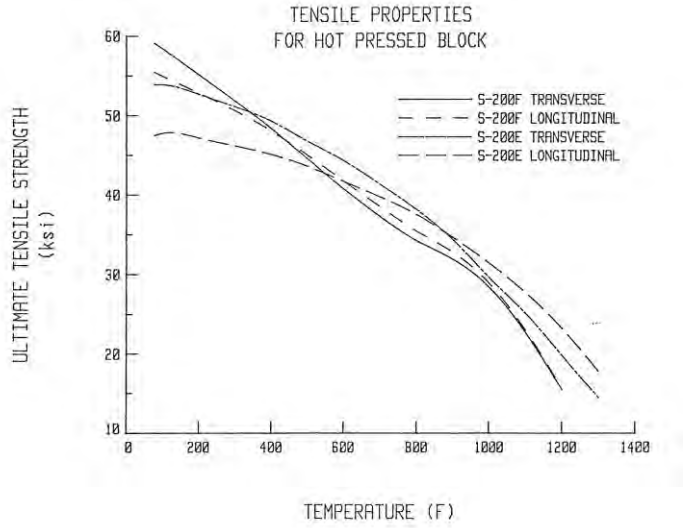

Figure 3.0221c: Ultimate tensile strength of Materion S200E and S200F Be as a function of temperature and sample orientation (30).

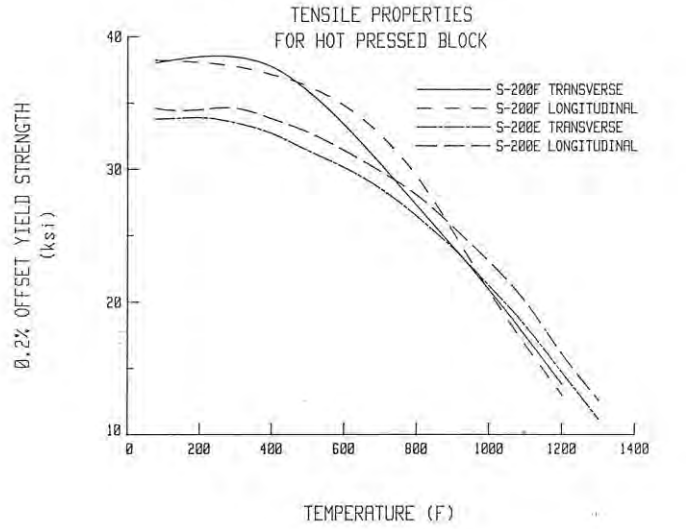

Figure 3.0221d: Tensile 0.2% offset yield strength of Materion S200E and S200F Be as a function of temperature and sample orientation (30).

Temperature (°C)		Ultimate strength (MPa)	Ultimate strength (ksi)	Yield strength (MPa)	Yield strength (ksi)	Elongation %
20	L[b]	421	61.1	270	39.1	3.0
20	T[c]	454	65.8	273	39.6	5.4
200	L	382	55.4	232	33.6	10.2
200	T	389	56.4	234	34.0	23.4
400	L	270	39.2	179	25.9	50.0
400	T	268	38.8	177	25.6	49.5
600	L	160	23.2	119	17.2	25.2
600	T	167	24.2	122	17.7	31.9

[b] Longitudinal direction (parallel to molding pressure).
[c] Transverse direction (perpendicular to molding pressure).

Figure 3.0221e: Ultimate strength and yield strength in tension of Materion S65B Be as a function of temperature and sample orientation (67).

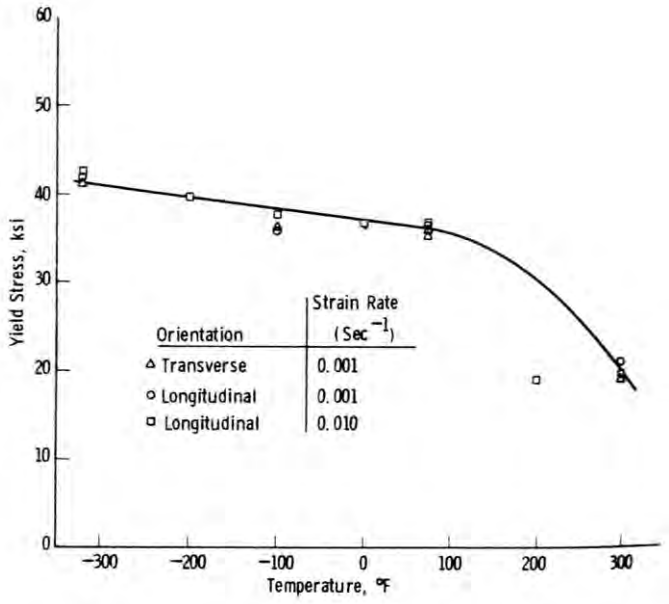

Figure 3.0221f: Yield stress of vacuum hot pressed Materion S200 Be as a function of temperature and sample orientation (78).

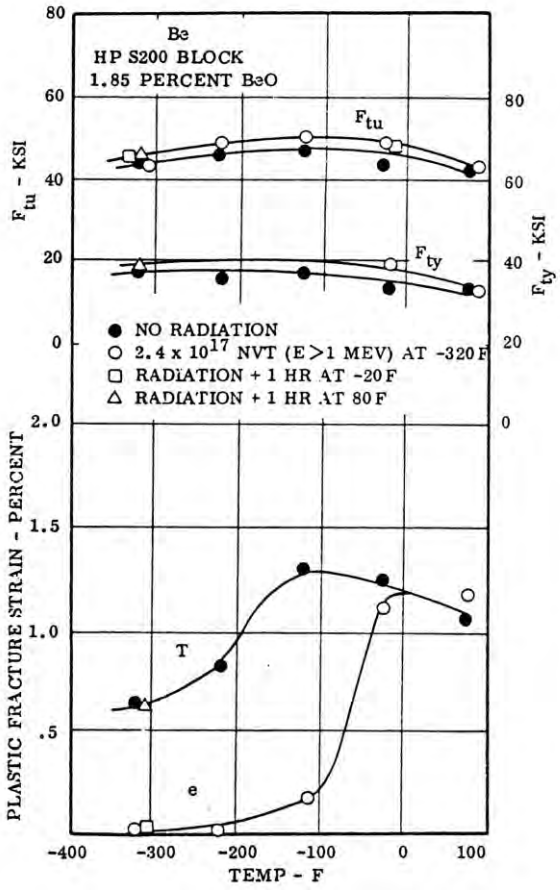

Figure 3.0221g: Tensile properties as a function of temperature and neutron radiation dose for Materion S200 Be block (66). F_{tu} = tensile ultimate strength, F_{ty} = tensile yield strength.

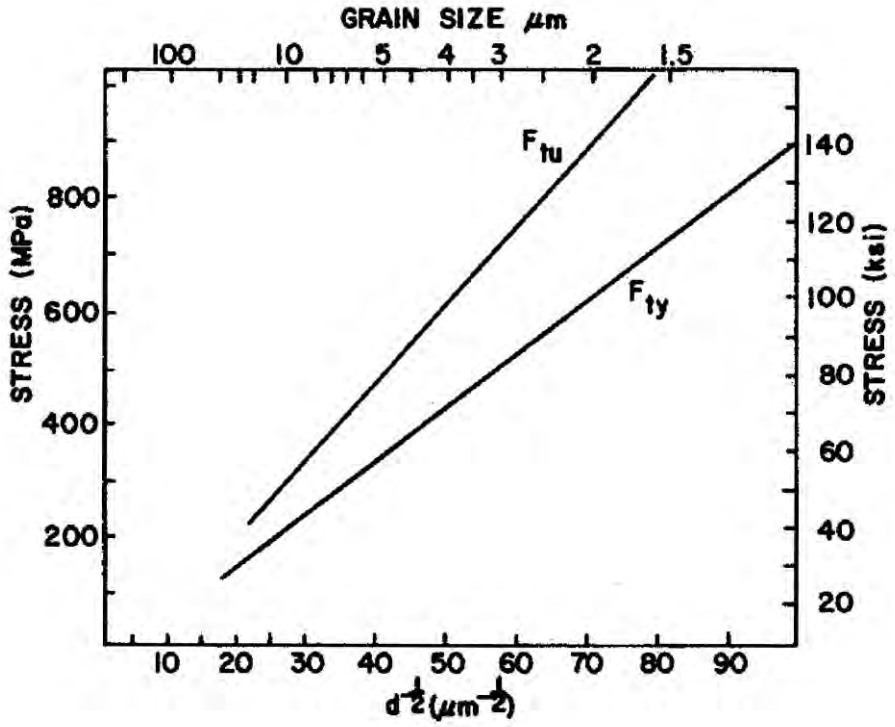

Figure 3.0221h: Stress as a function of grain diameter for KBI Be (65). d = grain diameter.

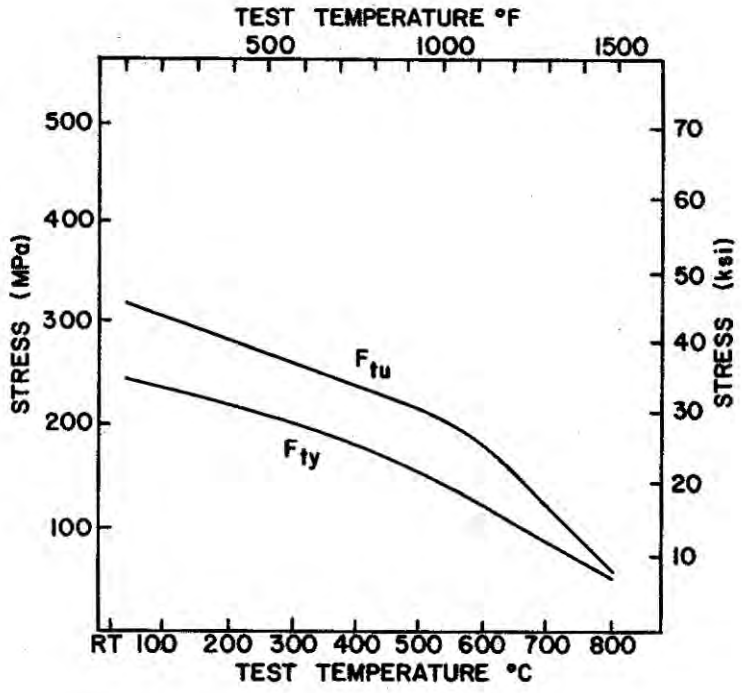

Figure 3.0221i: Stress as a function of temperature for KBI Be (65).

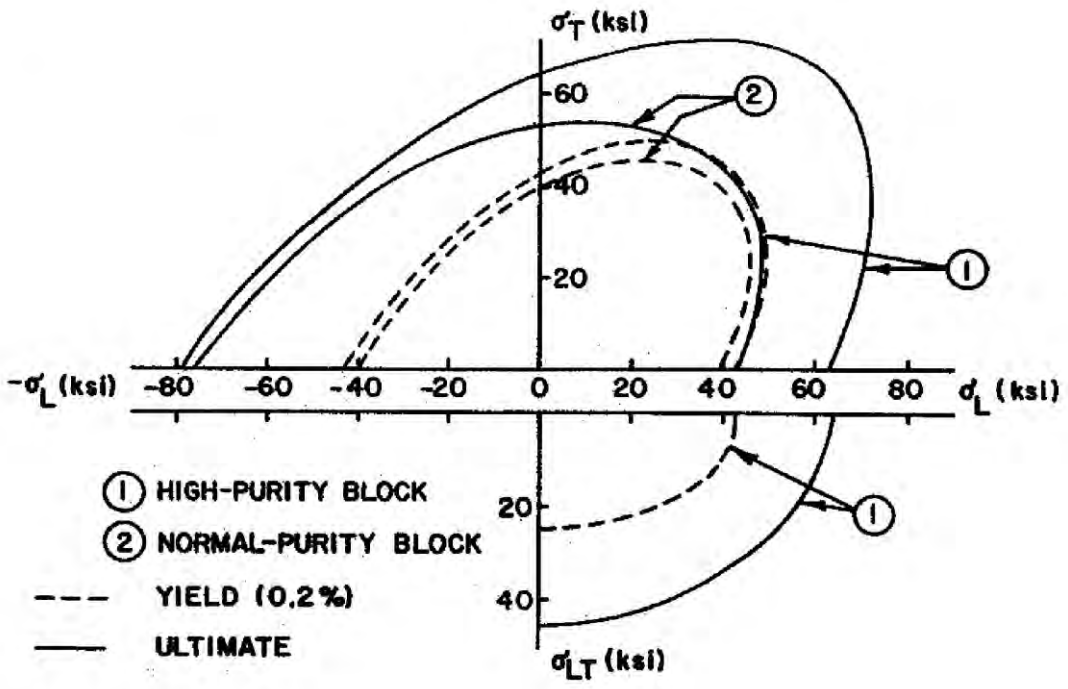

Figure 3.0221i: Effects of combined stress loading on the strength of Kawecki Berylco beryllium block (65). σ = stress, L = longitudinal, T = transverse.

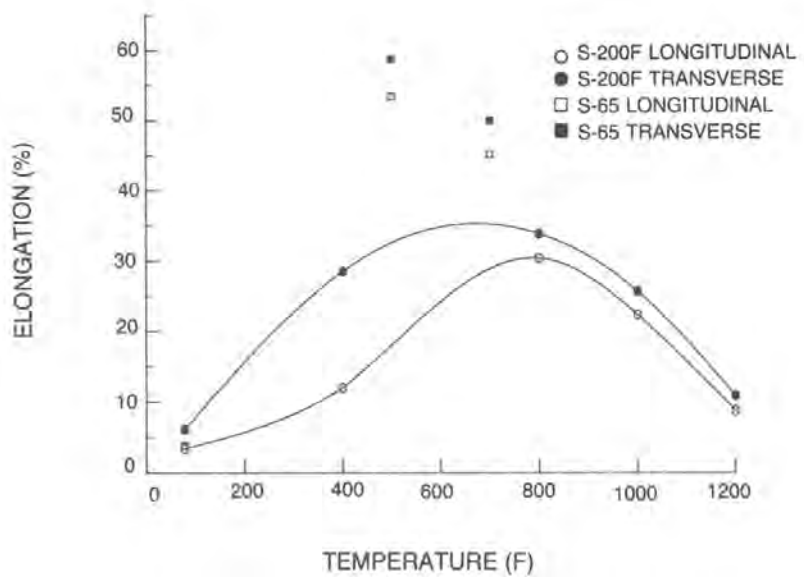

Figure 3.0222a: Elongation of Materion S200F and S65 Be as a function of temperature and sample orientation (3).

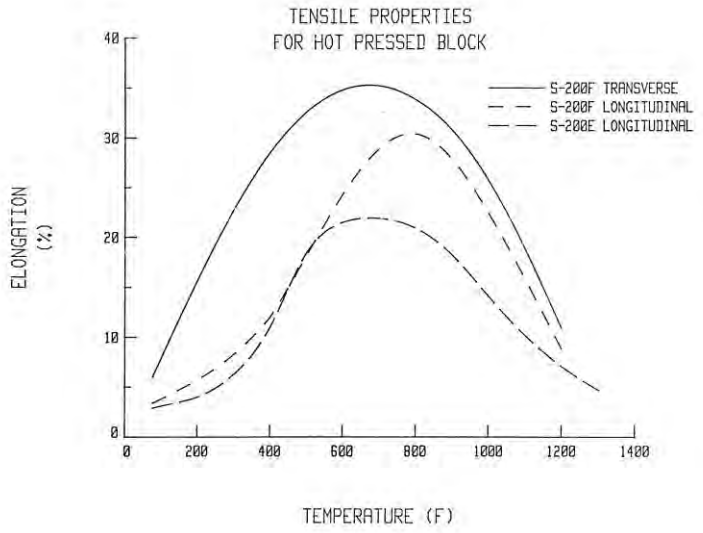

Figure 3.0222b: Tensile elongation of Materion S200E and S200F Be as a function of temperature and sample orientation (30).

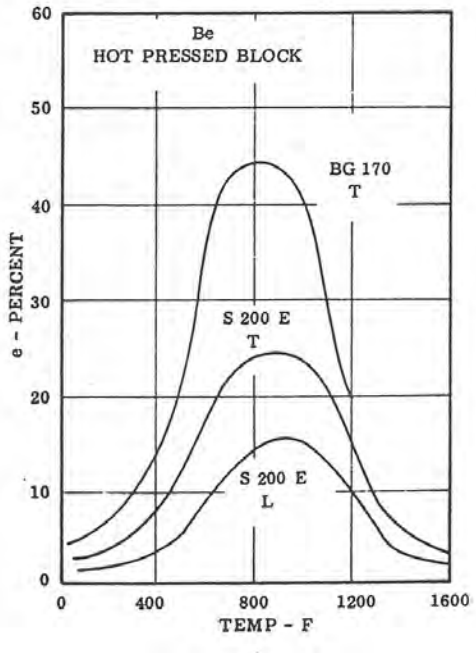

Figure 3.0222c: Average value of elongation as a function of temperature for several lots of Materion S200E and other Be (68). L = longitudinal, T = transverse.

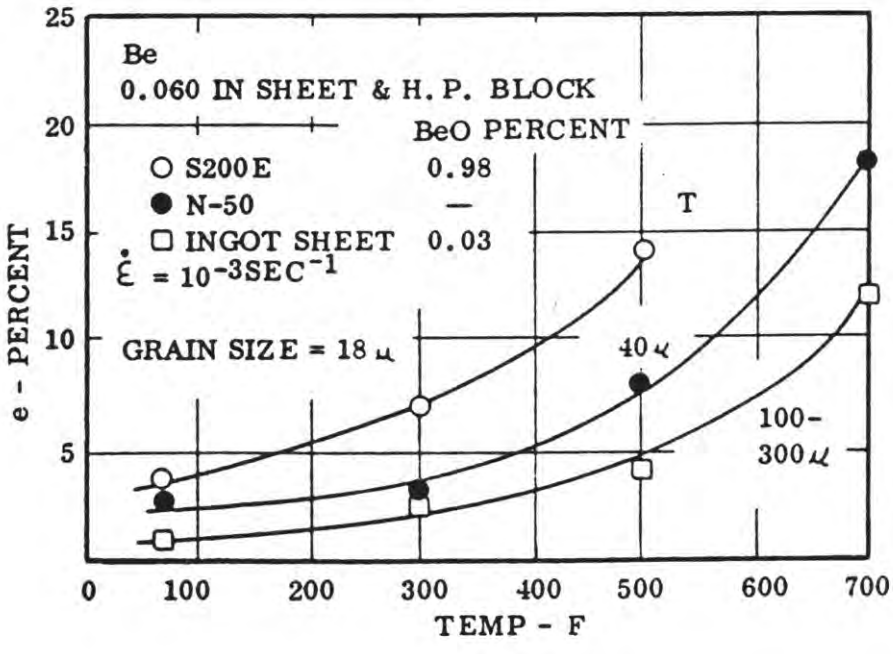

Figure 3.0222d: Elongation of Materion S200E and other Be as a function of grain size and temperature (1).

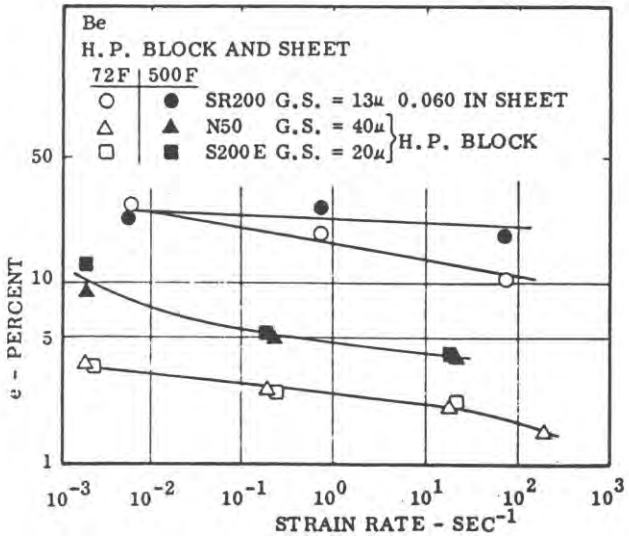

Figure 3.0222e: Elongation of Materion S200E and other Be as a function of strain rate and temperature (1).

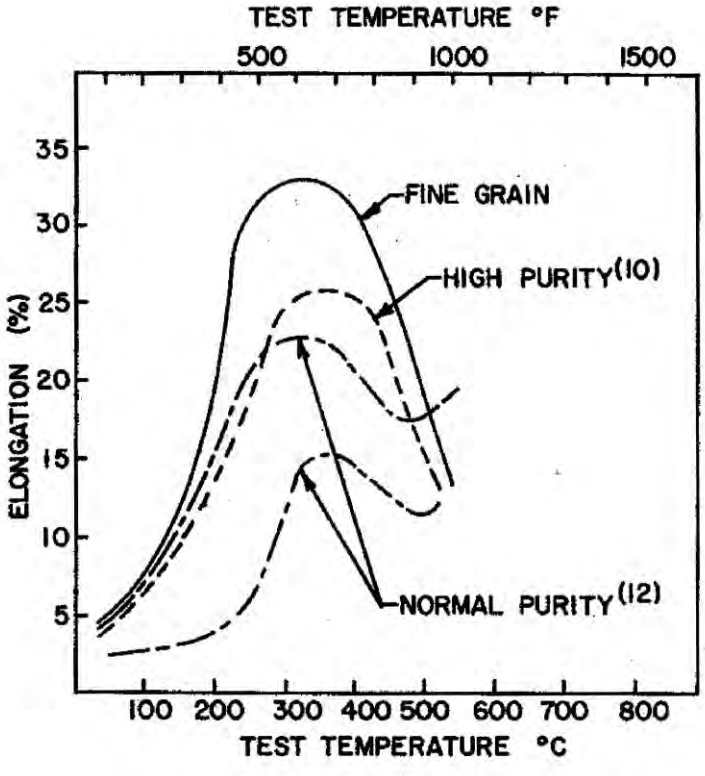

Figure 3.0222f: Elongation of KBI Be block as a function of temperature (65).

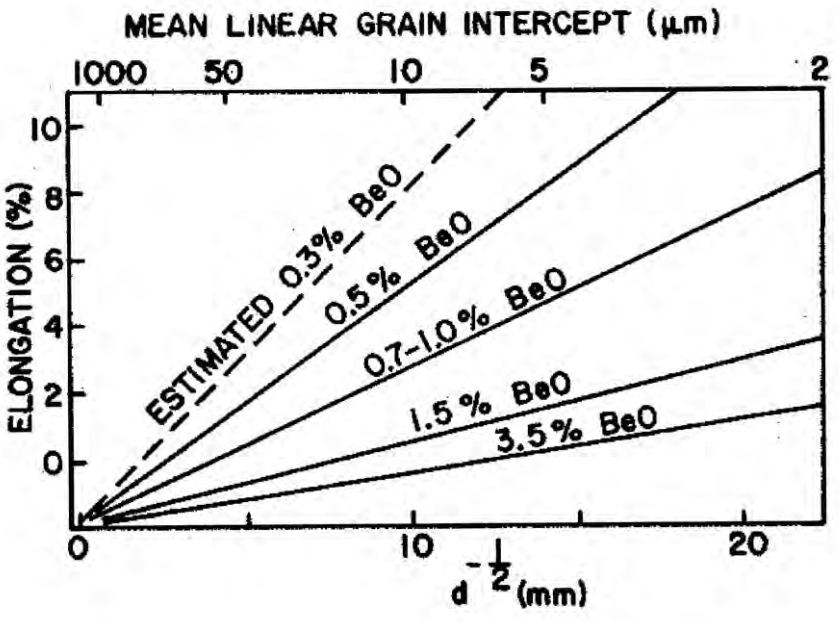

Figure 3.0222g: Elongation of KBI Be block as a function of grain size and BeO content (65). d = grain diameter.

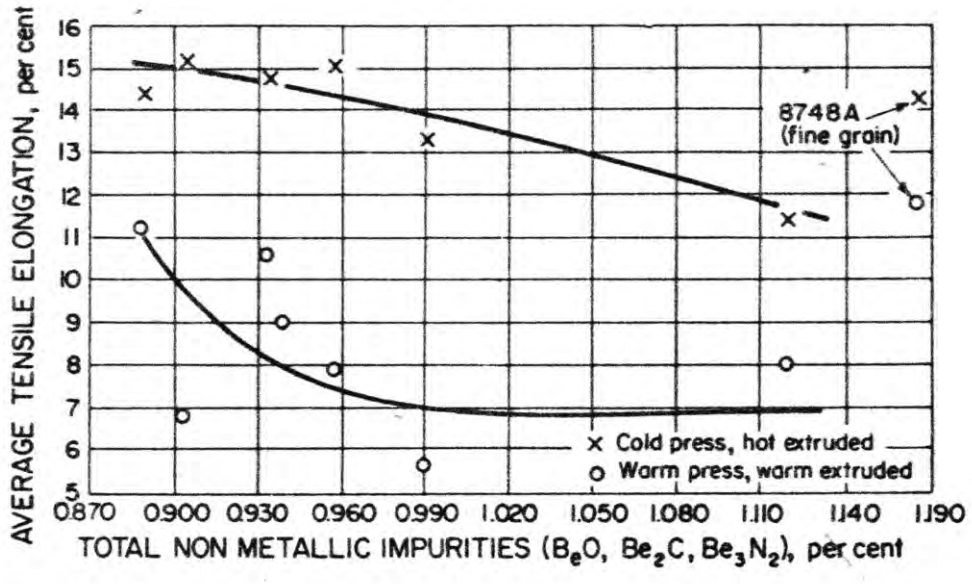

Figure 3.0222h: Elongation of Be rod as a function of impurity content (69).

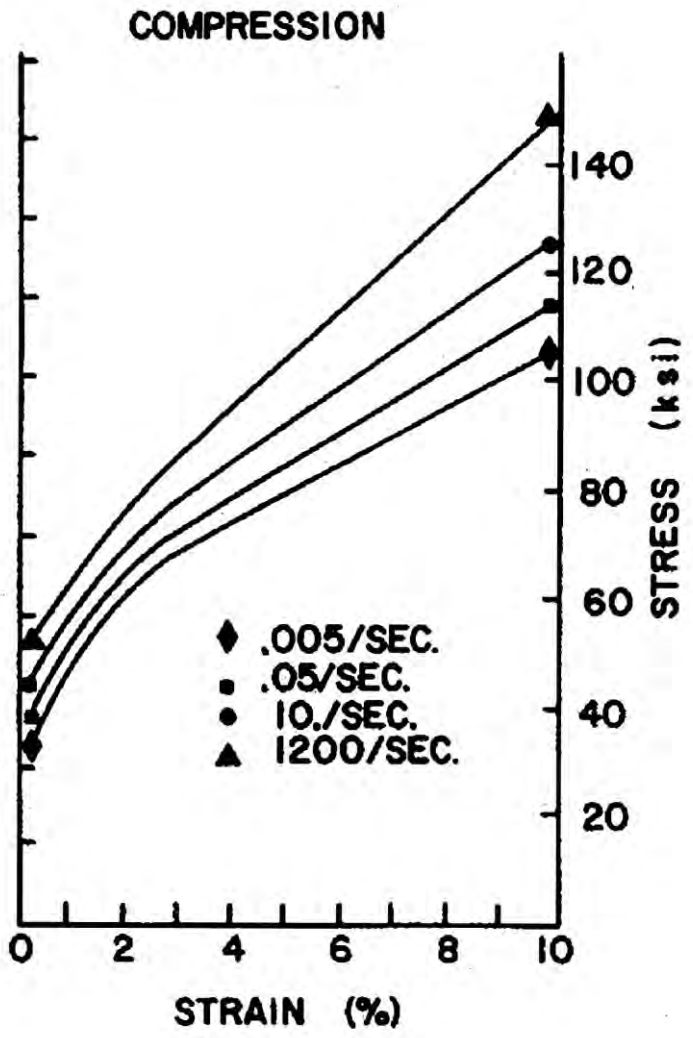

Figure 3.023a: Stress as a function of compressive strain at various strain rates and room temperature for KBI Be block (65).

Orientation	Compressive Yield Strength (ksi)
Longitudinal	37.2
Longitudinal	38.5
Transverse	37.3
Transverse	35.9
Transerse	35.8

Figure 3.023b: Compressive yield strength of Materion S200F Be as a function of sample orientation at 190°C (64).

Compression Properties	
0.2% Yield Strength (psi)	24,600
Proportional Limit (psi)	3,800
Elastic Modulus (10-6)	44.1
Poisson's Ratio	0.25 ± 0.005

Figure 3.023c: Compressive properties of Materion hot pressed powder, measured prior to 1955 (31).

Orientation	K_{IC} (ksi $\sqrt{in.}$)
LR	8.4
LR	8.7
LR	7.8 (invalid test)
LR	8.9
RL	9.6
RL	9.8
RL	10.4
RL	9.8

Figure 3.025a: Fracture toughness values for Materion S200F Be (64). K_{IC} = fracture toughness, LR = stress applied in longitudinal direction with crack propagation in the radial direction, RL = stress applied in the radial direction with the crack propagating in the longitudinal direction.

Material Number	Thickness, in.	Orientation	Yield Strength, ksi	Ultimate Strength, ksi	Elongation, %	U_T, lb-in./in.³	K,[b] max load, ksi-in.$^{1/2}$
S-200E							
R.T.	1.00	L	33.0	42.0	1.5	0.64	9.4 (L) WOL
			34.9	47.9	2.2	1.10	11.2 (T)
−100°F	1.00	L	32.0	48.0	1.3	0.63	8.5 (L)
		T	35.0	51.8	1.9	1.00	10.0 (T)
−320°F	1.00	L	38.0	42.0	0.6	0.25	7.6 (L)
		T	41.1	48.8	0.6	0.30	8.3 (T)
S-200I (GA)	0.35	L	40.1	42.4	1.0	0.43	13.2 (L) SEN (cleaved)
S-200I (GA)	0.50	L	40.1	42.4	1.0	0.43	11.7 (L) SEN (cleaved)
S-200II (LRL)	0.50	T					22.9 (T) (cleaved)
S-200D	0.50	T	41.0	57.0	3.3	1.89	14.5 (T) 3 pt bend
S-200	1.00	L	33.5	43.5	1.2	0.53	23.4 (T) WOL, as-machined, reduced to 12.0 for precracking correction

[b] All specimens fatigue precracked unless indicated otherwise.

L = Pressing direction.
T = Transverse to pressing direction.

Figure 3.025b: Fracture toughness values for Materion S200D, S200E and S200 hot pressed block (72). The data has been obtained using differing techniques. K = fracture toughness, U_T = true stress at fracture × true strain at fracture, GA = gas atomized, WOL = wedge opening loading, SEN = single edge notched specimen.

Material	Specimen Orientation	K_{Ic}			wt% BeO	Grain Size	Reference
		Mean (ksi √in)	Std. Dev. (ksi √in)	n		(μm)	
S-65H	L-T	9.0	-	1	0.70	6.6	Present Work
HIP'd GA	L-T	10.2	-	1	0.32	9.5	Present Work
VHP S-200E	L-T	9.4	0.425	5	1.1	NA	26
	T-L	11.2	0.209	3			
VHP S-200F	L-T	9.66	-	1	0.67	8.7	1
	T-L	11.2	-	1			
VHP S-200F	L-T	8.64	0.254	3	1.06	NA	24
	T-L	9.92	0.345	4			
VHP S-65	L-T	9.64	0.701	3	0.7	11.4	25
	T-L	9.92	0.655	3			
VHP GA Be	T-L	12.4	-	1	0.37	13.2	1
S-200FH	L-T	8.25	0.373	3	0.78	7.0	27
	T-L	8.33	0.291	3			

Figure 3.025c: Fracture toughness values for several Materion berylliums (73). K_{IC} = fracture toughness, VHP = vacuum hot pressed, HIP = hot isostatic pressed, GA = gas atomized. L-T = load applied parallel to longitudinal direction in VHP billet and crack propagation parallel to transverse direction, T-L = load applied parallel to transverse direction in VHP billet and crack propagation parallel to longitudinal direction.

Pressing I.D.	Direction	Position**	K_{IC} ksi √in	F_{tu} ksi	F_{ty} ksi	el %	Composition Wt%			Grain Size μm
							Fe	Al	BeO	
2572	LR RL	Middle	8.6 10.4	50.4 56.8	39.1 39.1	1.4 3.2	0.09	0.04	1.0	11.3
2485	LR RL	Top	8.8 10.4	54.2 58.2	40.8 40.1	1.6 2.7	0.08	0.03	0.9	11.3
2486	LR RL	Middle	9.2 10.4	52.9 58.9	38.7 39.3	1.7 3.1	0.07	0.03	1.1	11.3
2494	LR RL	Top	9.1 10.5	49.0 55.0	35.1 35.9	1.6 3.0	0.08	0.04	0.8	11.1
2549	LR RL	Middle	9.4† 11.3†	45.0 52.3	33.7 33.7	1.1 3.9	0.08	0.04	1.1	13.1
2468	LR RL	Middle	9.3 10.5	51.0 57.3	38.2 38.8	1.4 2.5	0.07	0.03	1.1	12.1
2573	LR RL	Middle	8.9 9.6	51.2 58.6	37.7 37.3	1.4 3.6	0.08	0.04	1.2	10.0
2510	LR RL	Top	8.6† 10.3	48.7 57.4	36.3 36.7	1.4 3.7	0.07	0.03	1.0	9.7

** Position in respect to the pressing

† Load-displacement record exhibited crack jumps

Figure 3.025d: Fracture toughness values for Materion S200E, along with mechanical and compositional properties (71). K_{IC} = fracture toughness, F_{tu} = ultimate tensile strength, F_{ty} = tensile yield strength, el = elongation, LR = crack plane normal to the pressing direction, RL = crack plane parallel to the pressing direction.

Pressing	Direction[b]	K_{Ic}, ksi · in.$^{1/2}$	F_{tu}, ksi	F_{ty}, ksi	Elongation, %	Composition, Weight %: Iron	Aluminum	Beryllium Oxide	Grain Size, μm
S65	LR	10.4	58.5	37.0	3.2	0.05	0.02	0.7	11.4
		9.0	...	...	...	...	...	...	...
		9.6	...	...	...	...	...	...	...
	RL	9.3	62.5	38.2	5.8	...	...	...	...
		9.8	...	...	...	...	...	...	...
		10.6	...	...	...	...	...	...	...
S200E	LR	9.4	58.4	42.5	1.6	0.07	0.04	1.7	8.4
		8.6	...	...	...	...	...	...	...
		8.9	...	...	...	...	...	...	...
	RL	9.1	65.1	42.5	1.6	...	...	...	...
		9.2	...	...	...	...	...	...	...
		8.9	...	...	...	...	...	...	...

Figure 3.025e: Fracture toughness values for Materion S200E, along with mechanical and compositional properties (74). K_{IC} = fracture toughness, F_{tu} = ultimate tensile strength, F_{ty} = tensile yield strength, el = elongation, LR = crack plane normal to the pressing direction, RL = crack plane parallel to the pressing direction (74).

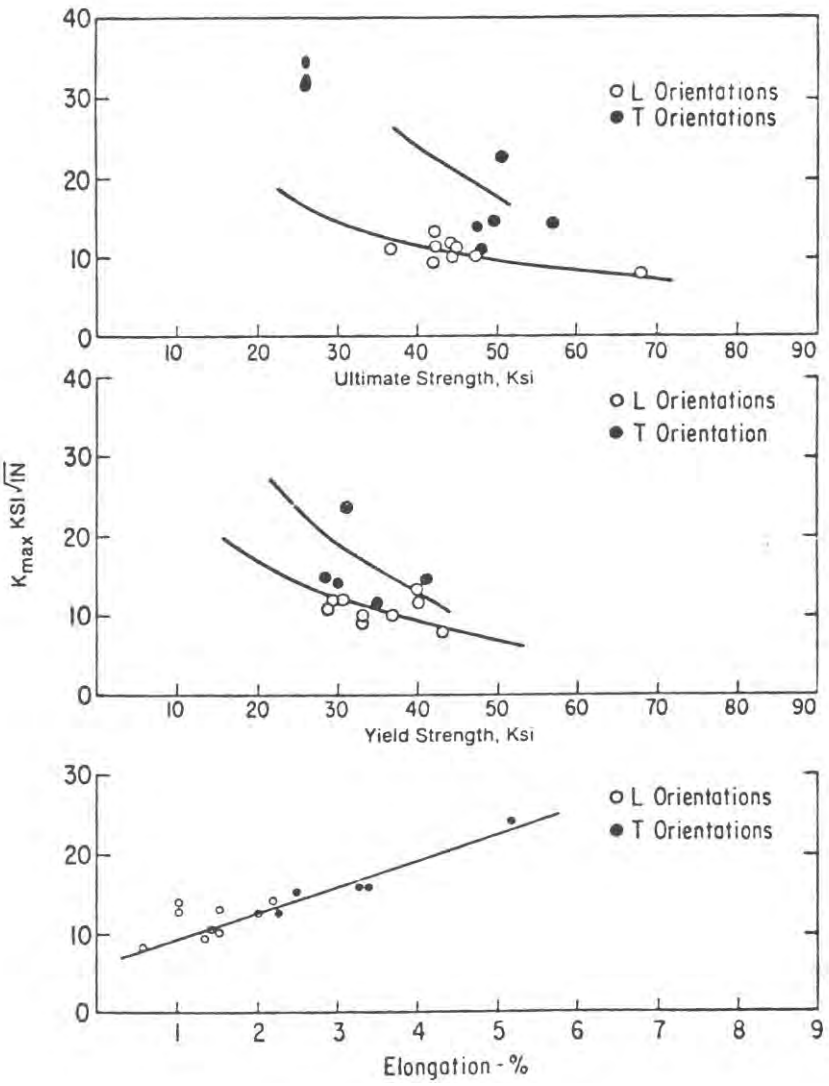

Figure 3.025f: Correlation of fracture toughness of hot pressed Be block to tensile properties (72). K = fracture toughness, L = longitudinal, T = tensile.

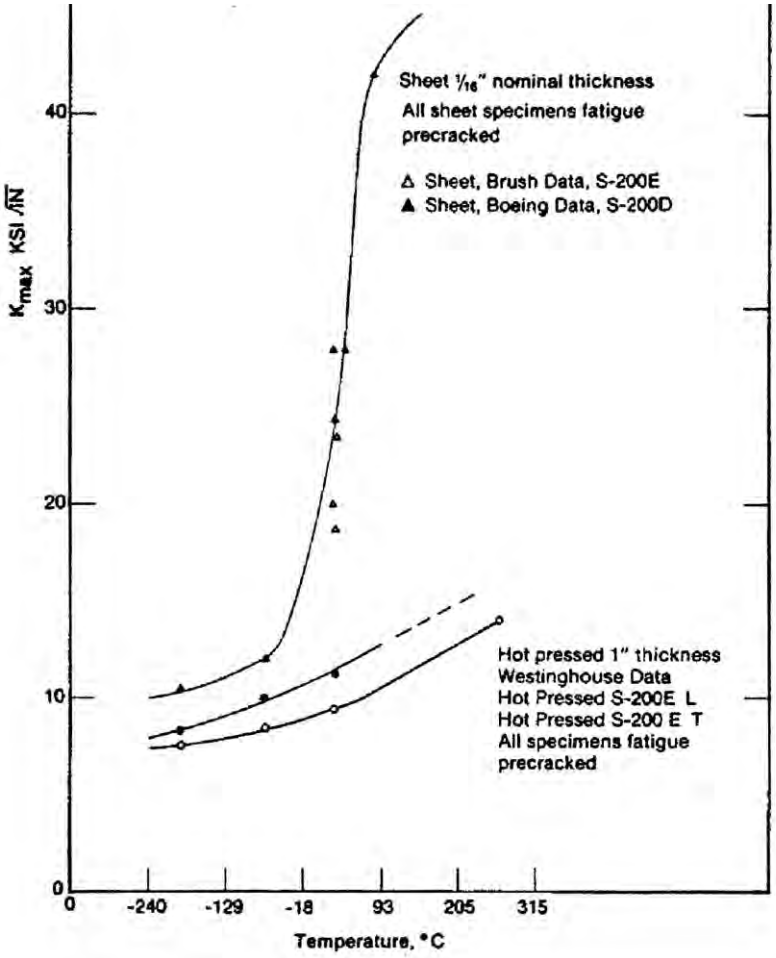

Figure 3.025g: Fracture toughness as a function of temperature for Materion S200E Be (72).

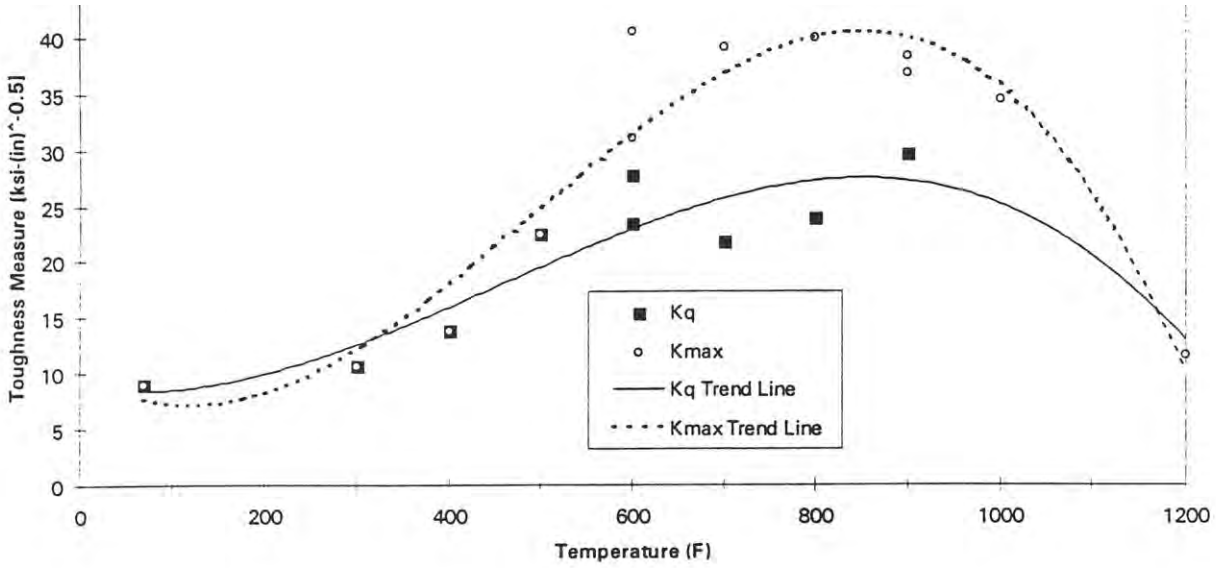

Figure 3.025h: Fracture toughness as a function of temperature for Materion S65 Be (73).

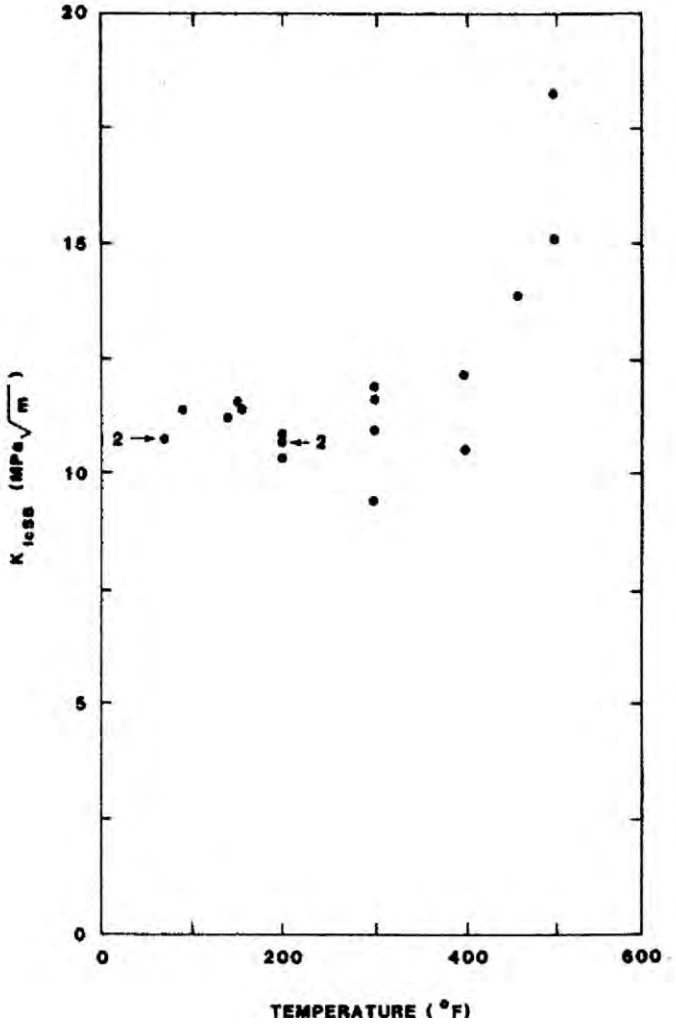

Figure 3.025j: Fracture toughness as a function of temperature for KBI CIP-HIP Be (76).

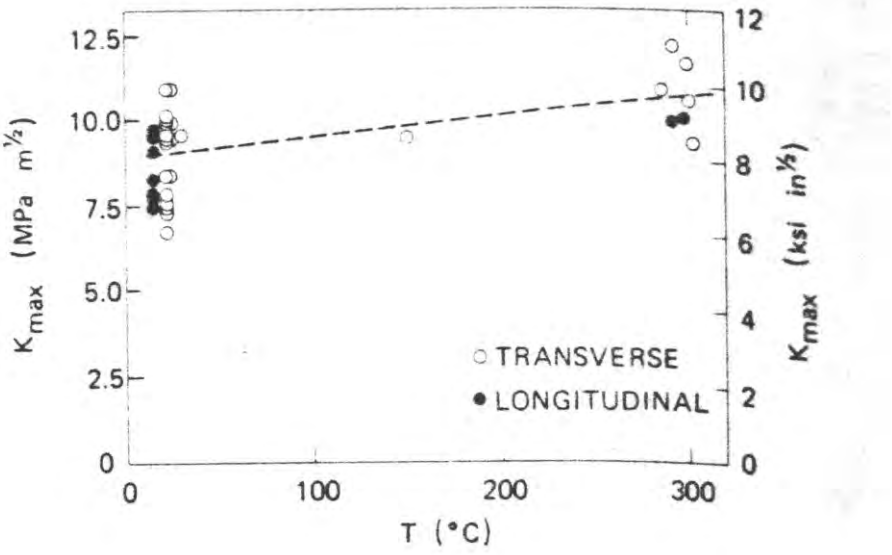

Figure 3.025i: Fracture toughness as a function of temperature for a high yield strength Be block (75).

Ageing or irradiation temperature (°C)	Neutron fluence, $E_n > 1$ MeV ($\times 10^{21}$ n cm^{-2})	Test temperature (°C)	Fracture toughness, K_{IC} (MPa $\sqrt{m}$)	Number of tests
0	0	23	11.3 ± 0.5	8
0	0	185	12.2 ± 1.2	2
0	0	230	14.9 ± 0.3	2
0	0	310	14.9	1
185	0	23	10.6 ± 0.9	3
200	0.94	23	7.5 ± 1.0	4
200	0.94	200	7.5 ± 0.8	4
230	0	23	10.6 ± 2.0	3
230	0	230	14.6 ± 0.7	2
230	1.40	23	6.8 ± 1.0	3
230	1.40	230	7.7 ± 0.3	4
350	0.94	250	8.3 ± 1.6	4
350	0.94	350	10.1 ± 0.6	3
435	0	250	15.3	1
435	1.40	250	9.5 ± 1.3	3
435	1.40	435	10.2 ± 2.2	2
600	0	250	15.9 ± 1.2	2
600	1.78	250	12.8 ± 1.5	8
600	1.78	600	$13.1 + 2.0$	5

Figure 3.025j: Effects of neutron irradiation and temperature on the fracture toughness of Materion S200F and S65 Be (77).

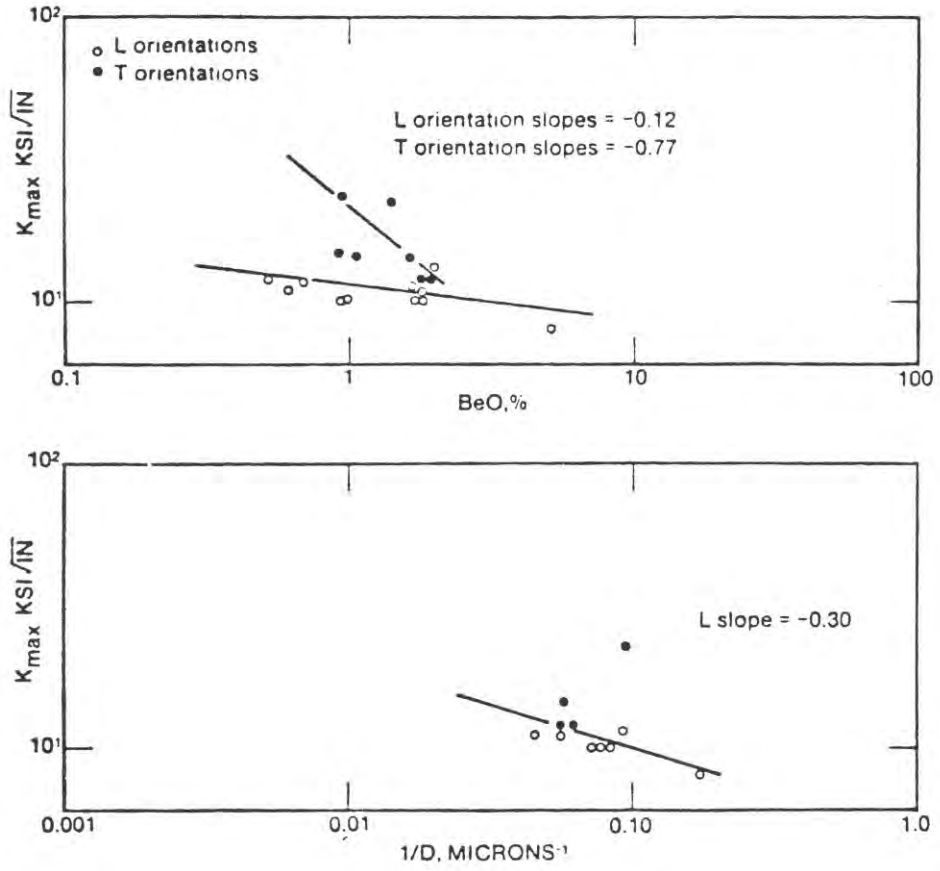

Figure 3.025k: Fracture toughness as a function of BeO content and grain size at room temperature for hot pressed block Be (72). D = grain diameter.

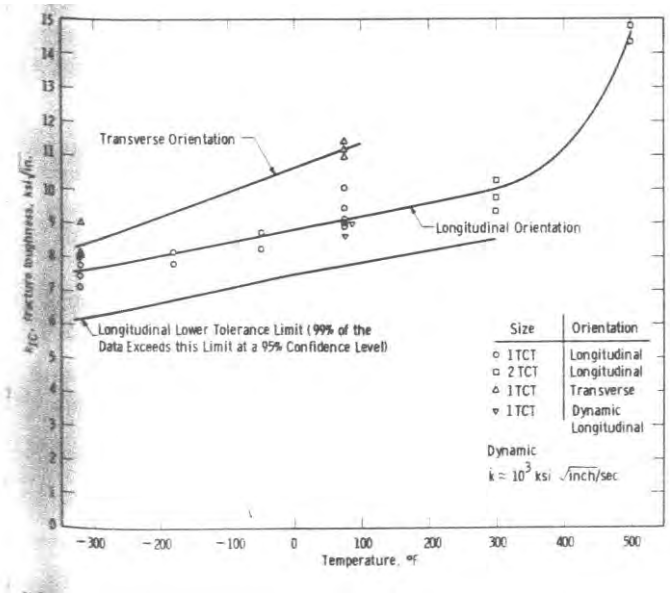

Figure 3.025l: Dynamic fracture toughness as a function of temperature for Materion vacuum hot pressed S200 beryllium (78).

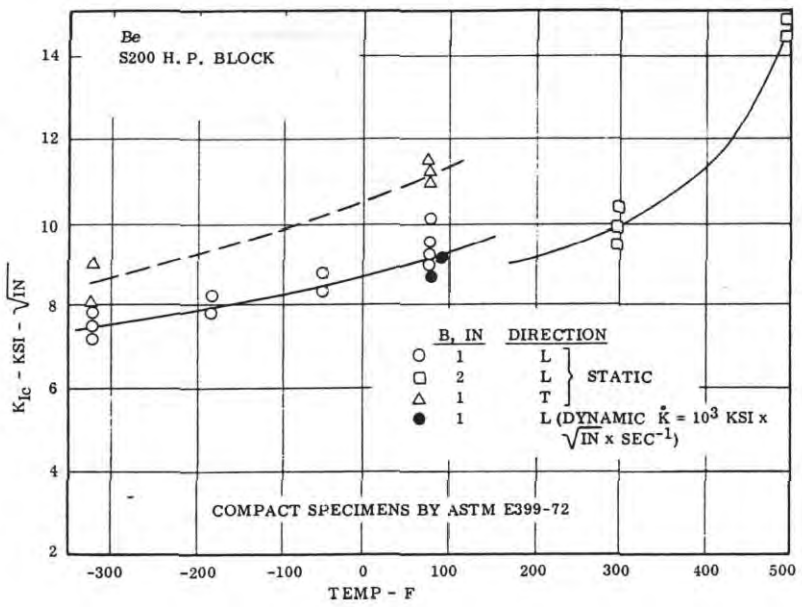

Figure 3.025m: Plane-strain fracture toughness as a function of temperature and test direction for Materion S200 hot pressed block (71). L = longitudinal, T = transverse.

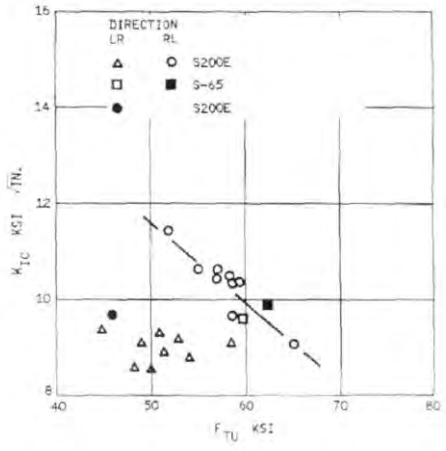

Figure 3.025n: Plane-strain fracture toughness as a function of tensile ultimate strength for Materion S200E and Materion S65 (71). LR = crack plane normal to the pressing direction, RL = crack plane parallel to the pressing direction, F_{TU} = ultimate tensile strength.

Movable specimen material and dia. in inches	Normal force in psi	Coefficient of static friction*
0.530 Be	8.1	0.49
0.530 Be	46	0.46
0.530 Be	85	0.46, 0.46, 0.46, 0.46
0.750 Be	4	0.47
0.750 Be	23	0.47
0.750 Be	42	0.46
0.940 Be	2.3	0.47
0.940 Be	15	0.45
0.940 Be	27	0.46
0.500 1040 St	9.2	0.40
0.500 1040 St	51	0.41
0.500 1040 St	93	0.42, 0.42, 0.43, 0.42
0.850 1040 St	3.3	0.43
0.850 1040 St	18	0.41
0.850 1040 St	33	0.42

*Results at 75% relative humidity and 74°F.

Figure 3.026a: Coefficients of static friction at room temperature and wet atmosphere for Be plate against Be rod and Be plate against 1040 steel rod, obtained by the "opposing horizontal force method." (79).

Movable specimen material and dia. in inches	Normal force in psi	Angle of inclination Θ	Coefficient of static friction* tan Θ
0.530 Be	0.03	31.5	0.61
0.530 Be	0.03	31	0.60
0.530 Be	0.03	31	0.60
0.750 Be	0.12	29.5	0.57
0.750 Be	0.12	30	0.58
0.750 Be	0.12	30	0.58
0.750 Be	4.0	24.5	0.46
0.750 Be	4.0	25	0.47
0.940 Be	0.07	30	0.58
0.940 Be	0.07	30.5	0.59
0.940 Be	0.07	30.5	0.59
0.940 Be	2.6	26	0.49
0.940 Be	2.6	26.5	0.50
0.940 Be	2.6	26.5	0.50
0.850 1040 St	0.28	29	0.55
0.850 1040 St	0.28	29.5	0.57
0.850 1040 St	0.28	29	0.55
0.850 1040 St	3.4	24.5	0.46
0.850 1040 St	3.4	23	0.42
0.850 1040 St	3.4	23.5	0.43

*66% relative humidity, 74°F.

Figure 3.026b: Coefficients of static friction at room temperature and wet atmosphere for Be plate against Be rod and Be plate against 1040 steel rod, obtained by the "inclined plane method." (79).

Movable specimen material and dia. in inches	Normal force in psi	Angle of inclination Θ	Coefficient of static friction* tan Θ
0.530 Be	0.03	31.5	0.61
0.530 Be	0.03	31	0.60
0.530 Be	0.03	31	0.60
0.750 Be	0.12	29.5	0.57
0.750 Be	0.12	30	0.58
0.750 Be	0.12	30	0.58
0.750 Be	4.0	24.5	0.46
0.750 Be	4.0	25	0.47
0.940 Be	0.07	30	0.58
0.940 Be	0.07	30.5	0.59
0.940 Be	0.07	30.5	0.59
0.940 Be	2.6	26	0.49
0.940 Be	2.6	26.5	0.50
0.940 Be	2.6	26.5	0.50
0.850 1040 St	0.28	29	0.55
0.850 1040 St	0.28	29.5	0.57
0.850 1040 St	0.28	29	0.55
0.850 1040 St	3.4	24.5	0.46
0.850 1040 St	3.4	23	0.42
0.850 1040 St	3.4	23.5	0.43

*66% relative humidity, 74°F.

Figure 3.026c: Coefficients of static friction at room temperature and dry atmosphere for Be plate against Be rod and Be plate against 1040 steel rod, obtained by the "inclined plane method." (79).

STEADY-STATE FRICTION COEFFICIENTS OF BERYLLIUM AND ANODIZED BERYLLIUM SURFACES				
DISK MATERIAL	STEADY-STATE FRICTION COEFFICIENTS			
	0.05 N	0.1 N	0.2 N	0.5 N
Unlubricated Be	0.72 ± 0.07	0.60 ± 0.03	0.45 ± 0.02	0.58 ± 0.06
Lubricated Be	0.66 ± 0.08	0.58 ± 0.05	0.50 ± 0.06	0.54 ± 0.07
Unlubricated Anodized Be	0.58 ± 0.03	0.48 ± 0.03	0.97 ± 0.07	0.90 ± 0.05
Lubricated Anodized Be	0.40 ± 0.04	0.36 ± 0.03	0.80 ± 0.04	0.42 ± 0.03

Pin material: Pyroceram.
Lubricant: Stearate-based propietary lubricant.

Figure 3.026d: Pin-on-disk sliding friction coefficients for pyroceram on beryllium and anodized beryllium surfaces (51).

NOTES: (1) - GSF = Gage Section Failure
RO = Run Out

Specimen Number	Test Number	Max. Stress (ksi)	Cycles ($\times 10^3$)	Results(1)
Longitudinal Group				
L-E-216	17	40.0	135	GSF
L-E-222	18	40.0	141	GSF
L-E-227	22	39.0	229	GSF
L-E-224	21	39.0	233	GSF
L-E-213	12	38.0	14,860	RO
L-E-220	13	38.0	15,609	RO
L-E-207	7	36.0	18,885	RO
L-E-209	9	36.0	25,686	RO
L-E-201	2	34.0	584	GSF
L-E-205	6	34.0	11,340	RO
L-E-203	3	34.0	13,554	RO

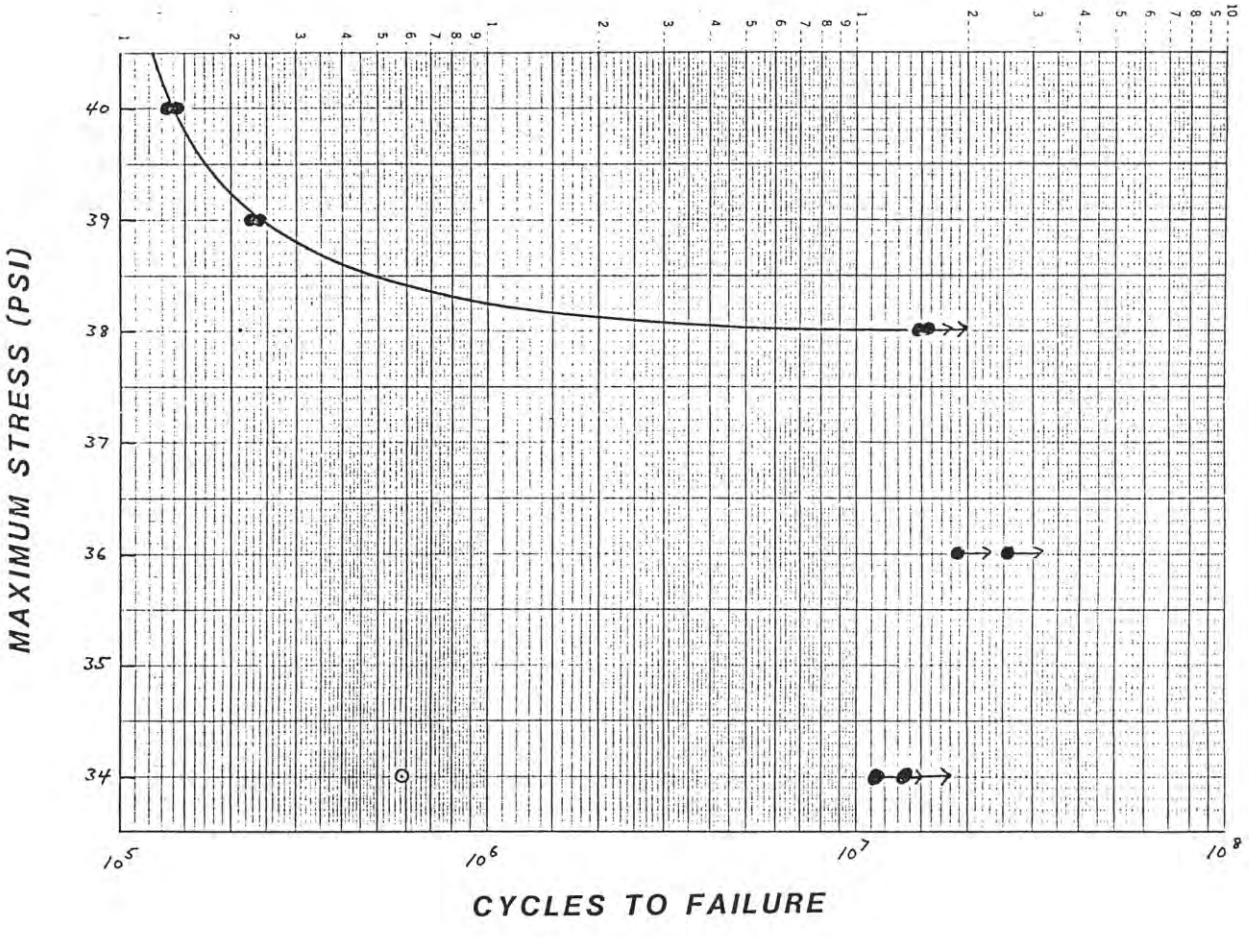

Figure 3.027a: Room temperature notch fatigue test data for longitudinal oriented Materion S200F Be (64).

NOTES: (1) - GSF = Gage Section Failure
RO = Run Out

Specimen Number	Test Number	Max. Stress (ksi)	Cycles (x 10^3)	Results(1)
Transverse Group				
T-A-120	15	40.0	377	GSF
T-A-121	16	40.0	686	GSF
T-A-125	19	39.0	1,309	GSF
T-A-134	23	39.0	4,033	GSF
T-A-130	20	39.0	15,766	RO
T-A-113	10	38.0	210	GSF
T-A-115	11	38.0	12,262	RO
T-A-118	14	38.0	30,473	RO
T-A-108	5	36.0	13,938	RO
T-A-110	8	36.0	17,186	RO
T-A-104	1	34.0	14,649	RO
T-A-106	4	34.0	30,819	RO

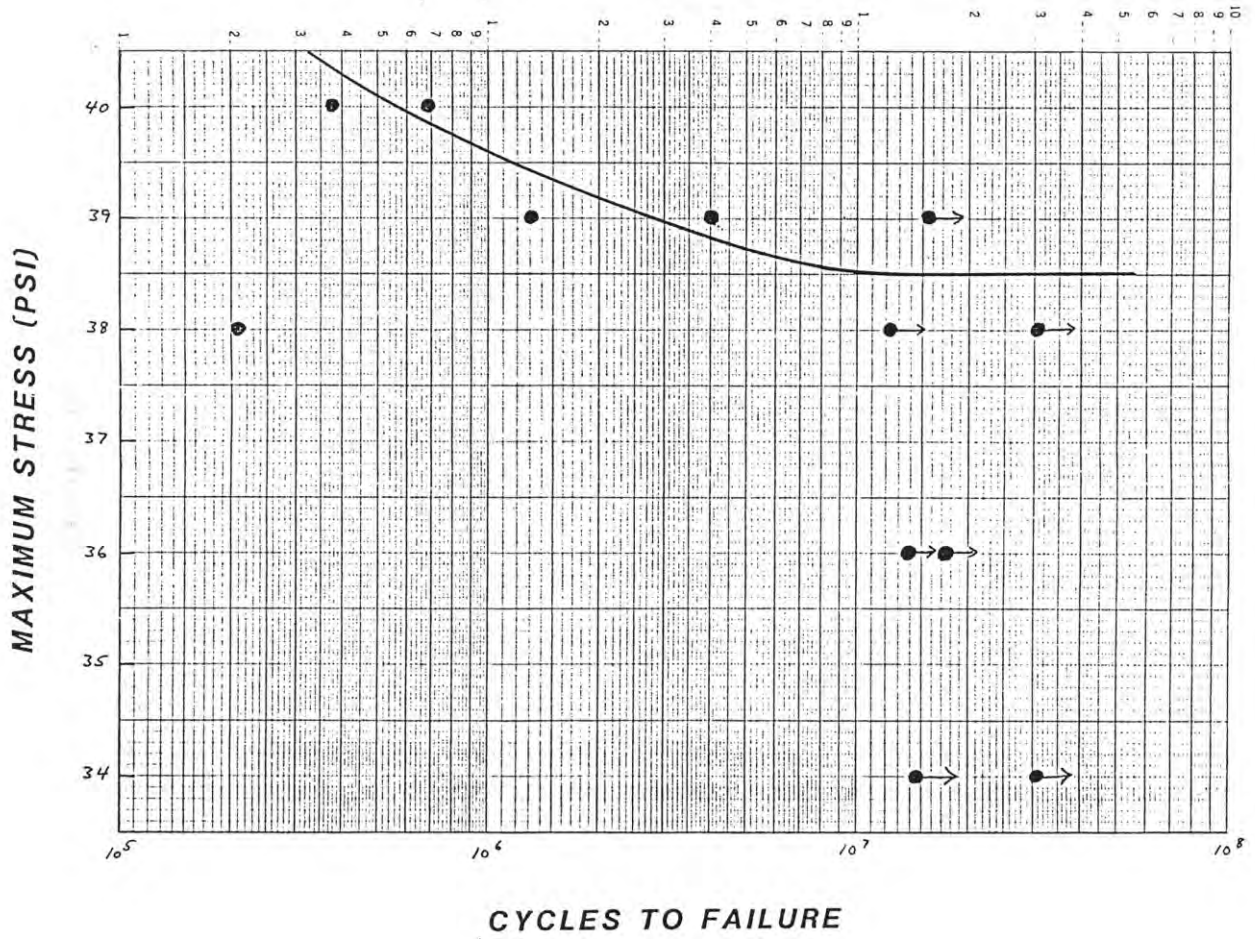

Figure 3.027b: Room temperature smooth fatigue test data for transverse oriented Materion S200F Be (64).

Test Sequence	Specimen ID	Stress Concentration Factor	Maximum Applied Stress (ksi)	Fatigue Life (cycles)	Comments
Longitudinal Orientation					
1	E-204	2.91	18	542,400	Failed
2	E-228	2.99	18	727,900	Failed
3	E-206	2.99	20	311,000	Failed
4	E-217	3.02	20	265,600	Failed
5	E-225	2.94	16	1,388,100	Failed
6	E-214	2.95	16	651,800	Failed
7	E-202	3.00	16	63,825,300	Run out
8	E-212	3.00	16	9,437,100	Failed
9	E-219	3.00	17	181,900	Failed
10	E-210	3.00	15	405,700	Failed
11	E-221	2.99	15	35,069,500	Run out
12	E-208	2.95	15	1,002,400	Failed
12	C-143	2.95	15	253,500	Failed

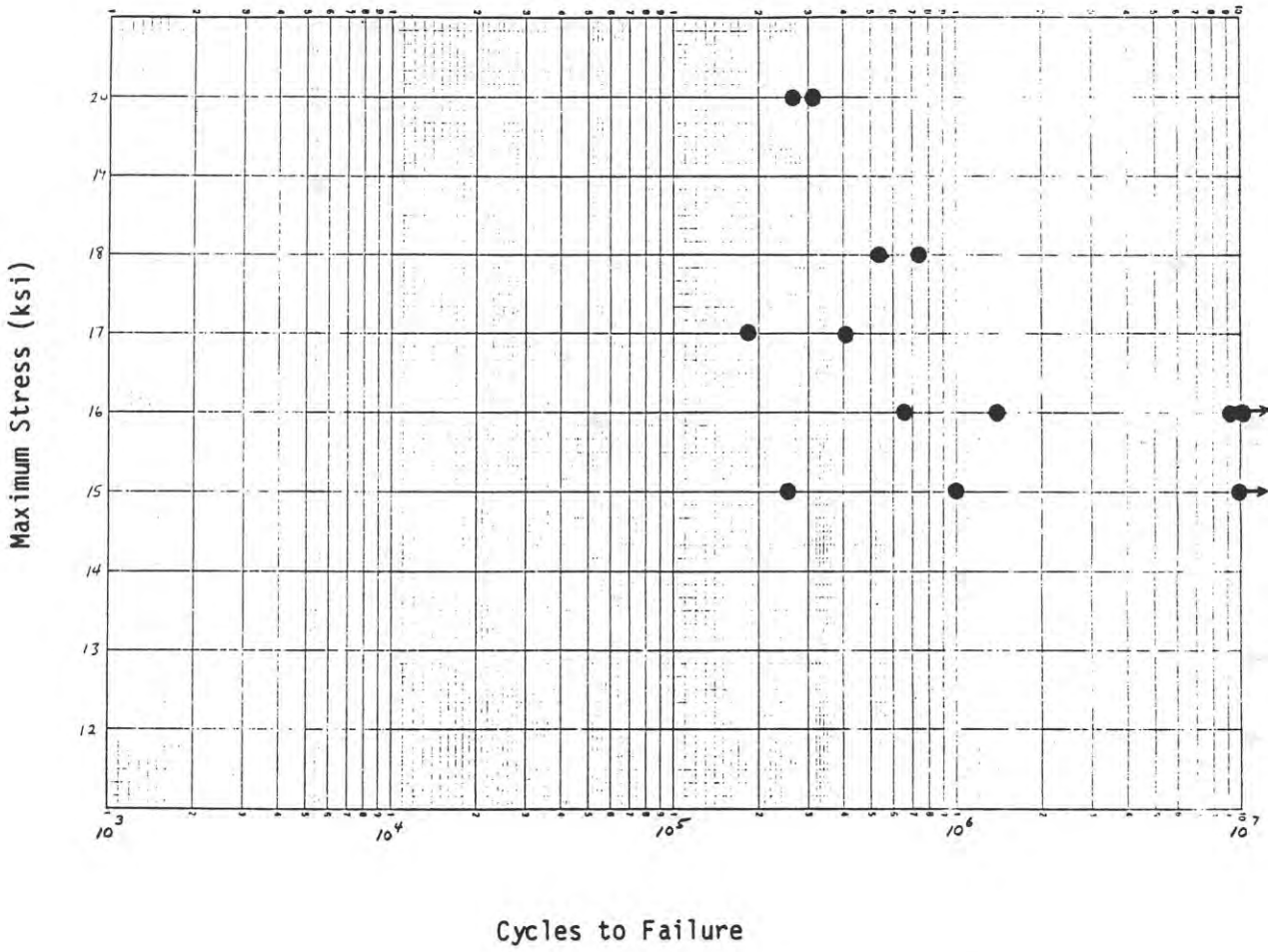

Figure 3.027c: Room temperature notch fatigue test data for longitudinal oriented Materion S200F Be (30).

Test Sequence	Specimen ID	Stress Concentration Factor	Maximum Applied Stress (ksi)	Fatigue Life (cycles)	Comments
Transverse Orientation					
1	A-119	3.05	19	5,000	Failed
2	A-126	3.01	16	50,100	Failed
3	A-116	3.04	14	311,000	Failed
4	A-109	3.03	16	18,411,800	Run out
5	A-122	3.02	14	953,800	Failed
6	A-129	3.01	12	101,120,800	Run out
7	A-112	3.04	13	267,500	Failed
8	A-124	3.02	13	101,673,500	Run out
9	A-114	2.95	16	102,732,900	Run out
10	A-133	2.99	18	5,497,500	Failed
11	A-111	2.98	18	162,400	Failed
12	A-107	2.99	18	672,200	Failed

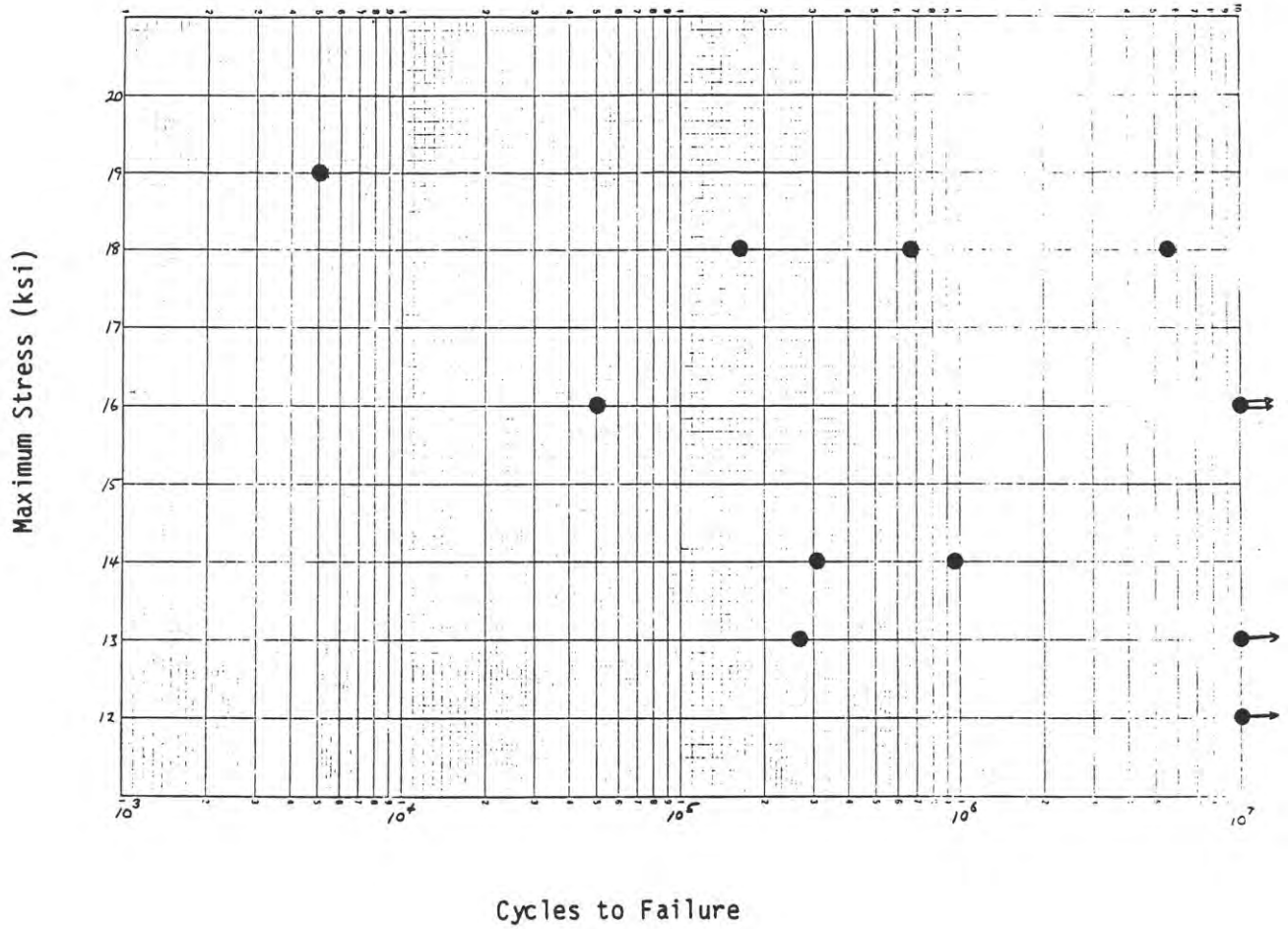

Figure 3.027d: Room temperature notch fatigue test data for transverse oriented Materion S200F Be (30).

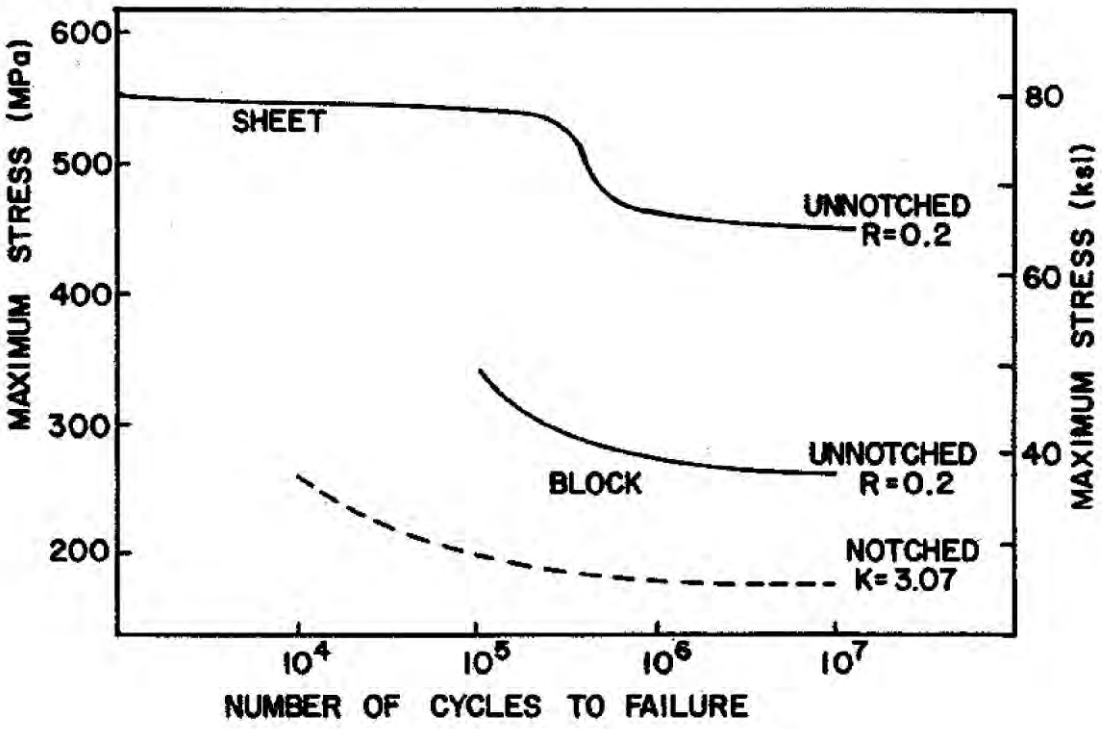

Figure 3.027e: Fatigue properties of KBI block and sheet Be (65).

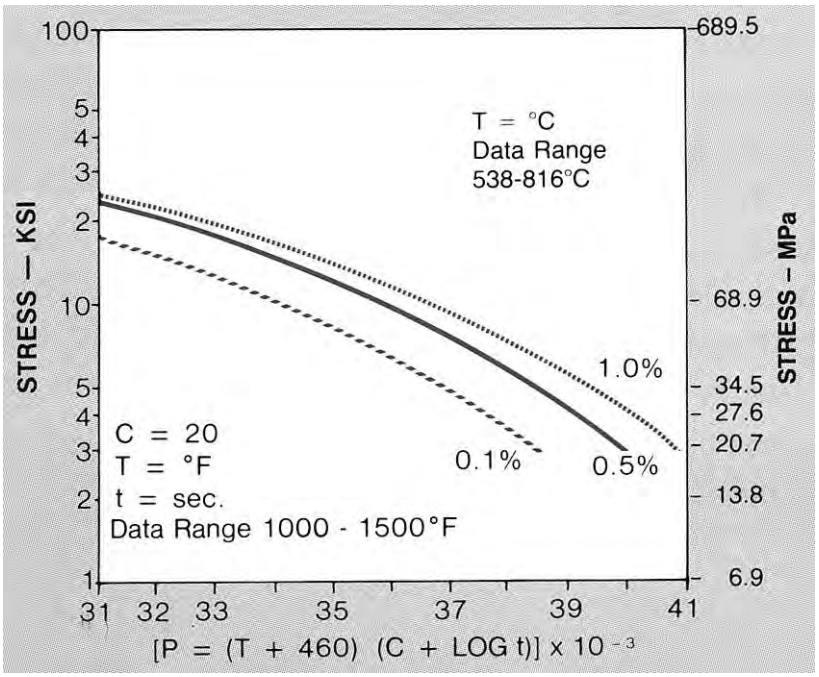

Figure 3.028a: Creep data using the Larson Miller parameter to obtain 0.1%, 0.5% or 1.0% creep for Materion S200F Be (63).

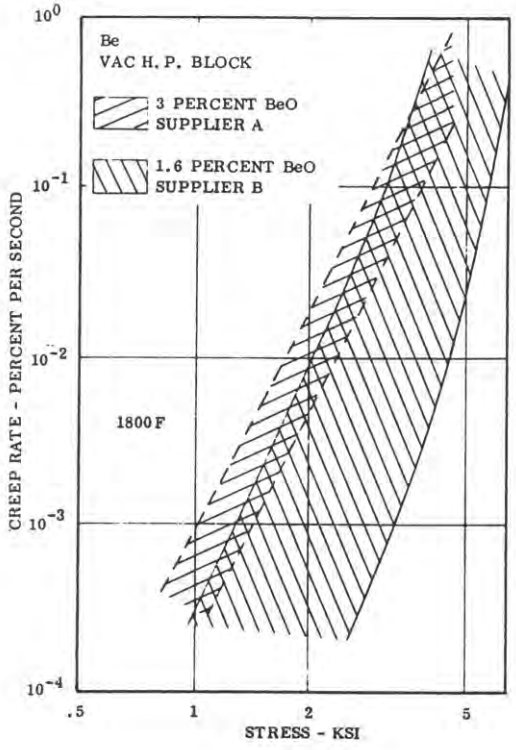

Figure 3.028b: Compression creep rate as a function of stress for vacuum hot pressed Be block (80).

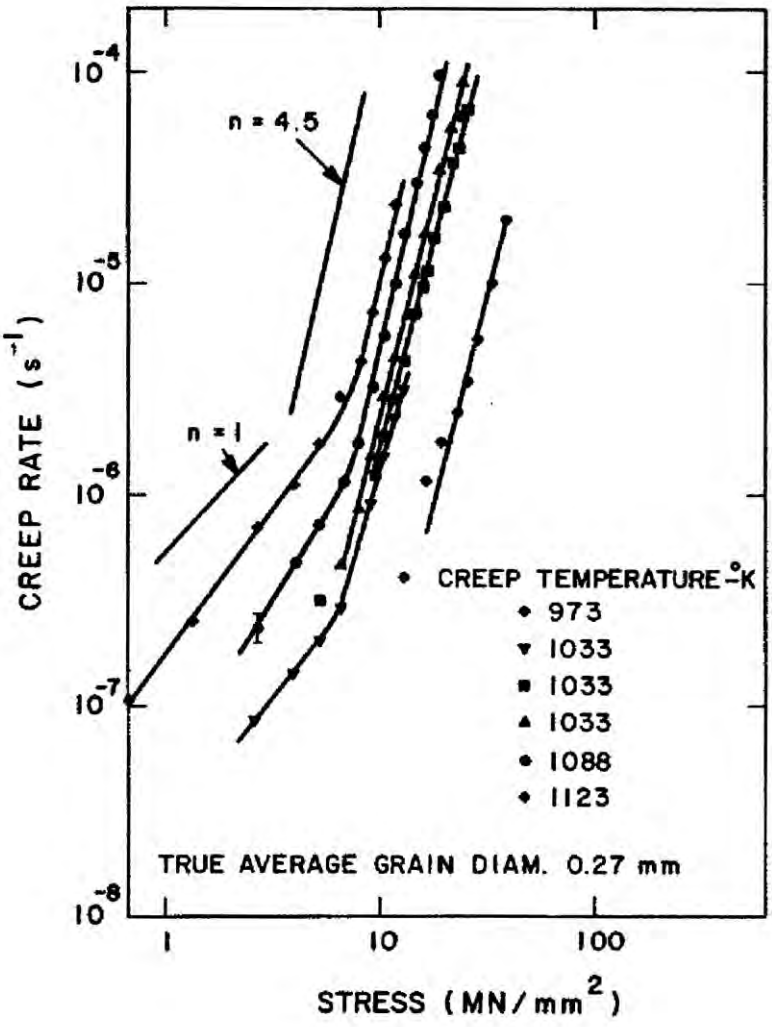

Figure 3.028c: Creep rate for Be as a function of temperature and stress (81).

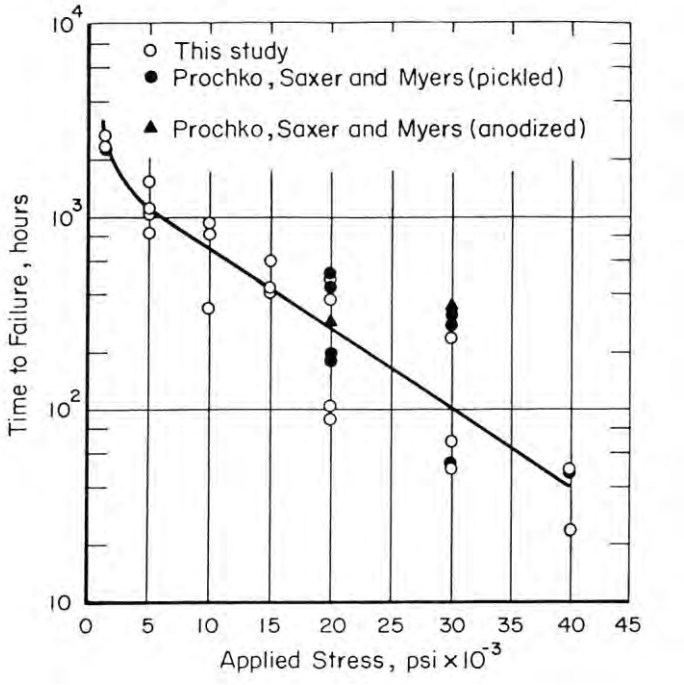

Figure 3.029: Time to failure as a function of applied stress during stress corrosion cracking for sheet Be in synthetic seawater at 25°C (40).

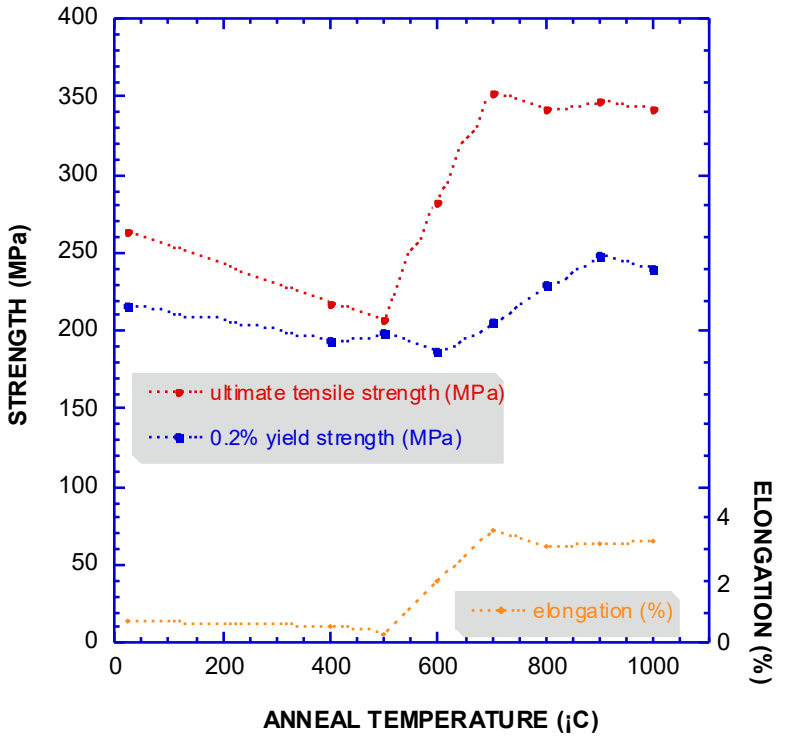

Figure 4.025a: Strength as a function of anneal temperature for machine damaged Materion S200E Be (2).

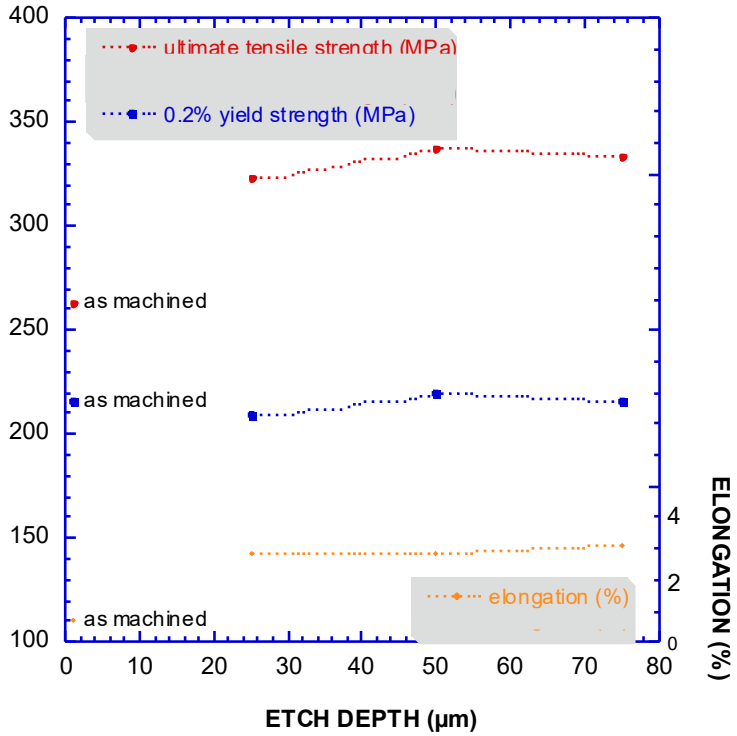

Figure 4.02 S200E Be (2).

BRUSHWELLMAN

ENGINEERED MATERIALS

Brush Wellman Inc. • Elmore Ohio 43416 • Phone 419/862-2745 • TWX 810/490-2300

RECOMMENDED ETCHING PROCEDURES/SOLUTIONS

These recommended procedures and solutions were compiled from a variety of industry sources and are offered as suggested ways to etch beryllium, but no guarantee or warranty is implied.

Etching is performed on machined beryllium surfaces in order to remove the machine damaged layer of material, twinned grain structures, which typically is .002" to .005" deep. Etching is performed typically prior to the final machining of critical dimensions. A typical process flow on producing machined beryllium components is as follows; rough machine to within .025/.035 per surface of final dimensions, stress relieve by heating to 1450°F in a vacuum or inert atmosphere, semi-finish machine to within .003" to .008", etch and finish machine.

Solutions

	Material	Volume (Percent)
I.	Nitric Acid (39° Baume)	25 ± 2
	Hydrofluoric Acid (60%)	0.25 to 1.0
	De-ionized or Distilled Water	Balance
II.	Nitric Acid	48.0
	Hydrofluoric Acid	2.0
	De-ionized or Distilled Water	Balance
III	Hydrofluoric Acid (48% Reagent Grade)	2.0
	Nitric Acid (70-71% Reagent Grade)	2.0
	Sulfuric Acid (96% Reagent Grade)	2.0
	Tap Water	Balance
IV.	Chromic Acid (Dry Technical Grade)	17 ± 0.5 oz/gal.
	Phosphoric Acid (75% Technical Grade)	75 ± 3 volume percent
	Sulfuric Acid (95 to 96.7% Reagent Grade)	15 ± 1 volume percent
	Deionized or Distilled Water	10 ± 1 volume percent

General Process

1. Heat solution to 75±F up to 100±F.
2. Clean parts before etching.
3. During etching agitate parts to allow free circulation of the etchant and to minimize gas entrapment.
4. Rinse parts in de-ionized or distilled water
5. Blow dry with clean warm air or dry nitrogen.
6. Handle etched parts with clean, lint-free gloves to avoid fingerprint and other stains.

Figure 4.025c: Materion Corporation recommended etching procedure for Be (82).

Thickness, in.	Included angle, deg	tensile strength, 1000 psi	Elongation in 2 in., %	Location of fracture
Beryllium-to-beryllium joints — aluminum filler				
¼	40	31.0	1	Beryllium plate and weld
¼	60	23.0	1	Beryllium plate and weld
½	40	17.0	1	Beryllium plate and weld
Beryllium-to-aluminum joints — aluminum filler				
¼	40	12.0	11	Aluminum
¼	60	13.0	11	Aluminum
½	40	13.5	1	Beryllium plate and beryllium fusion line

Base metal	Joint type	Brazing temp. °F	Test temp. °F	stress, 1000 psi
72 silver, 28 copper braze alloy				
Copper	Insert	1545	R.T.	7.7
Copper	Scarf	1445	R.T.	9.6
Monel	Double shear	1520	R.T.	42.4
347 S.S.	Double shear	1510	R.T.	6.6
405 S.S.	Lap	1525	700	7.7
Nickel	Double shear	1510	R.T.	20
Hastelloy-X	Lap	1470	R.T.	13.9
Hastelloy-X	Lap	1490	700	10.3
Inconel-X	Lap	1435	700	8.81
100 silver braze material				
Monel	Scarf	1790	R.T.	27.4
Monel	Double shear	1850	R.T.	11
347 S.S.	Double shear	1795	R.T.	24.2
Nickel	Double shear	1850	R.T.	30
Beryllium	Double shear	1775	R.T.	5.5
Aluminum braze material				
Beryllium	—	1600	R.T.	21.6

Figure 4.027: Properties of Be braze joints by braze-welding (top) and furnace brazing (bottom) (42).

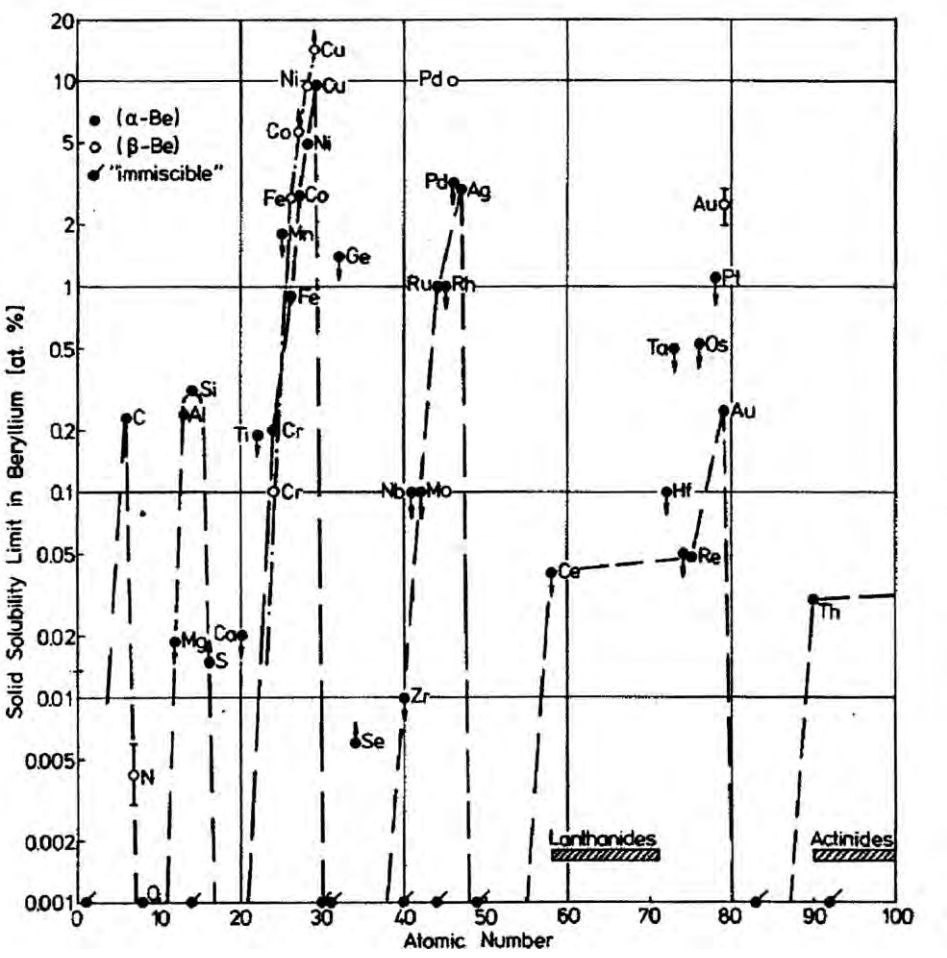

Figure 4.029a: Solid solubility of various elements in beryllium (86).

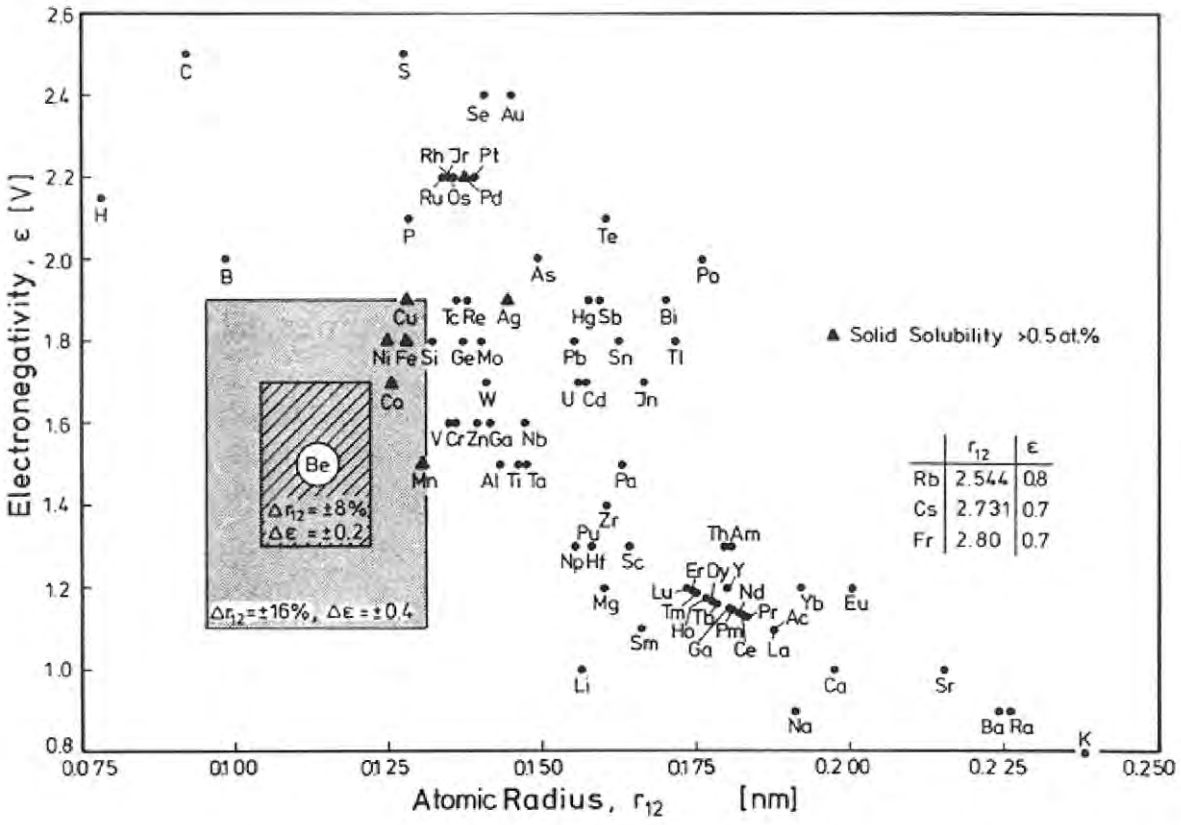

Figure 4.029b: Comparison of elements to beryllium in terms of atomic radius and electronegativity (86). r12 = atomic radius with coordination number 12.

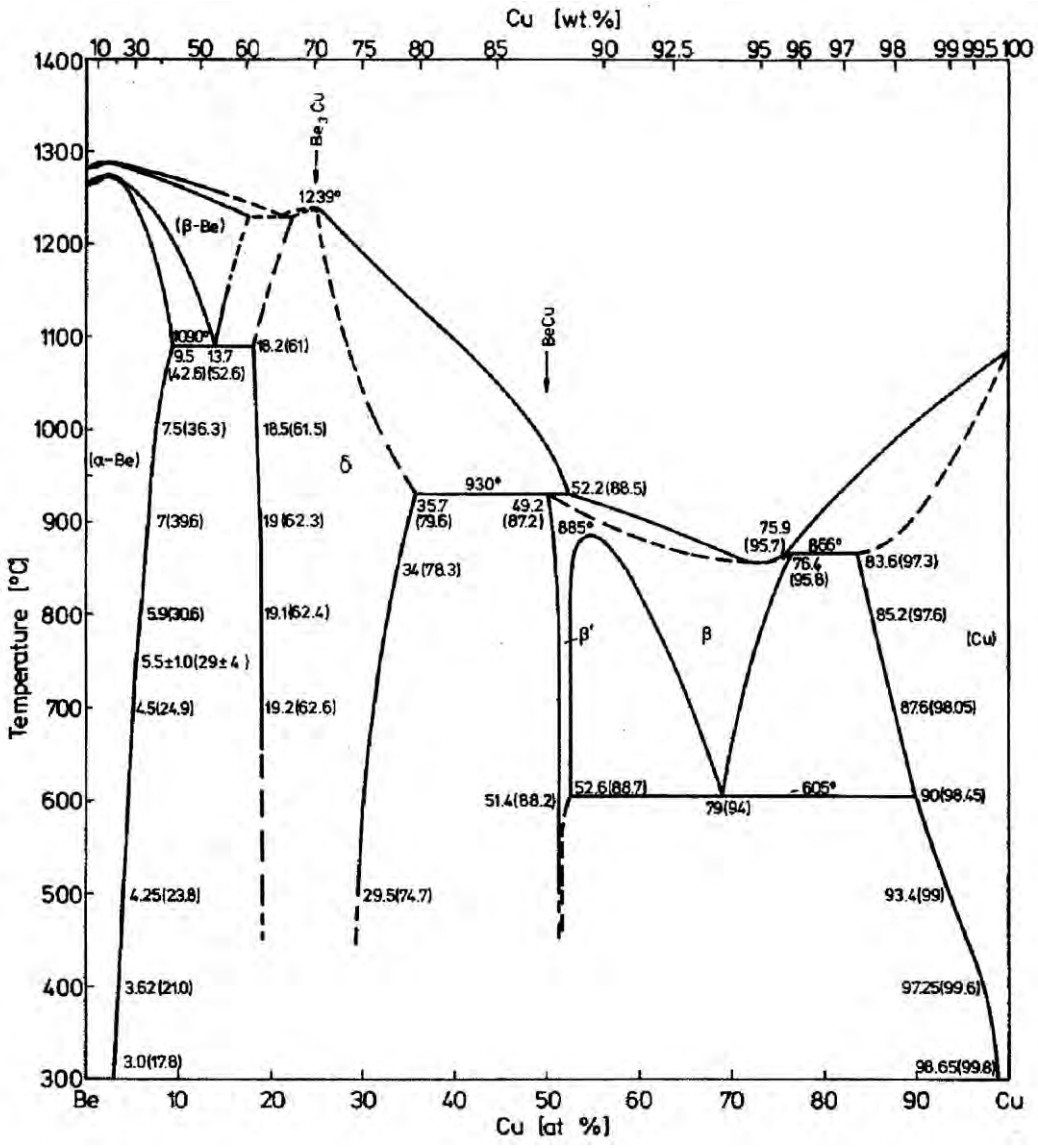

Figure 4.029c: Beryllium-copper phase diagram (86).

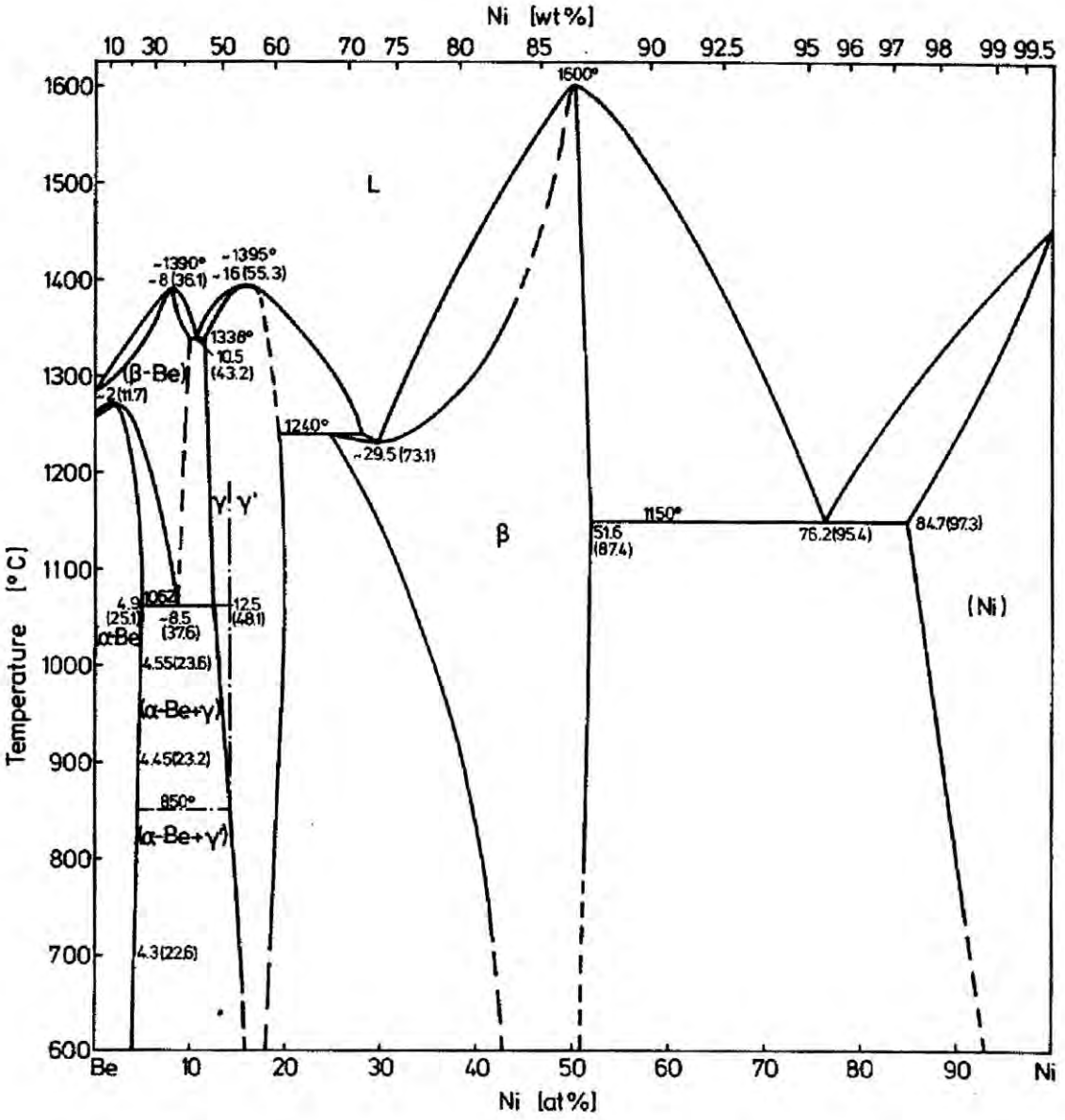

Figure 4.029d: Beryllium-nickel phase diagram (86).

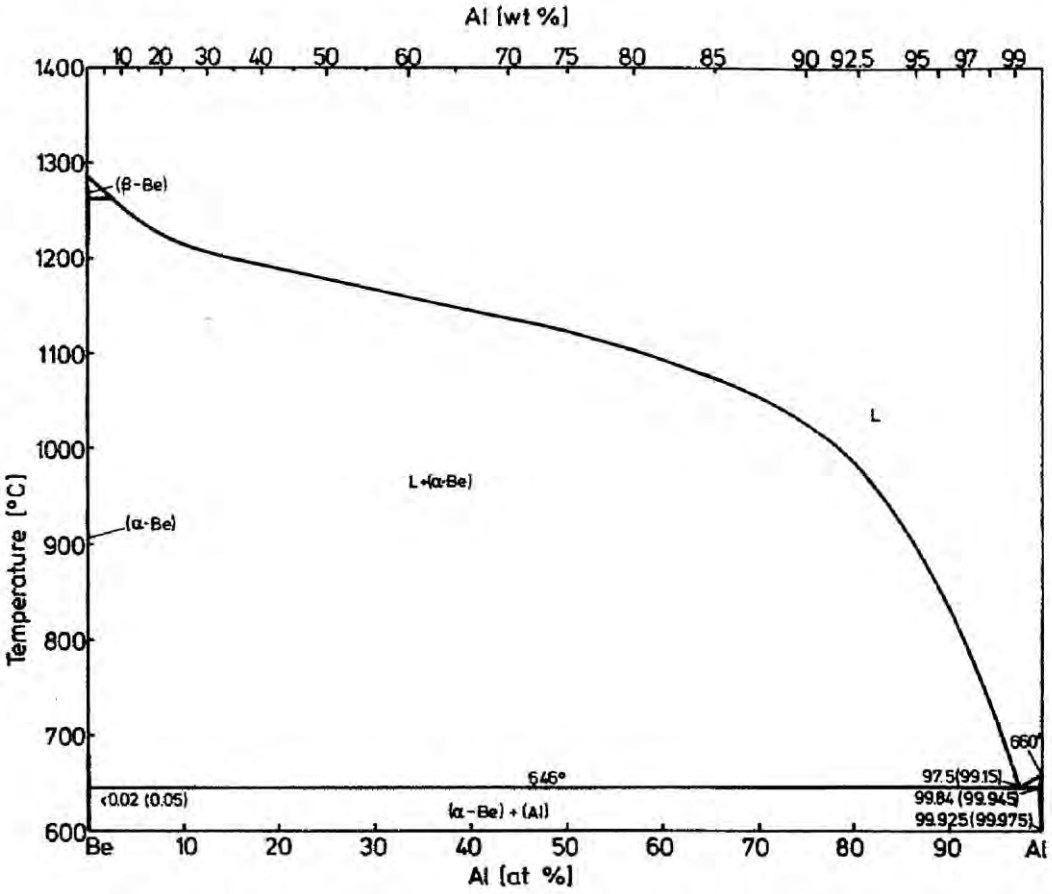

Figure 4.029d: Beryllium-aluminum phase diagram (86).

Phase (symbol)	Crystal structure		Lattice parameter (nm) a	b	c	c/a	Composition[a] (at %)	Remarks[c]
$Al_{8.3}Be_{1.2-1.4}Ce$	$BaAl_4$	bct	0.418	—	1.057	2.530	55–52 Al, 25–28 Be, 20 Ce	—
$AlBe_4Cr$	$MgZn_2$	Hexagonal	0.436	—	0.718	1.628	—	—
	$MgCu_2$	fcc	0.612	—	—	—	—	Excess Be (probably allotropic trans.)
$Be_2(Cu,Al)$	$AuBe_5$	fcc	0.6232	—	—	—	—	RSS of Be_2Cu
			0.6362	—	—	—	19 Al, 43 Be	—
$(Al,Be)Cu_3$								
(β_1)	Cu_3Al	bcc	0.576_4	—	—	—	19.7 Al, 5.9 Be	Quenched metastable
(β)	CsCl	bcc	0.292_7	—	—	—	Same composition	and ordered structure at 800°C CSS
$Al_8Be_{2.3}Fe$	—	Monoclinic	0.7718 β = 124°32	0.44554	0.45424	—	—	—
$AlBe_4Fe$	$MgCu_2$	fcc	0.606	—	—	—	—	—
			0.6054	—	—	—	—	—
			0.6057	—	—	—	$Be_4(Al,Fe)$	—
$(Al,Be)Fe_4$	BiF_3	Cubic	0.572	—	—	—	12.5 Al, 12.5 Be	Probably CSS
$AlBe_4Mn$	$MgCu_2$	fcc	0.611	—	—	—	17.6 Al, 66 Be	TP, range of homogeneity
$Al_{12}Be_2Mn_3$	—	—	—	—	—	—	—	TP, range of homogeneity
$AlBe_4Ni$	$MgCu_2$	fcc	0.601	—	—	—	—	—
AlBeTi	—	—	—	—	—	—	—	—
$Al_8Be_2Ti_5$	—	—	—	—	—	—	—	—
$Au_{1-x}W_xBe_{13}$	$ThMn_{12}$	Tetragonal	0.7243	—	0.4252	0.587	—	Probably TP

Phase (symbol)	Crystal structure		Lattice parameter (nm) a	b	c	c/a	Composition[a] (at %)	Remarks[c]
Be_2CaGe_2	$BaAl_4$	Tetragonal	0.402	—	0.992	2.468	—	—
$BeCo_2Ge$	$AlCu_2Mn$	Cubic	0.546	—	—	—	—	—
$Be_{16}Co_4Hf_6$	$Mn_{23}Th_6$	Cubic	1.100	—	—	—	—	—
$Be_{1.2}Co_{0.8}Mn$	$MgCu_2$	fcc	0.620	—	—	—	—	—
$BeCo_2Si$	$AlCu_2Mn$	Cubic	0.537	—	—	—	—	—
BeCoSi	CaF_2	Cubic	0.524	—	—	—	—	—
or Be_2CoSi	NaTl	Cubic	0.524	—	—	—	—	—
$Be_{16}Co_8Zr_6$	$Mn_{23}Th_6$	Cubic	1.110	—	—	—	—	—
$Be_2(Cr,Mo)$	$MgZn_2$	Hexagonal	0.4359	—	0.7136	1.637	16.7 Cr, 16.7 Mo	CSS
B_{11} (Cr,V)	$ThMn_{12}$	Tetragonal	—	—	—	—	—	CSS
Be_2 (Cu,Ge)	$MgCu_2$	fcc	0.6018	—	—	—	—	CSS
$Be_{16}Cu_8Hf_6$	$Mn_{23}Hf_6$	Cubic	1.108	—	—	—	—	TP
Be_4CuIn	$MgCu_2$	fcc	0.6028	—	—	—	—	—
$Be_2Cu_4Mg_5$	$MgCu_2$	fcc	0.687	—	—	—	—	Probably no TP
Be_4CuMg	$MgCu_2$	fcc	0.6004	—	—	—	—	Probably SS of Be_2Cu
$Be_{16}Cu_8Nb_6$	$Mn_{23}Th_6$	Cubic	1.083_3	—	—	—	—	—
Be_2Cu_6Si	Cu_6Zn_6	Cubic	0.829	—	—	—	Alloy: 25 Be, 50 Cu	—
Be_2 (Cu,Si)	$MgCu_2$	fcc	0.605	—	—	—	—	Probably SS of Be_2Cu
$Be_{16}Cu_8Ta_6$	$Mn_{23}Ta_6$	Cubic	1.077_5	—	—	—	15 Ta, 30 Cu	—
Be_xC_xTa	—	—	—	—	—	—	Approximately 16–20 Ta, 40–60 Cu	—
$Be_{16}Cu_8Ti_6$	$Mn_{23}Th_6$	Cubic	1.078_4	—	—	—	—	—

Phase (symbol)	Crystal structure		Lattice parameter (nm) a	b	c	c/a	Composition[a] (at %)	Remarks[c]
Be_2 (Cu,Zn)	$MgCu_2$	fcc	0.6031	—	—	—	—	Probably SS of Be_2Cu
$Be_{16}Cu_8Zr_6$	$Mn_{23}Th_6$	Cubic	1.118_6	—	—	—	—	—
$Be_2Fe_{1-x}Mn_x$	$MgZn_2$	Hexagonal	0.4265	—	0.693	1.625	4.5 Fe, 28.8 Mn	CSS
$Be_4Fe_{1-x}Mn_x$								RSS
BeFeSi (τ)	—	—	—	—	—	—	36.5 Be, 31.6 Fe	—
Be_3FeSi (ϕ)	—	—	—	—	—	—	—	TP, homogeneity range
$Be_{16}Hf_6Ni_6$	$Mn_{23}Th_6$	Cubic	1.099	—	—	—	—	—
$Be_{16}Hf_6Pd_6$	$Mn_{23}Th_6$	Cubic	1.120	—	—	—	—	—
BeHfSi	NiAs	Hexagonal	0.3693	0.7135	—	1.932	—	—
$(Be,Si)_2Mo$	$CrSi_2$	Hexagonal	0.461,	0.6459	—	1.399	$(Si_{0.5}Be_{0.1})_2$ Mo	—
$Be_{16}Nb_6Ni_6$	$Mn_{23}Th_6$	Cubic	1.073	—	—	—	—	—
Be_2 ($Nb_{1-x}Ti_x$)	$MgCu_2$	fcc	0.6498	—	—	—	66.67 Be, 16.67 Nb	CSS
$BeNi_6Si$	$AlCu_6Mn$	Cubic	0.543	—	—	—	—	—
$Be_{16}Ni_6Ta_6$	$Mn_{23}Th_6$	Cubic	1.068	—	—	—	—	—
$Be_{16}Ni_6Zr_6$	$Mn_{23}Th_6$	Cubic	1.106	—	—	—	—	—
$Be_{16}Pd_6Zr_6$	$Mn_{23}Th_6$	Cubic	1.125	—	—	—	—	—
$(Be,Si)_2Ta$	$MoSi_2$	bct	0.321	—	0.784	2.442	—	—
BeSiZr	—	Hexagonal	0.3722	—	0.7232	1.943	Si-rich	—
			0.3718	—	0.7217	1.941	Be-rich	—
Be_4 ($Ta_{1-x}Ti_x$)	$MgCu_2$	fcc	0.6487	—	—	—	66.67 Be, 21.67 Ta	CSS
$Be_{13}Th_{1-x}U_x$	$NaZu_{13}$	fcc	1.0383	—	—	—	Binary $Be_{13}Th$	CSS
			1.0247	—	—	—	Binary $Be_{13}U$	CSS

[a]If the composition is identical with the chemical formula, no composition is stated.

[c]CSS = complete solid solution, RSS = restricted solid solution, TP = stated as ternary phase.

Figure 4.029e: Ternary beryllide compounds (86).

Phase (symbol)	Crystal structure		Lattice parameter (nm) a	b	c	c/a	Composition (at %)[a]	Remarks
AlBBe	AgAsMg	fcc	0.493	—	—	—	—	—
AlBe $(B_{12})_2$	—	Tetragonal	0.882	—	0.508	0.576	$Al_{\sim 0.6}Be_{\sim 0.4}B_{12}$	Si is necessary in small amounts
$Al_{0.06}BeB_{3.06}$	—	Hexagonal	0.9800	—	0.9532	0.973	1.4 Al, 24.5 Be	—
B_2BeC_2	—	Hexagonal	1.084	—	0.618	0.570	—	—
$B_{12}BeC_2$	B_4C_3	Rhombohedral	0.5615	—	1.228	2.187	—	—
			(Hexagonal arrangement)					
$B_3Be_7Ni_6$	—	—	—	—	—	—	—	—
B_yBe_2Ni	$MgCu_2$	fcc	0.5762–0.5772	—	—	—	$(Ni_{0.63}B_{0.37})$ $(Be_{1.4}B_{0.6})$	Range of homogeneity
B_yBe2Si	α-AlB_{12}	Tetragonal	1.022	—	1.4215	1.391	—	—
BeLiN	—	Orthorhombic	0.875	0.816	0.765	—	—	—
BeLiP	—	Tetragonal	0.512	—	0.6015	1.175	—	—
Be_2MoS_4	—	fcc	1.081	—	—	—	—	—
$Be_4N_2O_3$	—	Hexagonal	0.277	—	3.458	12.484	—	Wurtzite type
$Be_5N_2O_5$	—	Hexagonal	0.2752	—	4.787	17.395	—	Wurtzite type
$Be_6N_2O_6$	—	Hexagonal	0.2738	—	6.105	22.297	—	Wurtzite type
Be_4N_4Si	—	Hexagonal	0.2862	—	1.922	6.716	—	Wurtzite type
$Be_9N_{10}Si_3$	—	Hexagonal	0.2857	—	3.657	12.800	—	Wurtzite type
$Be_5N_6Si_2$	—	Hexagonal	0.286	—	2.910	10.175	—	Wurtzite type
$Be_{11}N_{14}Si_3$	—	Hexagonal	0.286	—	5.098	17.825	—	Wurtzite type
$Be_6N_8Si_3$	—	Hexagonal	0.2862	—	6.511	22.750	—	Wurtzite type
BeN_2Si	ZnS (B_4)	Hexagonal	0.2869	—	0.4668	1.627	$Be_{1+x}Si_{1-x}N_{2-3/3x}$ $0 < x < 0.1$	—
		or Orthorhomb.	0.4977	0.5747	0.4674	—		—
BeN_2Th	—	Hexagonal	1.050_1	—	0.395_5	0.377	—	—

[a]If the composition is identical with the chemical formula, no composition is stated.

Figure 4.029f: Ternary beryllide compounds with nonmetals (86).